Heating of the interstellar medium in the Small Magellanic Cloud by massive stars

Bachelorarbeit aus der Physik

Vorgelegt von

Caroline Collischon

12.07.2017

Friedrich-Alexander-Universität Erlangen-Nürnberg

Betreuerin: Prof. Dr. Manami Sasaki

Abstract

The hot phase of the interstellar medium (ISM) is mainly heated by supernovae and the winds of massive stars which are the subject of this thesis. It emits diffuse X-rays whose distribution should follow the distribution of supernovae and stellar winds. The energy distribution of winds in the Small Magellanic Cloud (SMC) is estimated here based on the star formation history data by Harris and Zaritsky (2004) assuming a Salpeter initial mass function. Their calculation is based on the Zaritsky et al. (2002) catalogue using stars with $m_V \leq 21$ mag and Padua isochrones by Girardi et al. (2002). They provide results for 351 12'×12' regions of the SMC in logarithmic timesteps and for the metallicities $Z = 0.001$, $Z = 0.004$ and $Z = 0.008$.

Relations to calculate luminosity, effective temperature, stellar radius, mass-loss-rates and ages are chosen based on comparisons of observational data and theoretical models. For the luminosity, power-law fits $L/L_\odot = a \cdot (m/M_\odot)^b$ over data by Andersen (1991) for lower masses and Martins et al. (2005) for higher masses are used. For effective temperature and stellar radius logarithmic fits of the form $x = a \log(m/M_\odot) + b$ over the same data are used. For mass-loss the theoretical relation by Vink et al. (2001) is chosen not taking inhomogenities in the wind into account. As the simulated timescale is longer than the lifetime of the most massive stars, stellar ages based on the core hydrogen burning times in Charbonnel et al. (1993) for $Z = 0.004$ and Schaerer et al. (1993) for $Z = 0.008$ are used. Fits of the function $t = \frac{c}{m-a} + b$ for initial masses $m > 10\,M_\odot$ are calculated and give accurate estimates for ages $t \lesssim 20$ Myr. The effects of Wolf-Rayet stars and supernovae are not calculated, but should follow the spatial distribution of the wind output.

Energy output by winds in recent time is then calculated iteratively for stars formed since a few Myr ago from the relation $P = \frac{1}{2}\dot{m}v_\infty^2$ where $\dot{m}$ is the mass-loss rate and v_∞ is the terminal velocity of the wind. The energy output is integrated in 0.1 Myr timesteps for different timeframes and $1\,M_\odot$ massbins for masses ranging from 10 to 100 solar masses and multiplied with the expected amount of stars in each age and mass group. The different metallicity data are added. Depending on the region, an output of the order of 10^{45} to 10^{51} erg/arcmin^2 is found. No correlation is found between the spatial distribution of energy output up to 29 Myr ago and the diffuse X-ray emission of the SMC. The X-ray distribution rather roughly follows the star formation distribution between 40 Myr and 2.5 Gyr ago. Correlations of output with Hα emission, stellar distribution and strong X-ray point-sources in the southern half of the SMC are found. The diffuse emission might not stem from the ISM, but from unresolved, soft X-ray sources as is probably the case in the Milky Way (Revnivtsev et al. 2009). Still, since the X-ray distribution does not follow the stellar distribution as in the Galactic case but is rather shifted to the northwest, the true origin of the diffuse emission remains unclear and requires further study.

Contents

1. Introduction

1.1. Stellar bubbles and the interstellar medium

The interstellar medium (ISM) is composed of gas and dust occupying the space between star systems in galaxies. It has been found to consist of three phases characterised by different temperatures (McKee and Ostriker 1977): A hot low-density phase ($n \sim 10^{-2.5}\,\mathrm{cm^{-3}}, T \sim 10^6\,\mathrm{K}$) heated and ionised by supernova remnants (SNRs) and the winds of massive stars fills most of the volume. Additionally, there is a warm low-density phase ($n \sim 10^{-0.5}\,\mathrm{cm^{-3}}, T \sim 10^4\,\mathrm{K}$), heated and partially ionised by UV and soft stellar X-ray radiation, and a cold dense phase ($n \sim 10^{1.6}\,\mathrm{cm^{-3}}, T \sim 10^2\,\mathrm{K}$) in clouds surrounded by the warm phase. The hot phase mainly emits X-rays. Therefore, SNRs and bubbles around stars with strong winds can be studied in X-ray observations. The latter shall be of interest in this thesis.

Massive stars (mass $m \gtrsim 8 - 10\,M_\odot$) lose a significant amount of mass by stellar winds at rates of the order of $10^{-6}\,M_\odot/\mathrm{Myr}$ during their lifetime (Castor et al. 1975b). These winds compress the ambient medium and form a shock wave that creates a shell of swept-up ISM surrounding the star. Therefore, the strong stellar winds of massive stars are an important source of energy for the ISM (Castor et al. 1975a; Weaver et al. 1977). Weaver et al. (1977) expand the analysis of Castor et al. (1975a) and describe the evolution of such a bubble in three stages. First, the emitted wind expands adiabatically without relevant radiative losses and sweeps up the surrounding matter. The wind is compressed into a hot shell further away from the center and a cooler shell of ISM forms around it. In the next stage this outer shocked gas collapses into a thin shell due to radiation losses. The inner part of the shell absorbs energy by conduction and evaporates into the hot region. It becomes the main source of its mass in the second stage. In later evolution the wind dissipates into the surrounding medium and the system reaches a steady state if the star lives long enough. All this is surrounded by the cold ISM. The warm shell is partially ionised and therefore can be observed as a H II region with a temperature of $\sim 10^4\,\mathrm{K}$.

Calculations show that for a typical bubble (mass-loss rate $\dot{m} = 10^{-6}\,M_\odot/\mathrm{Myr}$, terminal velocity $v_\infty = 2000\,\mathrm{km/s}$) at an age of $10^6\,\mathrm{yr}$, the transition from shocked stellar wind to warm ISM occurs at a radius of $\sim 27\,\mathrm{pc}$. At this point the stellar bubbles should have a much lower X-ray luminosity compared to SNRs. Still, massive stars emit a significant amount of energy in the form of stellar winds over their lifetime. The output can be of the same order of magnitude as a supernova explosion (energies are equal for stars with about $55\,M_\odot$) and winds are more efficient at transferring energy to the ISM (Abbott 1982). Their overall input into the Galactic ISM is estimated to be $20 - 40\%$ of that of supernovae on average according to the same paper.

1.2. The Small Magellanic Cloud

The Magellanic Clouds are irregular dwarf galaxies orbiting the Milky Way. Their metallicities $Z = m_{metal}/m_{tot}$ are significantly lower than the solar value ($Z_{\odot} = 0.142$, Asplund et al. 2009, although often higher values are used in papers), especially in the Small Magellanic Cloud (SMC, $Z_{SMC} \sim 0.2 Z_{\odot}$, Russell and Dopita 1992) which will be the object of investigation of this thesis. An image in near-infrared taken at the VISTA telescope can be seen on the right in Fig. 1. It is located at a relatively small distance of 60 kpc (Hilditch et al. 2005) to the Sun in a direction far away from the Galactic disk. This makes it an ideal object for observing metal-poor environments without Galactic gas and dust in the line of sight. It emits diffuse X-ray radiation which is believed to originate from the hot phase in the ISM (Sturm 2012). A view in the energy band of $0.2 - 4.5$ keV by the XMM-Newton space telescope can be seen on the left in Fig. 1.
The SMC is forming stars and Harris and Zaritsky (2004) have obtained spatially resolved star formation history (SFH) data. They used stars with a brightness up to $m_V \leq 21$ mag from the Zaritsky et al. (2002) catalogue and performed fits to Padua isochrones (Girardi et al. 2002). Isochrones are curves in the Hertzsprung-Russell diagram showing stars of the same age and can thus be used to calculate SFHs for a given initial mass function (IMF). They used $\frac{\mathrm{d}N}{\mathrm{d}m} \propto m^{-2.35}$ and a binary fraction of 0.5. In the ISM a part of the stellar light is scattered or absorbed which may lead to errors. To take this interstellar extinction into account, they derived a hot-star extinction distribution for younger populations and a cool-star extinction distribution for older populations with a combination of both for intermediate ages. Photometric errors in their catalogue result mainly from crowding in high surface density areas. The structure of their results is further described in section 3.1.

Their results show several bursts in addition to a constant star formation rate (SFR) since about 3 Gyr ago. This means there must have been massive stars present in the last few Myr interacting with the ISM through stellar winds and supernovae, thus providing energy. Previous observations have already shown a linear correlation between the SFR and the X-ray luminosity of star-forming galaxies (e.g. Mineo et al. 2012).
In this thesis, the relation between the SFR and the X-ray luminosity of the hot ISM will be investigated from a more theoretical point of view by calculating the energy input starting from a SFH: The number of massive stars will be obtained for a given mass distribution and SFR. Then stellar parameters related to stellar mass-loss and the strength of the winds themselves will be estimated to calculate the energy input by stellar winds. This shall be done here taking the low metallicity into account. The mass-loss of Wolf-Rayet-stars (WR, a short-lived, evolved form of massive stars) is neglected because of their low number and relatively weak winds in the SMC compared to Galactic WR stars (Hainich et al. 2015). The influence of supernovae will not be treated here since a large number of the SNRs in the SMCs are known and well resolved in the X-ray data. In addition, their spatial distribution will be the same as that of the wind input.

The structure of this thesis is the following: Mass distribution, luminosity, effective

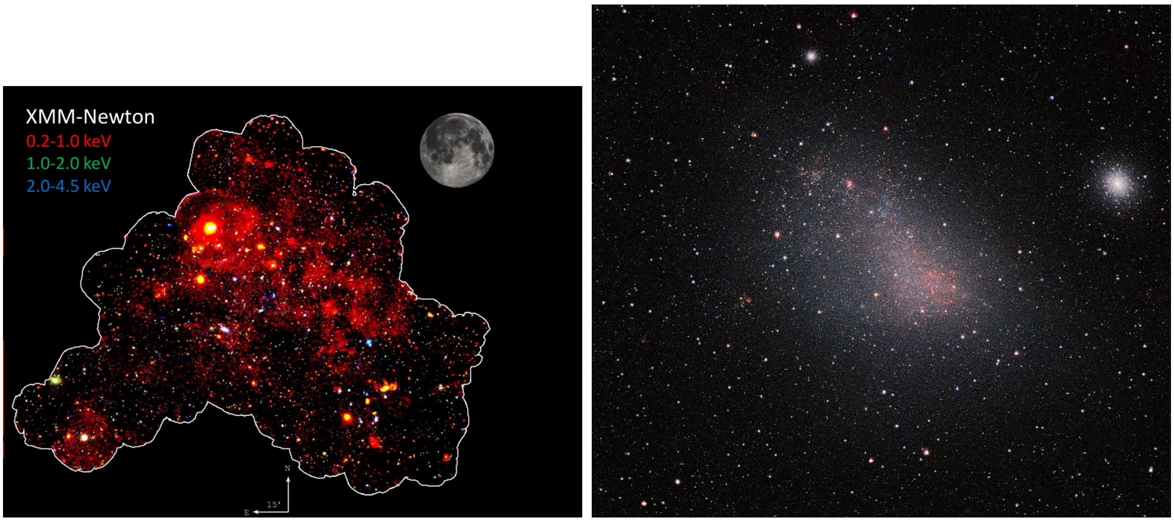

Fig. 1.— The SMC in XMM-Newton X-ray energies (Sturm and Haberl 2014, left) and in near-infrared (ESO/VISTA VMC, right). The globular cluster on the right is 47 Tucanae and unrelated to the SMC.

temperature, radius, mass loss and expected age of massive stars in respect to their mass from theoretical and observational data are obtained in section 2 to get statistical mass-parameter-relations. All values are calculated for main-sequence stars if applicable. In section 3, the results are then used to calculate the energy output by stellar winds of the most massive stars in recent time. The results are discussed in section 4.

2. Stellar parameters

Calculating stellar energy output, which is the aim of this thesis, means estimating the strength of stellar winds during the lifetime of a star. They are caused by mainly two effects: In the line-driving mechanism, metal ions of bright stars absorb photons from the stellar photosphere and therefore obtain momentum in a direction away from the star. A photon is then re-emitted in a random direction which on average does not yield momentum. Another mechanism is Thomson scattering, where a photon elastically scatters by any charged particle and provides radial momentum. If the average force exerted by radiation is higher than local gravity, the particle will escape. Metal ions have more transitions and thus larger cross sections than hydrogen or helium in the high energy part of the spectrum. They can share a part of their momentum with the less heavier elements through Coulomb scattering. This depends on the timescale of the momentum transfer compared to the timescale for drifting away from the passive atoms (Puls et al. 2008).

It can easily be seen that metallicity plays a big role in stellar winds and its effect will be weaker in the metal-poor SMC than in the Galaxy. In order to calculate the stellar wind output, the effective temperature, which is related to the position of the stellar flux maximum, and obviously the luminosity also need to be estimated. The stellar radius is also crucial for some models to calculate the surface escape velocity. All this will be the aim of this section:

existing models and data will be compared and mass-parameter-relations for the subsequent calculations will be chosen. This will be done for main-sequence stars where possible.

2.1. Mass distribution

Newly formed stars follow a mass distribution which is given by a so-called initial mass function (IMF):

$$\frac{\mathrm{d}N}{\mathrm{d}m} = \chi(m)$$

where dN is the number of stars in the mass interval dm. Often it is not given in the above form, but as a function of $\log m$, but the two forms can be deduced from each other: $\frac{\mathrm{d}N}{\mathrm{d}m} \propto \frac{\mathrm{d}N}{\mathrm{d}\log m} m^{-1}$. Studies suggest that in many cases it is given by a power-law (for a review see Bastian et al. 2010)

$$\frac{\mathrm{d}N}{\mathrm{d}m} \propto m^{-\alpha} \tag{1}$$

with $\alpha = 2.35$ first proposed by Salpeter (1955). For several clusters in the SMC the IMF is in agreement with such a Salpeter law (NGC 602, Schmalzl et al. 2008; NGC 346, Sabbi et al. 2008; NGC 330, Sirianni et al. 2002 and several young clusters and OB associations Massey 2003). Massive field stars, however, seem to follow a much steeper slope of $\alpha \sim 5$ as mentioned in Massey (2003).

In this analysis a Salpeter slope is used since Harris and Zaritsky (2004) also assumed $\alpha = 2.35$ and their data based on this reproduces the current situation. A different mass distribution would therefore not be useful with this data set.
The total star formation rate (SFR) is given in $M_\odot$/Myr for different timebins and regions of the SMC and will now be called μ. Integrating over the IMF will yield a SFR in 1/Myr which denotes the number of stars formed for a certain mass range per time, denoted as ν. The structure of the equations will remain the same as only a time derivative is added.
In order to calculate the number of stars resulting from a specific SFR for a fixed mass range in a region at a certain time, the total distribution has to be normalised first:

$$\frac{\mathrm{d}\nu}{\mathrm{d}m} = c\,m^{-2.35} \Rightarrow \mathrm{d}\nu = c\,m^{-2.35}\mathrm{d}m$$

$$\mathrm{d}\mu = m\,\mathrm{d}\nu = c\,m^{-1.35}\mathrm{d}m \;\Rightarrow \mu = \int_{m_{\min}}^{m_{\max}} c\,m^{-1.35}\mathrm{d}m = \frac{c}{0.35}(m_{\min}^{-0.35} - m_{\max}^{-0.35}) \tag{2}$$

Here $m_{\min}$ and $m_{\max}$ are the overall mass limits. The normalisation constant c then follows. The upper limit needs only to be selected sufficiently high as the integral converges for $m_{\max} \to \infty$; here $m_{\max} := 100$. The lower limit is more important as the function diverges for $m_{\min} \to 0$. Harris and Zaritsky (2004) used stars with $m_V \leq 21$. At a distance modulus of $d = 18.9\,$mag (Hilditch et al. 2005) this corresponds to an absolute magnitude of $M_V = m_V - d = 2.1$, a typical value for A5-A6 dwarfs, with a typical mass $\log(m/m_\odot) \simeq 0.32 \Rightarrow m \simeq 2\,m_\odot$ (Zombeck 2007). This value shall be used as the lower limit. A calculation for one region of the SMC at one timebin can be seen in Fig. 2.

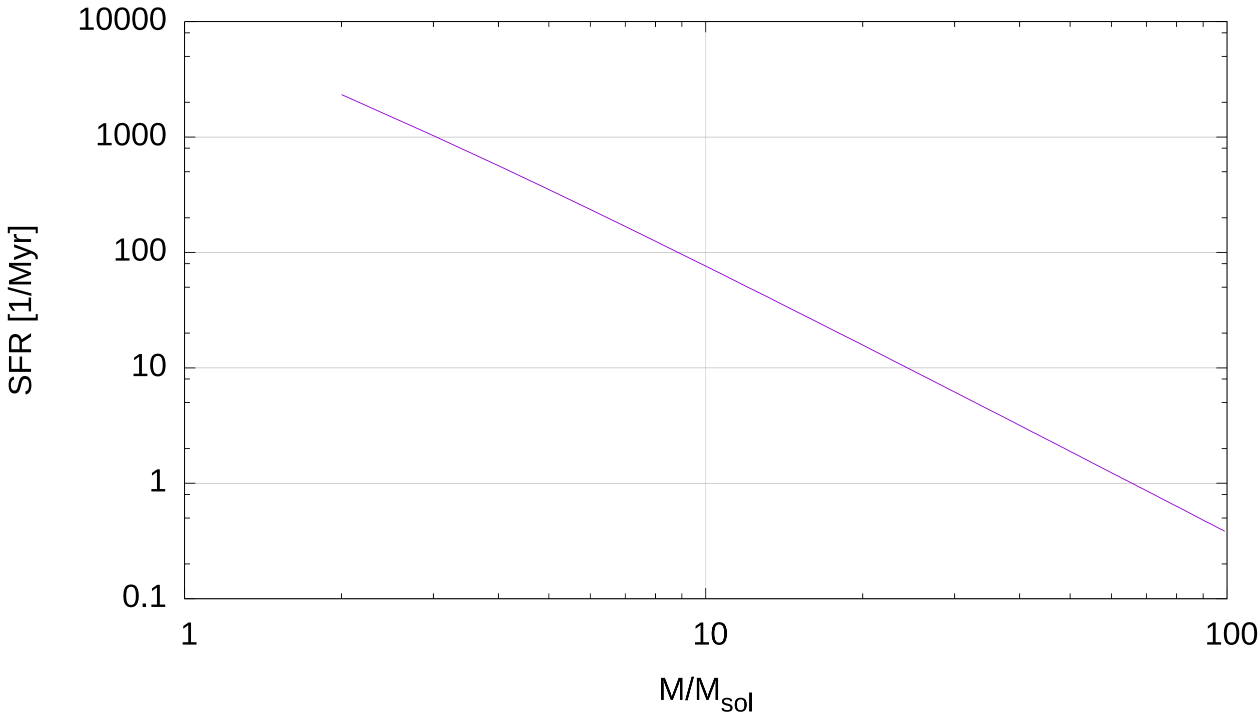

Fig. 2.— SFR over mass in region NO, $Z = 0.008$, $6.6 < \log t < 6.725$, bin width $1\,M_\odot$.

2.2. Luminosity

To obtain a mass-luminosity relation (MLR) I have considered observational data from Martins et al. (2005), table 4, and Hohle et al. (2010) (both Milky Way stars, averages for spectral types in Martins et al.), Massey et al. (2005) (several SMC and LMC stars) and Andersen (1991) (high precision binary star measurements). It is to be noted that the standard deviations in mass in Martins et al. (2005) range from $0.35 - 0.5$ and here 0.4 is used. From Hohle et al. (2010) mean masses and bolometric luminosities from single stars with $m > 8\,M_\odot$ are used. The masses depicted by Massey et al. (2005) are spectroscopic masses and some differ significantly from the evolutionary masses given in the same paper.
The theoretical MLR from Vitrichenko et al. (2007) and Nadyozhin and Razinkova (2005) (for $Z = 0.008$ and for solar values) have been compared to this observational data. In addition, power-laws were fitted to the data points of Martins et al. (2005) and Andersen (1991). The result can be seen in Fig. 3.

The MLR by Vitrichenko et al. (2007) results from a power-law fit over stars with masses $m > 10\,M_\odot$ in the catalogues of de Jager (1980), Svechnikov and Kuznetsova (1990) and Svechnikov (1969). It is given by

$$\frac{L}{L_\odot} = 19 \left(\frac{M}{M_\odot}\right)^{2.76} \tag{3}$$

and it is steeper than the IMF and thus not realistic as the overall L would diverge. They also note that this relation is steeper for high masses than the theory and the data they considered.

It is caused by the low statistics of stars with $m > 25\,M_\odot$ in their data.
Nadyozhin and Razinkova (2005) model the structure of spherical stars in hydrostatic and thermal equilibrium and homogeneous chemical composition (such as in zero age main sequence, ZAMS). Their resulting curve yields a much lower luminosity and is given by

$$L_0 = \frac{4\pi c G M_\odot}{\mu^2 \kappa_0}\lambda(\mu^2 M) = \frac{1}{1.5426\cdot 10^{-5}\mu^2(1+X)}\lambda(\mu^2 M)L_\odot \tag{4}$$

with

$$\begin{aligned}
\kappa_0 &= 0.2(1+X)\mathrm{cm}^2\mathrm{g}^{-1} \\
\lambda &= 0.00157(\mu^2\, M)^3 && (\mu^2\, M \leqslant 2.4) \\
\log\lambda &= -2.907029 \\
&\quad + 3.552793\log(\mu^2\, M) \\
&\quad - 0.7717945\log^2(\mu^2\, M) \\
&\quad + 0.078623\log^3(\mu^2\, M) && (2.4 < \mu^2\, M < 100) \\
\lambda &= \mu^2\, M\left(1 - \frac{4.5}{\sqrt{\mu^2\, M}}\right) && (\mu^2\, M \geqslant 100)
\end{aligned}$$

Here μ is the mean molecular mass, $1/\mu = \frac{X}{\mu_X} + \frac{Y}{\mu_Y} + \frac{Z}{\mu_Z}$, $\mu_i = \frac{A_i}{Z_i+1}$ for fully ionised atoms. X, Y and Z are the hydrogen, helium and metal mass fraction. Y is set to the solar value $Y_s = 0.2485$ (Basu and Antia 2004), Z is given by the SFH data, Z_i and A_i are the atomic proton and mass number; X follows from $1 = X + Y + Z$. μ can then be calculated using $A_i \simeq 2Z_i$ for light nuclei:

$$\mu^{-1} = 2X + \frac{3}{4}Y + \frac{1}{2}Z$$

Apparently the Vitrichenko et al. (2007)-relation and the Andersen-fit leads to a too high luminosity among the highest masses, whereas the Martins-fit is too high for the lower masses. Nadyozhin and Razinkova (2005) give a luminosity much lower than average for a big part of the mass range. It seems most appropriate to take the Andersen-fit for the lower masses and the Martins-fit for the higher masses. The resulting formula is

$$L = \min((257 \pm 16)m^{1.948\pm0.016},\ (9\pm4)m^{2.97\pm0.13}) \tag{5}$$

in solar units.

2.3. Temperature and radius

To obtain estimates for effective temperatures and radii, a similar method as in the previous section has been used.
The radius has been plotted over mass with data by Martins et al. (2005), Massey et al. (2005) and Andersen (1991) in Fig. 4. The datapoints can be well represented with a logarithmic function $R/R_\odot = a\log(m/M_\odot) + b$ with $a = 4.6 \pm 0.4$ and $b = -5.5 \pm 1.3$. A power-law fit is also possible, but it does not follow the data as well as the logarithm. A similar analysis

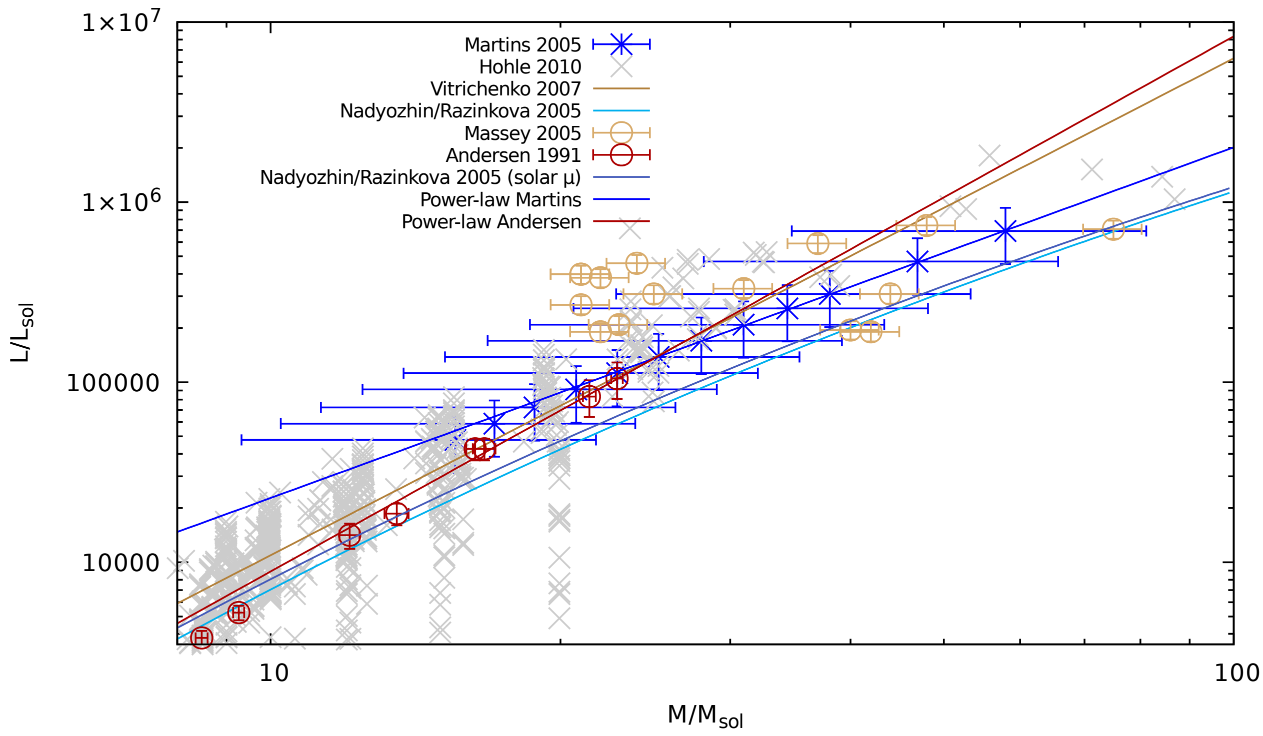

Fig. 3.— Mass-luminosity relation data from various sources and power-law fits.

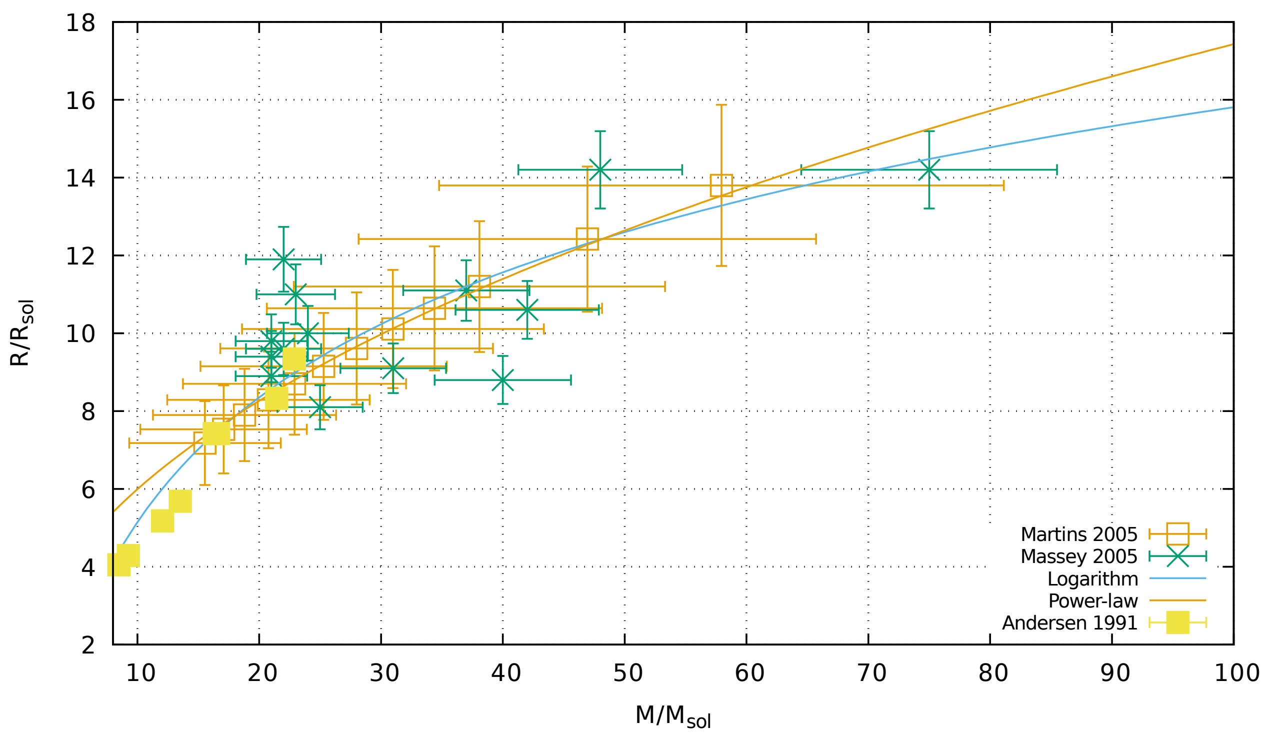

Fig. 4.— Mass-radius relation data from various sources and fits.

has been carried out for effective temperatures, but Hohle et al. (2010) data have been added as the relation is not as clear as in the previous case (Fig. 5). Especially the data of Massey et al. (2005) seem to be significantly hotter than the rest, but are outweighed by the data by Hohle et al. (2010). Again the data of Andersen (1991) and Martins et al. (2005) were fitted with a logarithmic function. The resulting parameters a and b in $T/\mathrm{K} = a\log(m/M_\odot) + b$ are $a = 11600 \pm 500$, $b = -1800 \pm 1100$ and $a = 9850 \pm 60$, $b = 4990 \pm 180$, respectively. The minimum value of both fits will be used for further calculation.

2.4. Mass loss

All these parameters can now be used to derive the stellar mass loss. For this purpose several models have been created and will be compared here.
The first model considered here is based on the theory of Castor et al. (1975b). They simulated line-driven and continuum-driven winds for local thermodynamic equilibrium and for a given temperature distribution. Their estimate is based on a large catalogue of C III lines. Mass loss is calculated as

$$\dot{m} = \frac{L}{v_\infty \cdot c} \tag{6}$$

where

$$v_\infty = a v_{esc} = a\left(\frac{2\,G\,m}{R} \cdot (1 - L/L_{\mathrm{edd}})\right)^{0.5} \tag{7}$$

is the terminal wind velocity with $L_{\mathrm{edd}} = 4\pi G \cdot m \cdot m_p \cdot c/\sigma_T$ as the Eddington luminosity, G gravitational constant, m_p proton mass and σ_T the Thomson cross-section for electrons. The Eddington luminosity is defined as the luminosity where the force from radiation acting outward is equal to gravity. $a = \frac{v_\infty}{v_{\mathrm{esc}}} = 2.6$ for high temperatures ($T \gtrsim 25\,000\,\mathrm{K}$, Vink et al. 2001), which can be assumed for most massive stars. A correction for non-solar metallicity can be introduced by $\dot{m} \propto Z^{0.69}$ (Vink et al. 2001) and $v_\infty \propto Z^{0.12}$ (Leitherer et al. 1992). Note that the first factor has been derived assuming $Z_\odot = 0.019$ as stated by Allen (1973) and the second one for $Z_\odot = 0.02$ although this is higher than more recent studies state (Asplund et al. 2009). Leitherer et al. (1992) mention however that the metallicity dependence of v_∞ in general is not very strong and the given factor is the result of a power-law fit, whereas the real dependence is not monotonous.
Another recipe is given by Vink et al. (2001) and Vink et al. (2000). They used a Monte Carlo method which simulates the path and interactions of a large number of photons travelling through the wind. Here mass-loss follows two formulas depending on the temperature. This is caused by a bi-stability jump near $T_{\mathrm{eff}} \simeq 25\,000\,\mathrm{K}$ where Fe IV recombines to Fe III which

provides more efficient absorption lines. The two formulas are given by

$$\begin{aligned}\dot{M}(L, M, v_\infty/v_{\rm esc}, T_{\rm eff}) = &- 6.697\\ &+ 2.194 \log(L/10^5)\\ &- 1.313 \log(m/30)\\ &- 1.226 \log\left(\frac{v_\infty/v_{esc}}{2}\right)\\ &+ 9.33 \log(T_{\rm eff}/40000)\\ &- 10.92 \log^2(T_{\rm eff}/40000)\\ &+ 0.85 \log(Z/Z_\odot)\\ &(27\,500 < T_{\rm eff} < 50\,000\,{\rm K}),\end{aligned}$$

here $v_\infty/v_{esc} = 2.6$;

$$\begin{aligned}\dot{M}(L, M, v_\infty/v_{\rm esc}, T_{\rm eff}) = &- 6.688\\ &+ 2.210 \log(L/10^5)\\ &- 1.339 \log(m/30)\\ &- 1.601 \log\left(\frac{v_\infty/v_{esc}}{2}\right)\\ &+ 1.07 \log(T_{\rm eff}/20000)\\ &+ 0.85 \log(Z/Z_\odot)\\ &(12\,500 < T_{\rm eff} < 22\,500\,{\rm K}),\end{aligned}$$

here $v_\infty/v_{esc} = 1.3$.
The exact $T_{\rm eff}^{\rm jump}$ can be calculated from eq. (15) in Vink et al. (2001): $T_{\rm eff}^{\rm jump} = 61.2 + 2.59 \log\langle\rho\rangle$. $\langle\rho\rangle$ is the average wind density at 50% of the terminal wind velocity and $\log\langle\rho\rangle = -14.94 + 3.2\,\Gamma_e$ with $\Gamma_e = \frac{\sigma_e L}{4\pi G m c} = 7.66 \cdot 10^{-5} \sigma_e (L/L_\odot)(m_\odot/m)$. $\sigma_e \simeq \sigma_T/m_p$ is the electron scattering cross-section per unit mass as derived in Lamers and Leitherer (1993).
Another approximation for mass loss during core hydrogen burning is given by Vanbeveren et al. (1998), which results from a fit to observational data:

$$\log(-\dot{m}) = 1.67 \log L - 1.55 \log T_{\rm eff} - 8.29 \tag{8}$$

These models have been plotted in Fig. 6 for $Z = 0.004$ along with several datasets (Massey et al. 2005, Massey et al. 2009, Muijres et al. 2012, Mokiem et al. 2006). Again Massey et al. analysed LMC and SMC stars and gave spectroscopic and evolutionary masses; spectroscopic masses are shown. The same holds for Mokiem et al. (2006), who only observed stars of the SMC cluster NGC 346. Muijres et al. (2012) based their work on the calibrations by Martins et al. (2005). They used two different models, denoted as A and B. Again, spectroscopic masses are shown.
Two problems are currently present regarding stellar winds. The first one is the so-called clumping correction: usually models assume spherically symmetric winds. If this is not the

case in reality, correction factors have to be added. For the Massey et al. (2009) data, a clumping correction $\sqrt{1/f}$ with f between 6 to 10 or lower should be applied. In the plot $f = 7$ has been assumed to give a rough estimate. In addition to this, for luminosities $L \lesssim 10^{5.2} L_\odot$ the observed mass loss becomes much lower than the predicted value and the reasons are unclear (see e.g. Muijres et al. 2012 or, for a review, Puls et al. 2008). This so-called weak-wind-problem will be neglected here as it is unknown whether the problem lies in the observations, the models, or both. If we find a discrepancy between observational results and the results of this thesis, this might be a possible cause.

Apparently the datapoints are scattered over a wide region which makes it difficult to make a final statement. However it seems, at least for the presented data, that the model based on Vink et al. (2001) fits the best. Castor et al. (1975b) might also give a good approximation, but the mass loss seems to be too high for smaller masses, especially considering the weak-wind-problem. It is clear that the numbers given need to be treated with caution.

2.5. Age

It is to be expected that the most massive stars do not live as long as the relevant timescale. To take ages into account, I use lifetimes given in Charbonnel et al. (1993) for $Z = 0.004$ and Schaerer et al. (1993) for $Z = 0.008$. These works present the durations of core hydrogen, helium, and carbon burning phases. Since core hydrogen burning is by far the longest phase, only this will be taken into account. To obtain the lifetime for arbitrary (high) masses, the durations have been plotted and fits with the function $t = \frac{c}{m-a} + b$ have been calculated (see Fig. 7).

In order to obtain the best results for the highest masses (and shortest lifetimes), only data points with $m > 10\,M_\odot$ have been taken into account. For $Z = 0.004$ one gets $a = 5.54 \pm 0.10$, $b = 1.911 \pm 0.023$, $c = 107.3 \pm 1.2$ and for $Z = 0.008$ $a = 5.74 \pm 0.16$, $b = 1.83 \pm 0.04$, $c = 103.1 \pm 2.0$. As it can be seen the function fits perfectly for short lifetimes. If the timespan of the estimation does not exceed $\simeq 20\,$Myr, this is a very good approximation; if not the ages of less massive stars will be drastically overestimated and a different fit will be necessary.

3. Calculation of the energy output

3.1. Structure of the given SFH-data

Harris and Zaritsky (2004) give locally resolved data by dividing the SMC into 351 subregions reaching from $0^{\mathrm{h}}\,25^{\mathrm{m}}$, $-74°\,57”$ to $1^{\mathrm{h}}\,16^{\mathrm{m}}$, $-70°\,32”$. This area is separated into 12’×12’ blocks, 23 lines in declination and 20 rows in right ascension. These blocks are

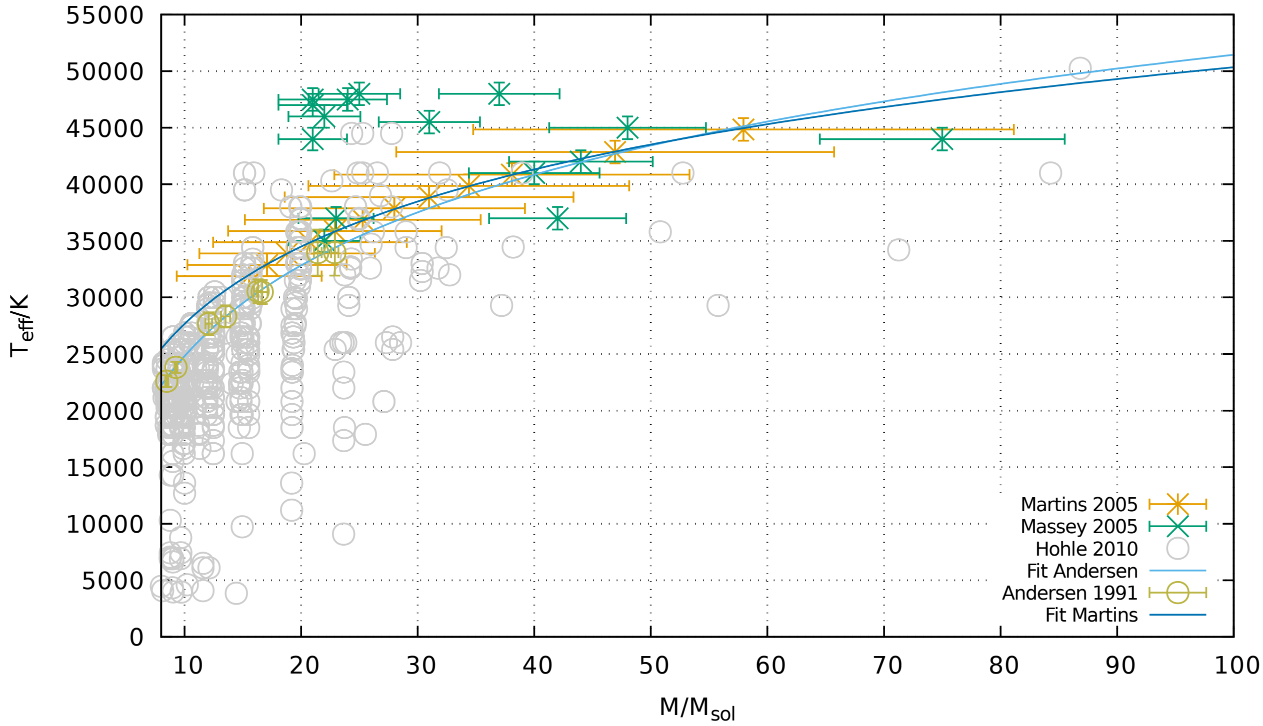

Fig. 5.— Mass-$T_{\rm eff}$ relation data from various sources and fits.

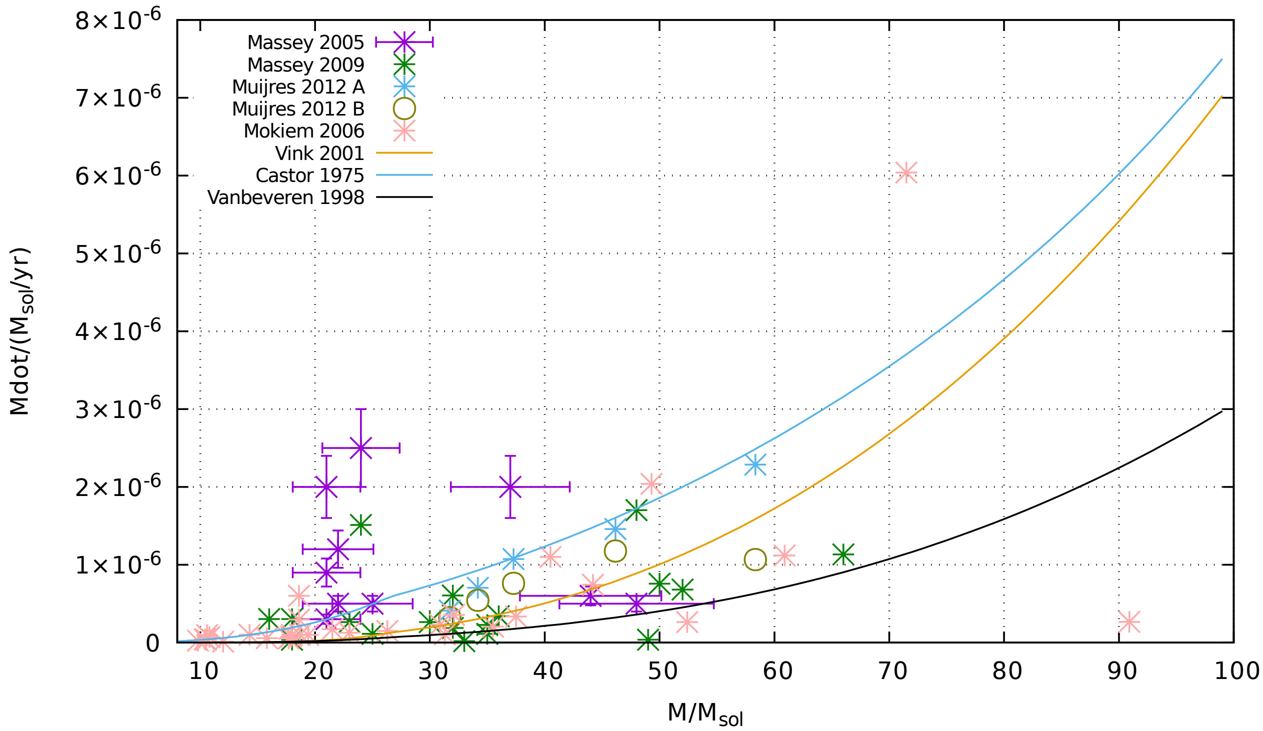

Fig. 6.— Stellar mass loss from various sources, $Z = 0.004$. Clumping correction $f = 7$ for Massey et al. (2009).

identified with a two-letter-code where the first letter denotes right ascension and the second one declination. In my further analysis these will be treated as integers starting from zero (within the program, e.g. A$\mapsto$ 0, E$\mapsto$ 4) or one (in plots and tables, A$\mapsto$ 1, E$\mapsto$ 5). For a conversion table see Tab. 1. It needs to be noted that the right ascension letters increase from right to left (in the direction of right ascension). Some areas have been masked in the original catalogue because of foreground structures (resulting in SFR= 0) and some less densely populated ones had to be combined to get a stable SFH, but this does not affect the data structure.

The time-bins are logarithmically divided into 18 bins ranging from $10^{10.05}$ to $10^{6.6}$ years ago which is less accurate than the given isochrones. This is chosen so that photometric errors of the original data are taken into account; the bin width represents the resolution of the simulation.

Harris and Zaritsky (2004) present data for different metallicities with $Z = 0.001$, $Z = 0.004$, and $Z = 0.008$. They state that there is no need for interpolation with their given dataset. Star formation with $Z = 0.001$ only appeared in the oldest age bins (age > 100 Myr) because of the subsequent chemical enrichment. These low-metallicity data will be neglected since the most massive stars have a much shorter lifetime.

Apart from the best-fit SFR, the lowest and highest realistic SFR are given. These will be used as a basis for error estimation.

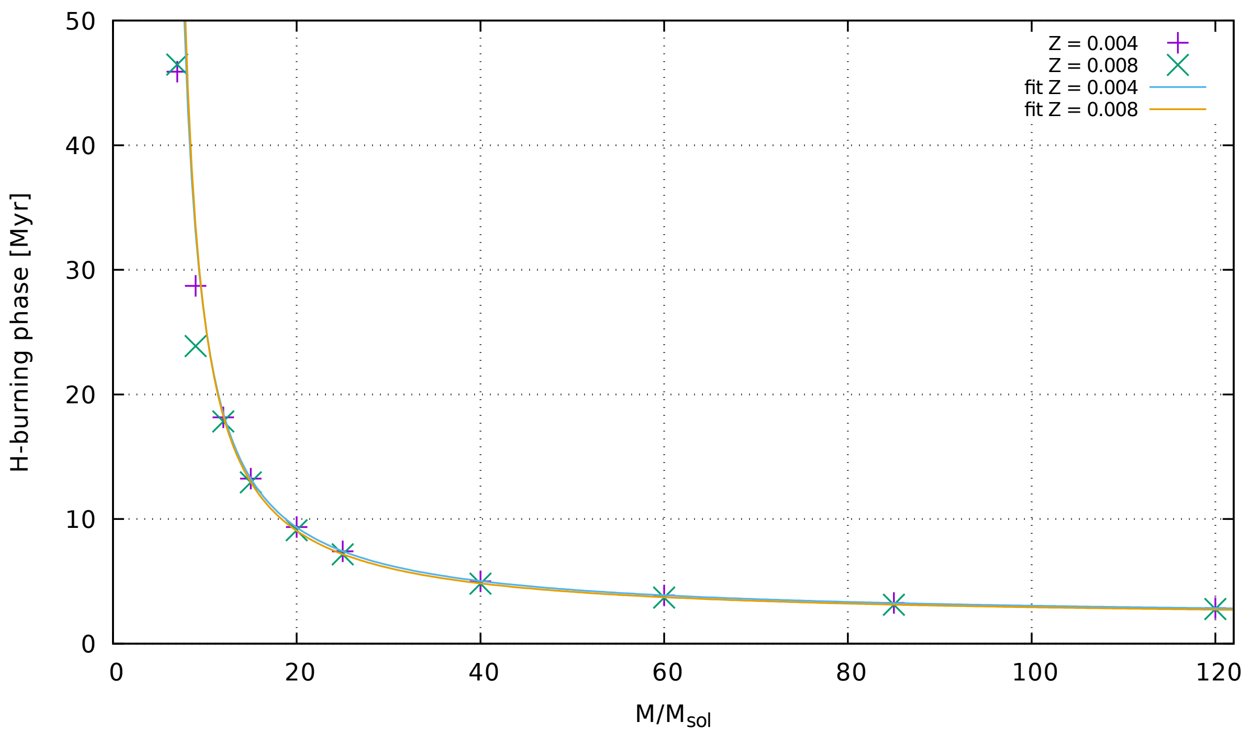

Fig. 7.— Durations of core hydrogen burning and fits; Charbonnel et al. (1993) for $Z = 0.004$ and Schaerer et al. (1993) for $Z = 0.008$.

3.2. Iteration over time and mass

To obtain the energy output of a star, the mechanical wind power

$$P = \frac{1}{2}\dot{m}v_\infty^2 \tag{9}$$

can be used for a simple approximation of the power of stellar winds of a star affecting the ISM (Weaver et al. 1977). Although the actual process is much more complicated, this gives the total kinetic energy lost by the star to the surrounding bubble. One then needs to integrate this input over time for all stars present. Since I use a wide stellar mass distribution given by the IMF, it is also necessary to iterate over mass and calculate the number of stars for each given mass bin. The sum of the output energy for each timestep gives the overall energy provided to the ISM by stars that formed in a certain period.
This calculation, along with all formulas chosen in the last section, has been implemented in C++ in the program ”tableselect”. The full code can be seen in Appendix A and can be compiled with the command `g++ -Wall -o "tableselect" "tableselect.cpp" -std=c++11 -fopenmp` using C++11 and openmp. The relevant function for calculating the output is simStars. When provided with a starting time (`t0`, in Myr), the SFH for one region, a lower and a higher mass limit, whether to use $Z = 0.004$ or $Z = 0.008$ data and whether to use expected (`what=6`), upper (`what=8`) or lower limit SFH (`what=7`), it will iterate over time starting `t0` Myr ago with step size dt. Newly formed stars according to the SFH are introduced in groups in mass bins with width dm (by default set to 1) for each time frame with star formation. For all pre-existing star groups, energy loss is calculated as $E = P \cdot \mathrm{d}t \cdot N$ and added to the variable `energy` which is returned in the end. Additionally, time of formation, lower mass limit of the bin, total lost mass, lost mass in the current step, v_∞ at the current step, L at the current step and expected, lowest and highest possible number of stars is saved for each group at each step. The latter three result from the SFH. If the time passed since formation is longer than the expected lifetime, the group is no longer present in the next step. For details see the code starting from line 414. All data is used in solar units where applicable. A graphical representation is given in fig. 8.

Since all data is saved in the three-dimensional `vector<vector<vector<double>>> all` more detailed analysis can be made by returning this instead of only the energy. Its first index denotes the timestep, the second one a star group at this time and the third one gives access to the parameters of the group in the order mentioned above. Simple changes in the code also make it possible to start the energy integration not at the simulation starting time `t0`, but at another time here called `tstart`. By default it is set to 99999 Myr which is equivalent to an integration over the whole simulated time. Setting it to e.g. 10 Myr with `t0` = 20 Myr would mean that star formation and evolution since 20 Myr ago is calculated, but the returned energy is only the energy emitted in the last 10 Myr.

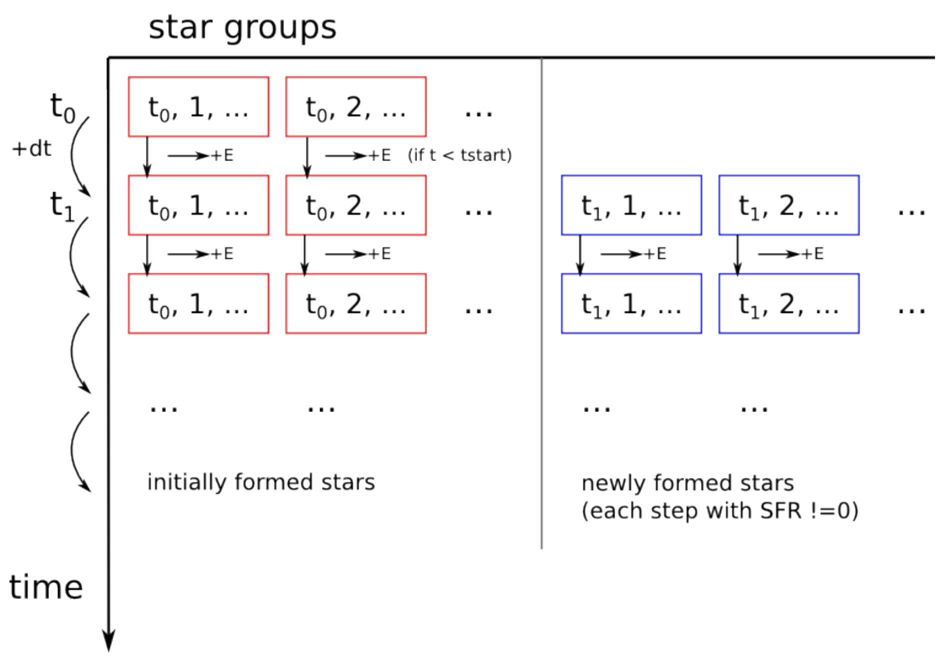

Fig. 8.— Schematic overview of the function simStars. Each coloured rectangle represents a group of stars with time of formation, initial mass and other parameters. In each step, energy output is calculated if the stars have not yet died and if the integration starting time has passed ("+E") and new star groups are added if SFR(t) $\neq 0$ (blue rectangles).

3.3. Maps of energy output

Using the output of simStars for each region and adding all metallicities with the function energyMap, maps of the SMC have been created for various starting times and masses between 10 and 100 $M_\odot$. Here the energy was integrated over the whole simulated time. They are shown in Figs. 9 for expected emission, 10 for the lower limit and 11 for upper limit. The images for `t0` = 29 Myr are actually outside the range in which the stellar age fit gives accurate lifetimes, but is included for an estimate of the effects of longer timescales. The corresponding tables can be found in the appendix starting from Table 2. The table entries are ordered in the same way as the images.
In addition, maps have been created for star formation starting times `t0 =` 20 and 29 Myr where energy integration starts only `tstart =` 10 Myr ago. They are shown in Fig. 12. The tables can be found in the appendix starting from Tab. 20. It can be seen that for these maps different starting times do not make a big difference due to the short lifetimes of the most massive stars. Stars living longer than 10 Myr have masses smaller than 20 $M_\odot$ (Fig. 7) and thus relatively weak winds (Fig. 6). As a result these maps present the sum of the total energy output of stars formed since 10 Myr and 15 Myr ago. This is useful for further analysis: it is not necessary to consider stars formed long time ago if only the energy input in recent times is relevant.

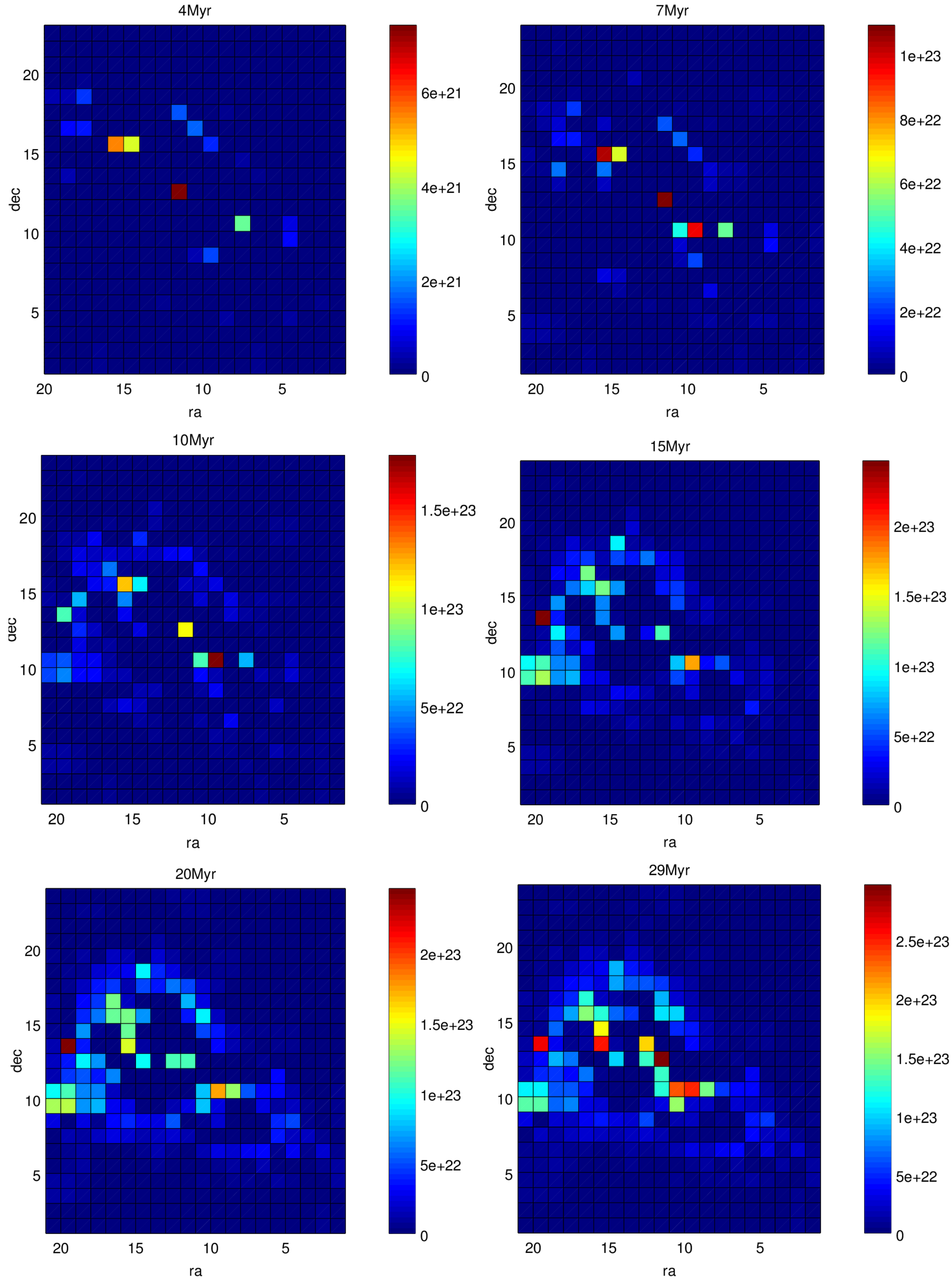

Fig. 9.— Energy output by stars formed in the last t Myr. Energy scale in 10^{30} erg. Corresponding tables 2 to 7, binsize $12' \times 12'$.

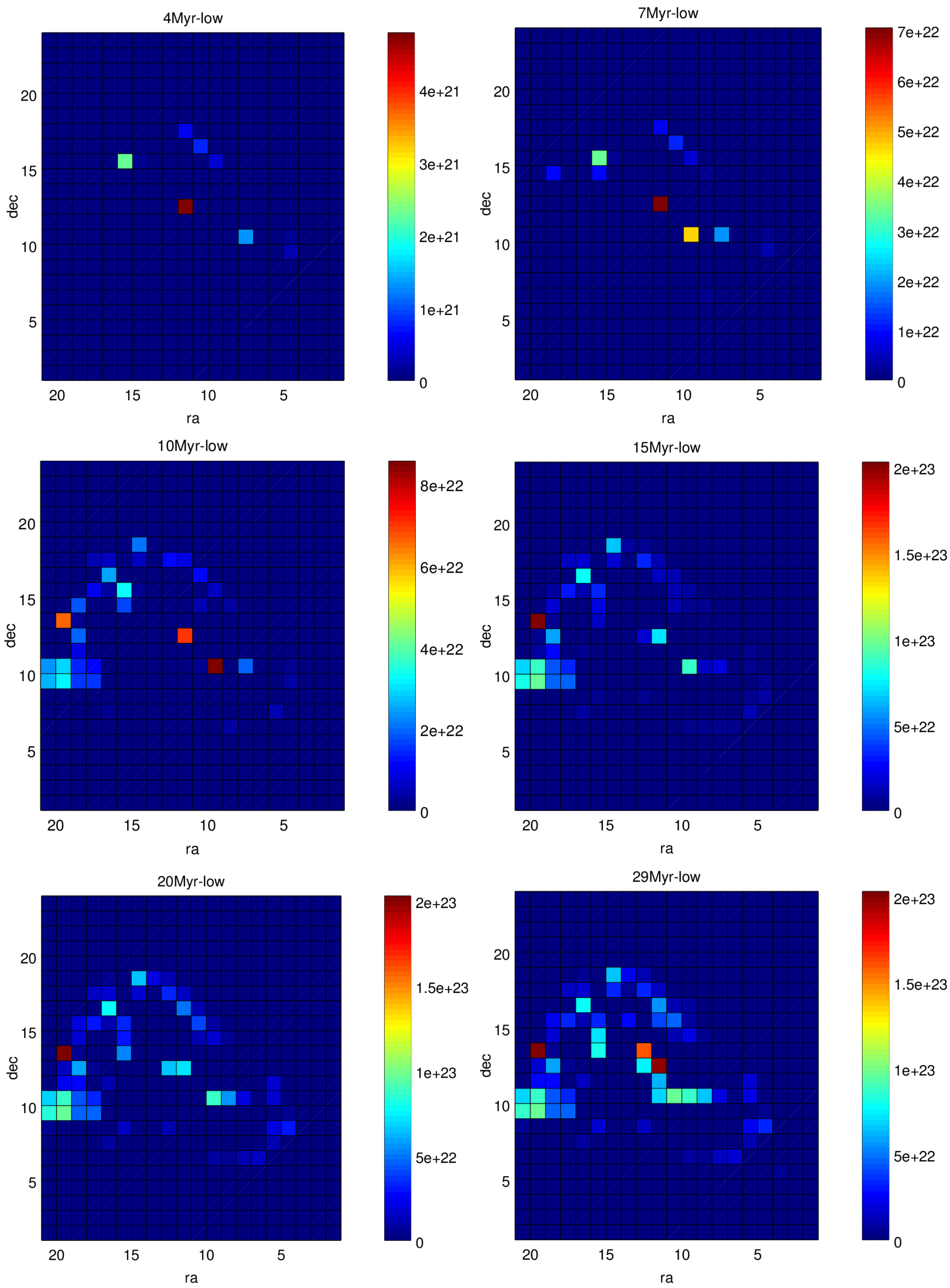

Fig. 10.— Energy output by stars formed in the last t Myr (lower limit of SFH). Energy scale in 10^{30} erg. Corresponding tables 8 to 13, binsize $12' \times 12'$.

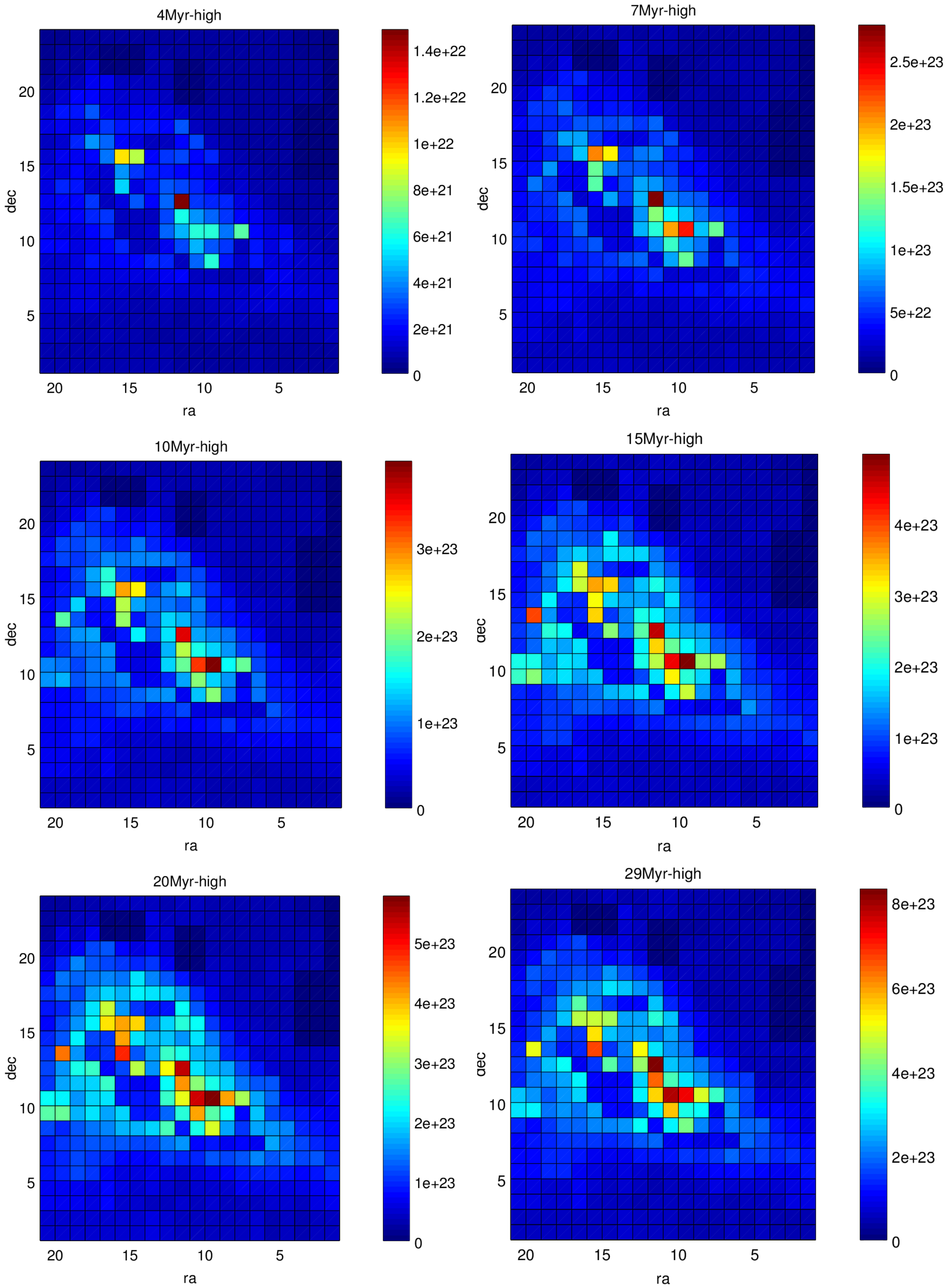

Fig. 11.— Energy output by stars formed in the last t Myr (upper limit of SFH). Energy scale in 10^{30} erg. Corresponding tables 14 to 19, binsize $12' \times 12'$.

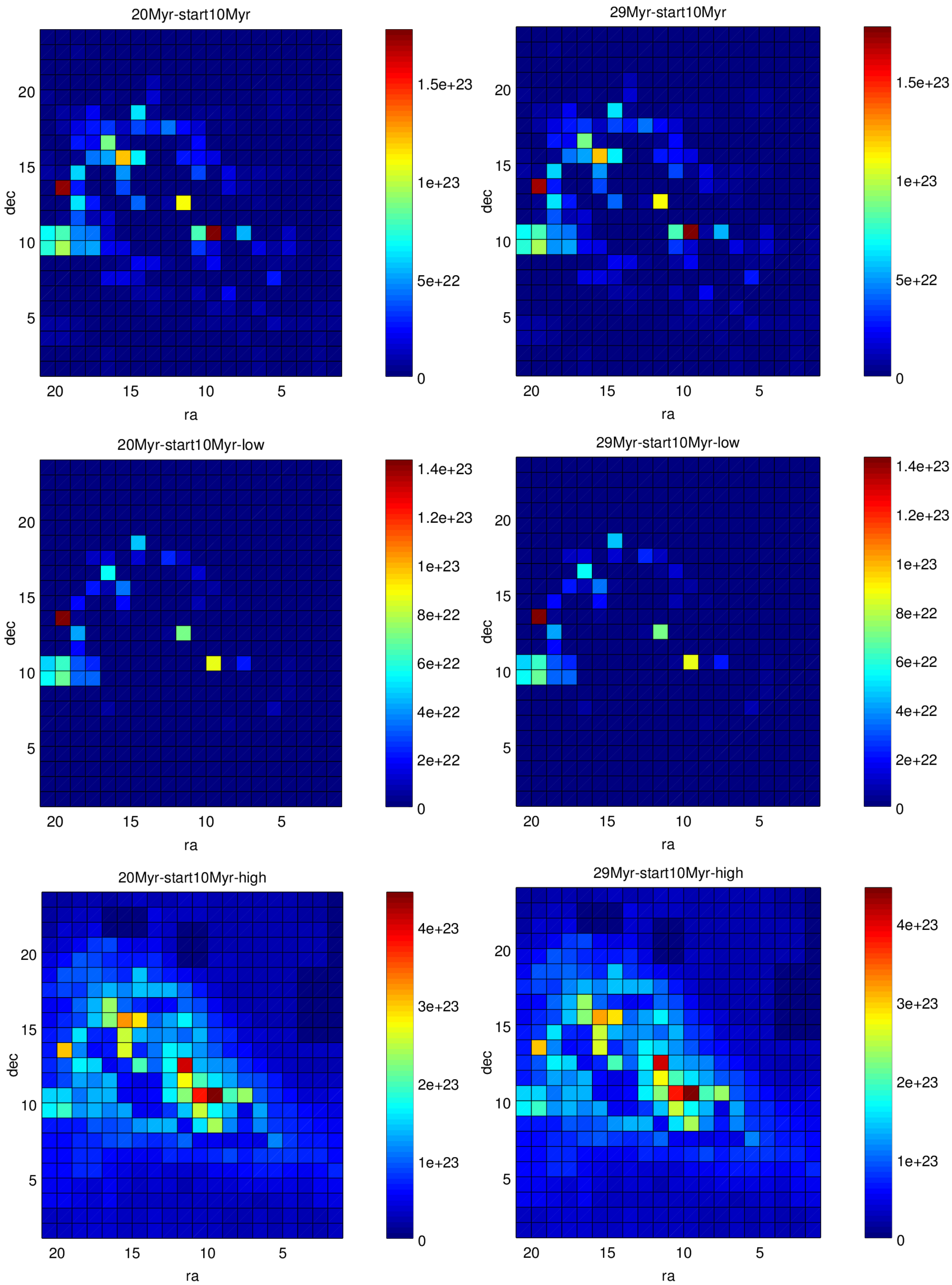

Fig. 12.— Energy emitted in the last 10 Myr by stars formed in the last 20 (left) or 29 Myr (right). Top: expected amount, middle: lower limit, bottom: upper limit. Corresponding tables 20 to 25, binsize $12' \times 12'$.

4. Discussion

4.1. General remarks

The calculated mechanical energy input for each region is of the order 10^{45} (regions with weakest star formation) to 10^{51} erg/arcmin^2 (single strong regions) for the expected SFR. The upper limit SFR is about a factor of 2-3 higher for the regions with maximum energy input and only the masked regions have SFR = 0. The lower limit is about a factor of 1.5 to 2 smaller and less regions contain star formation. As already discussed in Section 2, there are additional uncertainties caused by the rather wide distribution of stellar parameters in the observational data. This applies especially to the mass-loss data, where the problems of weak winds and clumping are not yet resolved. These effects are not included in the error estimation. Nevertheless the variation of expected energy output resulting from this uncertainty should be still within the bounds given by the upper/lower limit data as the uncertainties in SFR are already quite high.
These numbers are comparable to those obtained by Sasaki et al. (2011) for the LMC superbubble N 158. They state an energy input by 67 O- and B-stars of $L_{OB} = 3.4 \cdot 10^{37}\,\frac{\mathrm{erg}}{\mathrm{s}}$ over 1.1 Myr which gives a total energy of $E = 1.18 \cdot 10^{51}$ erg. The same order of magnitude is obtained by Kavanagh et al. (2012) who find an input of $(3.5 \pm 1.7) \cdot 10^{51}$ erg by stellar winds for the LMC superbubble N 206.
Not included in the calculations presented here are effects of supernovae and Wolf-Rayet (WR) stars. Because of the low number and relatively weak winds of WR stars in the SMC (Hainich et al. 2015), their effects may be added manually. In order to take supernovae into account, a "supernova counter" can easily be added to simStars, but would require to change the output data type to e.g. a `vector<double>` or to a string containing energy and the number of supernovae.
The shape of their distribution will be the same as the star formation distribution, but shifted a few Myr in time. For the longer times simulated here the distribution should be roughly the same as in Fig. 9.

4.2. Comparison to available data

The calculated energy maps can be compared to X-Ray, Hα and B-band Digitized Sky Survey data. For this purpose, the regions as mentioned in sec. 3.1, an approximate outline of the SMC and the regions of highest energy output have been marked in green, red and yellow, respectively. More precisely, all regions with an output of more than 10^{53} erg by stars formed in the last 29 Myr are marked yellow. Additionally, high mass X-ray binaries (HMXB) listed in Sturm et al. (2013) and SNRs listed in Badenes et al. (2010) have been added. HMXBs are close binary systems where a compact object (e.g. a neutron stars or black hole) accretes mass from a massive companion star which produces X-ray emission. Because of the high mass of the companion, these systems need to be relatively young. SNRs are visible for about 10^5 yr after the explosion through a shockwave of ejected material. HMXBs and SNRs should follow the distribution of the SFR with an offset of a few Myr and directly contribute to the X-ray emission as point-sources. This means their distribution should correlate with the calculated maps of this thesis. The resulting maps can be seen in Fig. 13 and a selection of energy maps with the contours added in Fig. 14.

Apparently the energy output in the timescale up to 29 Myr does not correlate with the X-ray emission. However, the southwestern yellow region fits with the marked point-sources, the Hα emission and the stellar population. The same holds for the southeastern square.
The northern part of the central northern yellow region correlates both with X-Ray and Hα emission and the energy maps show that in the last 10 Myr the energy output here was significant. It can be mentioned that NGC 346 is clearly visible in the Hα data directly right to the yellow border, but not part of the yellow region. In the top and middle rows of Fig. 14 it is however distinguishable in region (14,15). Since this it is not strongly expressed in the bottom row for which the yellow region was defined it is not marked, but still present in the energy maps.
The single eastern yellow square does not fit with any other data, but has a high value in all energy maps starting at least 10 Myr ago, including the lower limit maps. Since it is only a single region, it is possible, that it is an artefact in the SFH data. Otherwise at least a significant stellar population would be expected here.
The northwestern rectangle lies in an area where both weak Hα emission and few stars are present, but not more than in its neighbouring regions. Comparing to the energy maps, the output here was not as high as in the other yellow regions and the adjacent regions have only slightly smaller values. It is rather part of a ring-like structure around the inner border of the whole red region which is not present in the other data.

In general, the X-ray emitting regions seem to be shifted to the northwest compared to the stellar distribution. The shape of the emission looks similar to a shifted version of the star formation 2.5 Gyr ago and slightly correlates with the SFR 40 Myr ago as can be seen in Fig. 15, but the lack of X-ray emission in the southern half of the grid remains hard to explain. It is possible that a major part of the apparently diffuse emission stems from unresolved older point-sources from between 40 Myr and 2.5 Gyr ago. A similar result has been found for the Galactic X-ray ridge emission (Revnivtsev et al. 2009): the apparently diffuse emission likely is produced by unresolved soft sources such as accreting white dwarfs in binary systems, binary stars with coronal activity and coronally active Sun-like stars that are too faint to be resolved. However for the Galactic case, the X-ray emission is correlated to the stellar distribution (Revnivtsev et al. 2006) which is not the case here and a much broader distribution would be expected. Additionally, there might still be truly diffuse emission, but to make a final statement a deeper understanding of the properties of the SMC gas such as its dynamics, magnetic fields and tidal forces by interactions with the LMC and the Milky Way would be required.
In contrast, the distribution of the younger point-sources fits well with the distribution of

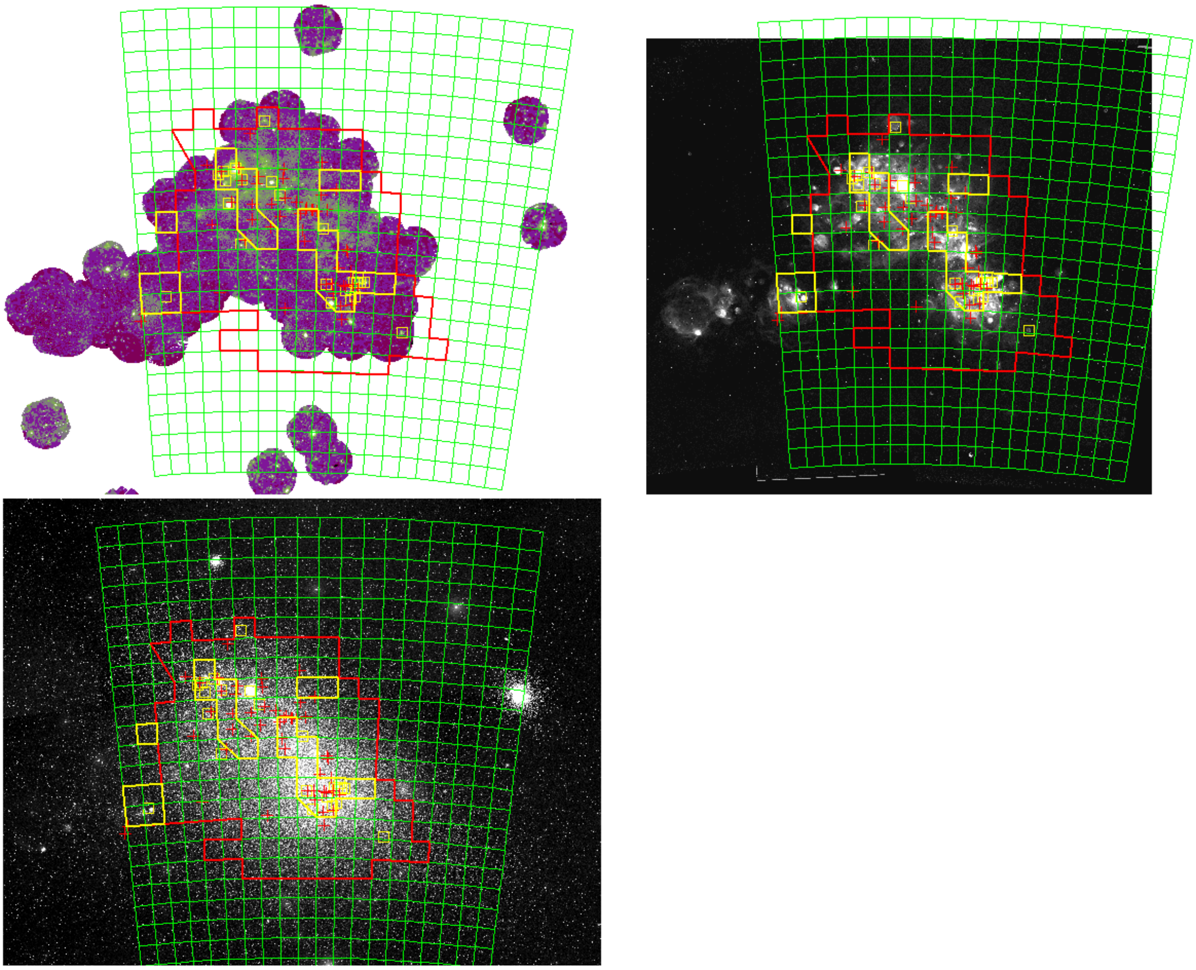

Fig. 13.— SMC in different datasets. Top left: XMM-Newton data by Haberl et al. (2012), Top right: Hα view by the Magellanic Cloud Emission Line Survey (MCELS, Smith et al. 2005), Bottom: Digitized Sky Survey B-band. Red Crosses: high mass X-ray binaries (Sturm et al. 2013), yellow boxes: supernova remnants (Badenes et al. 2010), green grid: region borders in SFH data. Red region marks approximate outline of SMC in energy maps, yellow line marks regions with highest energy output in energy maps.

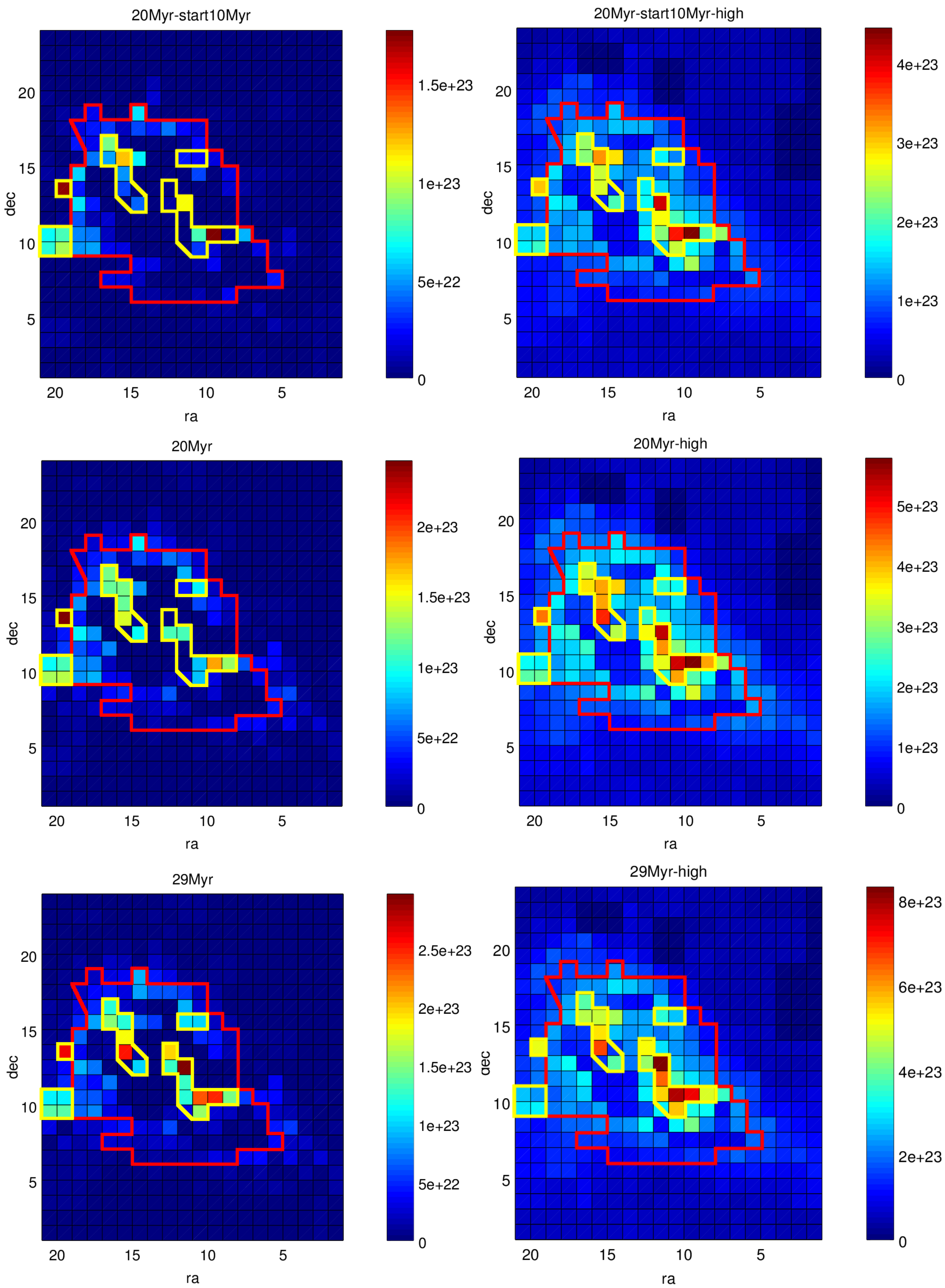

Fig. 14.— Energy emitted in 10^{30} erg in the last t Myr by stars formed in the last 20 Myr (top `tstart` = 10 Myr, middle `tstart` = `t0`) or 29 Myr (bottom). Left: expected SFR, right: upper limit SFR. Red line denotes approximate contours of SMC, yellow line denotes regions with highest output.

stars and, in the southern yellow region, with the calculated energy output. This correlation is not surprising: a high recent SFR should be visible in the data calculated here, the stellar population and in the young X-ray sources. It is a problem that this only holds in the southern part of the SMC where there is a lack of X-ray emission. The exact origin of the diffuse X-ray emission thus remains unclear and requires further study.

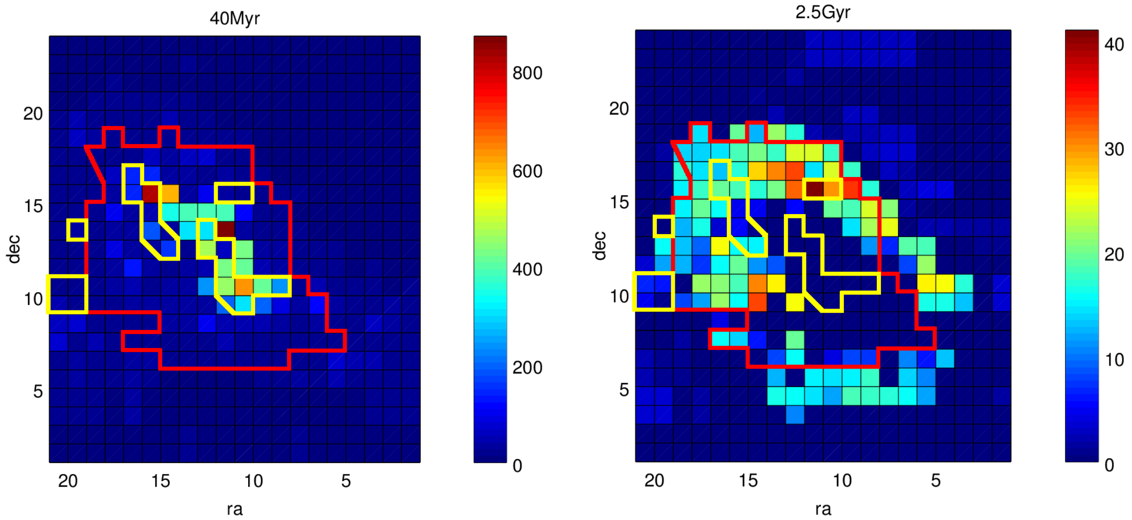

Fig. 15.— SFR [1/Myr] for stars with mass $10\,M_{\odot} < m < 100\,M_{\odot}$ in the SFH-bins 40 Myr (left) and 2.5 Gyr ago (right).

5. Summary

The energy output by stellar winds of massive stars into the ISM in the SMC has been calculated to be $10^{45} - 10^{51}$ erg/arcmin^2 depending on the 12'×12'-region. This was based on the SFH by Harris and Zaritsky (2004). They used a Salpeter slope IMF and Padua isochrones by Girardi et al. (2002) and the $m_V \leq 21$ stars in the Zaritsky et al. (2002) catalogue. Relations for calculating luminosity, effective temperature, stellar radius, mass-loss rate and stellar ages from stellar mass and metallicity have been derived. A MLR was obtained by power-law fits of the function $L/L_{\odot} = a \cdot (m/M_{\odot})^b$ to data by Andersen (1991) for lower masses and Martins et al. (2005) for higher masses. Logarithmic mass-temperature and mass-radius relations from fits of the shape $x = a\log(m/M_{\odot}) + b$ to the same data were used. The theoretical stellar mass-loss-rate by Vink et al. (2001) was chosen, but here both observational and theoretical uncertainties are higher and other theoretical predictions might also give correct estimates. Stellar ages based on the core hydrogen burning times in Charbonnel et al. (1993) for $Z = 0.004$ and Schaerer et al. (1993) for $Z = 0.008$ are used. Fits of the function $t = \frac{c}{m-a} + b$ for initial masses $m > 10\,M_{\odot}$ are calculated and give accurate estimates for ages $t \lesssim 20$ Myr. For simulations of longer timescales a combination of two fit functions would be more accurate. Output by Wolf-Rayet stars and supernovae has not been considered, but should follow the same distribution as stellar winds. Errors are based on the

SFH-errors given by Harris and Zaritsky (2004); the errors resulting from uncertainties in mass-parameter-relations for the expected SFR should lie within these borders.
The final results have been obtained by integrating over the total wind power of one star $P = \frac{1}{2}\dot{m}v_\infty^2$ for 0.1 Myr timesteps and $1\,M_\odot$ massbins and multiplying with the estimated amount of stars in each age- and mass-group. The obtained energy output by stellar winds does not seem to correlate with the SMC X-ray emission distribution and correlates with Hα, stellar distribution, and point-source distribution mainly in the southern part of the SMC. The X-ray distribution roughly follows the SFR 2.5 Gyr to 40 Myr ago in the northern part of the SMC. Thus a possible origin for the diffuse emission are unresolved old point-sources like in the Galactic X-ray ridge emission such as accreting white dwarfs and coronally active binaries (Revnivtsev et al. 2009). Since the X-ray emission does not follow the stellar distribution like in the Galaxy, this solution is problematic.

REFERENCES

Abbott, D. C. (1982). The return of mass and energy to the interstellar medium by winds from early-type stars. *ApJ*, 263:723–735.

Allen, C. W. (1973). *Astrophysical quantities.*

Andersen, J. (1991). Accurate masses and radii of normal stars. *A&A Rev.*, 3:91–126.

Asplund, M., Grevesse, N., Sauval, A. J., and Scott, P. (2009). The Chemical Composition of the Sun. *ARA&A*, 47:481–522.

Badenes, C., Maoz, D., and Draine, B. T. (2010). On the size distribution of supernova remnants in the Magellanic Clouds. *MNRAS*, 407:1301–1313.

Bastian, N., Covey, K. R., and Meyer, M. R. (2010). A Universal Stellar Initial Mass Function? A Critical Look at Variations. *ARA&A*, 48:339–389.

Basu, S. and Antia, H. M. (2004). Constraining Solar Abundances Using Helioseismology. *ApJ*, 606:L85–L88.

Castor, J., McCray, R., and Weaver, R. (1975a). Interstellar bubbles. *ApJ*, 200:L107–L110.

Castor, J. I., Abbott, D. C., and Klein, R. I. (1975b). Radiation-driven winds in Of stars. *ApJ*, 195:157–174.

Charbonnel, C., Meynet, G., Maeder, A., Schaller, G., and Schaerer, D. (1993). Grids of Stellar Models - Part Three - from 0.8 to 120-SOLAR-MASSES at Z=0.004. *A&AS*, 101:415.

de Jager, C. (1980). The brightest stars. *Geophysics and Astrophysics Monographs*, 19.

Girardi, L., Bertelli, G., Bressan, A., Chiosi, C., Groenewegen, M. A. T., Marigo, P., Salasnich, B., and Weiss, A. (2002). Theoretical isochrones in several photometric systems. I. Johnson-Cousins-Glass, HST/WFPC2, HST/NICMOS, Washington, and ESO Imaging Survey filter sets. *A&A*, 391:195–212.

Haberl, F., Sturm, R., Ballet, J., Bomans, D. J., Buckley, D. A. H., Coe, M. J., Corbet, R., Ehle, M., Filipovic, M. D., Gilfanov, M., Hatzidimitriou, D., La Palombara, N., Mereghetti, S., Pietsch, W., Snowden, S., and Tiengo, A. (2012). The XMM-Newton survey of the Small Magellanic Cloud. *A&A*, 545:A128.

Hainich, R., Pasemann, D., Todt, H., Shenar, T., Sander, A., and Hamann, W.-R. (2015). Wolf-Rayet stars in the Small Magellanic Cloud. I. Analysis of the single WN stars. *A&A*, 581:A21.

Harris, J. and Zaritsky, D. (2004). The Star Formation History of the Small Magellanic Cloud. *AJ*, 127:1531–1544.

Hilditch, R. W., Howarth, I. D., and Harries, T. J. (2005). Forty eclipsing binaries in the Small Magellanic Cloud: fundamental parameters and Cloud distance. *MNRAS*, 357:304–324.

Hohle, M. M., Neuhäuser, R., and Schutz, B. F. (2010). Masses and luminosities of O- and B-type stars and red supergiants. *Astronomische Nachrichten*, 331:349.

Kavanagh, P. J., Sasaki, M., and Points, S. D. (2012). XMM-Newton view of the N 206 superbubble in the Large Magellanic Cloud. *A&A*, 547:A19.

Lamers, H. J. G. L. M. and Leitherer, C. (1993). What are the mass-loss rates of O stars? *ApJ*, 412:771–791.

Leitherer, C., Robert, C., and Drissen, L. (1992). Deposition of mass, momentum, and energy by massive stars into the interstellar medium. *ApJ*, 401:596–617.

Martins, F., Schaerer, D., and Hillier, D. J. (2005). A new calibration of stellar parameters of Galactic O stars. *A&A*, 436:1049–1065.

Massey, P. (2003). MASSIVE STARS IN THE LOCAL GROUP: Implications for Stellar Evolution and Star Formation. *ARA&A*, 41:15–56.

Massey, P., Puls, J., Pauldrach, A. W. A., Bresolin, F., Kudritzki, R. P., and Simon, T. (2005). The Physical Properties and Effective Temperature Scale of O-Type Stars as a Function of Metallicity. II. Analysis of 20 More Magellanic Cloud Stars and Results from the Complete Sample. *ApJ*, 627:477–519.

Massey, P., Zangari, A. M., Morrell, N. I., Puls, J., DeGioia-Eastwood, K., Bresolin, F., and Kudritzki, R.-P. (2009). The Physical Properties and Effective Temperature Scale of O-Type Stars as a Function of Metallicity. III. More Results From the Magellanic Clouds. *ApJ*, 692:618–652.

McKee, C. F. and Ostriker, J. P. (1977). A theory of the interstellar medium - Three components regulated by supernova explosions in an inhomogeneous substrate. *ApJ*, 218:148–169.

Mineo, S., Gilfanov, M., and Sunyaev, R. (2012). X-ray emission from star-forming galaxies - II. Hot interstellarmedium. *MNRAS*, 426:1870–1883.

Mokiem, M. R., de Koter, A., Evans, C. J., Puls, J., Smartt, S. J., Crowther, P. A., Herrero, A., Langer, N., Lennon, D. J., Najarro, F., Villamariz, M. R., and Yoon, S.-C. (2006). The VLT-FLAMES survey of massive stars: mass loss and rotation of early-type stars in the SMC. *A&A*, 456:1131–1151.

Muijres, L. E., Vink, J. S., de Koter, A., Müller, P. E., and Langer, N. (2012). Predictions for mass-loss rates and terminal wind velocities of massive O-type stars. *A&A*, 537:A37.

Nadyozhin, D. K. and Razinkova, T. L. (2005). Similarity Theory of Stellar Models and the Structure of Very Massive Stars. *Astronomy Letters*, 31:695–705.

Puls, J., Vink, J. S., and Najarro, F. (2008). Mass loss from hot massive stars. *A&A Rev.*, 16:209–325.

Revnivtsev, M., Sazonov, S., Churazov, E., Forman, W., Vikhlinin, A., and Sunyaev, R. (2009). Discrete sources as the origin of the Galactic X-ray ridge emission. *Nature*, 458:1142–1144.

Revnivtsev, M., Sazonov, S., Gilfanov, M., Churazov, E., and Sunyaev, R. (2006). Origin of the Galactic ridge X-ray emission. *A&A*, 452:169–178.

Russell, S. C. and Dopita, M. A. (1992). Abundances of the heavy elements in the Magellanic Clouds. III - Interpretation of results. *ApJ*, 384:508–522.

Sabbi, E., Sirianni, M., Nota, A., Tosi, M., Gallagher, J., Smith, L. J., Angeretti, L., Meixner, M., Oey, M. S., Walterbos, R., and Pasquali, A. (2008). The Stellar Mass Distribution in the Giant Star Forming Region NGC 346. *AJ*, 135:173–181.

Salpeter, E. E. (1955). The Luminosity Function and Stellar Evolution. *ApJ*, 121:161.

Sasaki, M., Breitschwerdt, D., Baumgartner, V., and Haberl, F. (2011). XMM-Newton observations of the superbubble in N 158 in the LMC. *A&A*, 528:A136.

Schaerer, D., Meynet, G., Maeder, A., and Schaller, G. (1993). Grids of stellar models. II - From 0.8 to 120 solar masses at Z = 0.008. *A&AS*, 98:523–527.

Schmalzl, M., Gouliermis, D. A., Dolphin, A. E., and Henning, T. (2008). The Initial Mass Function of the Stellar Association NGC 602 in the Small Magellanic Cloud with Hubble Space Telescope ACS Observations. *ApJ*, 681:290–302.

Sirianni, M., Nota, A., De Marchi, G., Leitherer, C., and Clampin, M. (2002). The Low End of the Initial Mass Function in Young Clusters. II. Evidence for Primordial Mass Segregation in NGC 330 in the Small Magellanic Cloud. *ApJ*, 579:275–288.

Smith, R. C., Points, S. D., Chu, Y.-H., Winkler, P. F., Aguilera, C., Leiton, R., and MCELS Team (2005). The Magellanic Emission Line Survey (MCELS). In *American Astronomical Society Meeting Abstracts*, volume 37 of *Bulletin of the American Astronomical Society*, page 1200.

Sturm, R. (2012). *An X-ray investigation of the Small Magellanic Cloud with XMM-Newton*. Dissertation, Technische Universität München, München.

Sturm, R. and Haberl, F. (2014). The diffuse X-ray emission of the Small Magellanic Cloud. In *The X-ray Universe 2014*, page 191.

Sturm, R., Haberl, F., Pietsch, W., Ballet, J., Hatzidimitriou, D., Buckley, D. A. H., Coe, M., Ehle, M., Filipović, M. D., La Palombara, N., and Tiengo, A. (2013). The XMM-Newton survey of the Small Magellanic Cloud: The X-ray point-source catalogue. *A&A*, 558:A3.

Svechnikov, M. A. (1969). Catalogue of orbital elements, masses and luminosities of close binary systems. *Uch. zap. Ural'skogo un-ta, No. 88, 178 p.*, 88.

Svechnikov, M. A. and Kuznetsova, E. F. (1990). *Katalog priblizhennykh fotometricheskikh i absoliutnykh elementov zatmennykh peremennykh zvezd.*

Vanbeveren, D., De Loore, C., and Van Rensbergen, W. (1998). Massive stars. *A&A Rev.*, 9:63–152.

Vink, J. S., de Koter, A., and Lamers, H. J. G. L. M. (2000). New theoretical mass-loss rates of O and B stars. *A&A*, 362:295–309.

Vink, J. S., de Koter, A., and Lamers, H. J. G. L. M. (2001). Mass-loss predictions for O and B stars as a function of metallicity. *A&A*, 369:574–588.

Vitrichenko, E. A., Nadyozhin, D. K., and Razinkova, T. L. (2007). Mass-luminosity relation for massive stars. *Astronomy Letters*, 33:251–258.

Weaver, R., McCray, R., Castor, J., Shapiro, P., and Moore, R. (1977). Interstellar bubbles. II - Structure and evolution. *ApJ*, 218:377–395.

Zaritsky, D., Harris, J., Thompson, I. B., Grebel, E. K., and Massey, P. (2002). The Magellanic Clouds Photometric Survey: The Small Magellanic Cloud Stellar Catalog and Extinction Map. *AJ*, 123:855–872.

Zombeck, M. (2007). *Handbook of Space Astronomy and Astrophysics: Third Edition*. Cambridge University Press.

This manuscript was prepared with the AAS LaTeX macros v5.2.

A. C++ source code

```
#include <fstream>
#include <vector>
#include <iostream>
//#include <numeric>  // fuer partial_sum
#include <cmath>
#include <chrono>
#include <sstream>
#include <stdint.h>
#include <ccfits>

using namespace CCfits;
using namespace std;

double startM = 2; //for normalisation
double endM = 100;

double c = 3e8; //m/s
double pi = 3.141592654;
double G = 1.327e20; // m^3/Msol/s^2
double Lsol = 3.86e26; //W
double SB = 5.6704e-8; //Stefan-Boltzmann-constant, W*m^-2*K^-4
double mp = 1.67262e-27; //kg
double sT = 6.652459e-29; //m^2
double a = 2.6; //for mdot,vinf
double Ys = 0.2485; //solar He-mass fraction

vector<vector<double>> readdat(string area) //Reads SFH of area of
    table2_harriszaritsky.txt
{
    ifstream ifs ("table2_harriszaritsky.txt");
  vector<vector<double>> table;
  vector<double> sammel;
  vector<double> leer;
  string str;
  string ar = "";
  double num;
  int lcount = 0;
  char c;

    while (!ifs.eof())
    {
    c = ifs.get();
    lcount++;
      if (lcount == 1) ar = c;
    else if (lcount  == 2)
    {
      ar = ar + c;
    }
    else if (lcount  == 5 && !(ar.compare(area)))
```

```
    {
      str = str + c;
      sammel.push_back(stod(str));
      str ="";
    }
    else if (lcount == 8 && !(ar.compare(area)))
    {
      str = str + c;
      sammel.push_back(stod(str));
      str ="";
    }
    else if (lcount == 12 && !(ar.compare(area)))
    {
      str = str + c;
      sammel.push_back(stod(str));
      str ="";
    }
    else if (lcount == 15 && !(ar.compare(area)))
    {
      str = str + c;
      sammel.push_back(stod(str));
      str ="";
    }
    else if (lcount == 21 && !(ar.compare(area)))
    {
      str = str + c;
      sammel.push_back(stod(str));
      str ="";
    }
    else if (lcount == 28 && !(ar.compare(area)))
    {
      str = str + c;
      sammel.push_back(stod(str));
      str ="";
    }
    else if (lcount == 34 && !(ar.compare(area)))
    {
      str = str + c;
      sammel.push_back(stod(str));
      str ="";
    }
    else if (lcount == 40 && !(ar.compare(area)))
    {
      str = str + c;
      sammel.push_back(stod(str));
      str ="";
    }
    else if (lcount == 46 && !(ar.compare(area)))
    {
      str = str + c;
```

```
        sammel.push_back(stod(str));
        str ="";
      }
      else if (lcount  == 53 && !(ar.compare(area)))
      {
        str = str + c;
        sammel.push_back(stod(str));
        str ="";
      }
      else if (lcount  == 60 && !(ar.compare(area)))
      {
        str = str + c;
        sammel.push_back(stod(str));
        str ="";
      }
      else if (lcount == 67 && !(ar.compare(area)))
          {

        str = str + c;
        //cout << str << endl;
              sammel.push_back(stod(str));
              table.push_back(sammel);
              sammel = leer;
              str = "";
          }
      else if(c == '\n')
      {
        lcount = 0;
        str = "";
      }
      else if (lcount > 67) num++;
      else if (!(ar.compare(area)))
      {
        str = str + c;
      }
      else if (table.size()==18)
      {
        break;
      }

    }
    ifs.close();

      return table;
}

void printtable(string name, string description, int jstart, vector<vector<
    double>> tab, bool mapstyle) //Prints table starting from column j
{//mapstyle: if true, last line and column is repeated for easier plotting
    ofstream ofs(name);
```

```
    ofs << description << endl;
    if(!mapstyle)
    {
        for(uint_fast8_t i=0;i<tab.size();i++)
        {
            for(uint_fast8_t j=jstart;j<tab.at(i).size();j++){
                ofs << tab.at(i).at(j) << " ";}
            ofs << endl;
        }
    }
    else
    {
        for(uint_fast8_t i=0;i<tab.size();i++)
        {
            for(uint_fast8_t j=jstart;j<tab.at(i).size();j++){
                ofs << tab.at(i).at(j) << " ";
                }

            ofs << tab.at(i).at(tab.at(i).size()-1) << endl; //repeat last entry
        }
        for(uint_fast8_t j=jstart;j<tab.at(0).size();j++)
        {
            ofs << tab.at(tab.size()-1).at(j) << " "; //repeat last line
        }

        ofs << tab.at(tab.size()-1).at(tab.at(0).size()-1) << endl; //last entry
    }
   ofs.close();
}

void printLatextable(string name, vector<vector<double>> tab) //Prints latex
    format table
{
    ofstream ofs(name);

    for(uint_fast8_t i=0;i<tab.size();i++)
    {
        ofs.precision(2); //numper of decimals
        ofs << i+1 << " & "; //line numbers (enter column numbers in latex
    directly)
        for(uint_fast8_t j=0;j<tab.at(i).size()-1;j++)
        {
            ofs << scientific << tab.at(i).at(j) << " & ";
        }
        ofs << tab.at(i).at(tab.at(i).size()-1) << "\\\\" << endl;
    }

   ofs.close();
}
```

```
void printLatextableFlipped(string name, vector<vector<double>> tab) //Prints latex format table flipped to represent the actual location
{
    ofstream ofs(name);

    for(uint_fast8_t i=0;i<tab.at(0).size();i++)
    {
        ofs.precision(2); //numper of decimals
        ofs << tab.at(0).size()-i << " & "; //line numbers (enter column numbers in latex directly)
        //cout << tab.at(0).size()-i << endl;
        for(uint_fast8_t j=0;j<tab.size()-1;j++)
        {
            ofs << scientific << tab.at(tab.size()-1-j).at(tab.at(0).size()-i-1) << " & ";
            //cout << tab.size()-1-j << " " << tab.at(0).size()-i-1 << endl;
        }
        //ofs << tab.at(tab.size()-1).at(i) << "\\\\" << endl;
        ofs << tab.at(0).at(tab.at(0).size()-i-1) << "\\\\" << endl;
    }

  ofs.close();
}

double getRekt(int i){ //Ra in map in min, A <> i=0
    double R0 = 25;
    double Rekt = R0+51./19.*i;
    return Rekt;
}

double getDec(int j){  //Dec in map in deg, A <> j=0
    double D0 = -74.-57./60.;
    double Dec = D0+j*12.05/60;
    return Dec;
}

void plotmap(string name, string description, vector<vector<double>> tab) //Prints Ra, Dec, value for given map-shaped table
{
    ofstream ofs(name);
    ofs << description << endl;
    for(uint_fast8_t i=0;i<tab.size();i++)
    {
    for(uint_fast8_t j=0;j<tab.at(i).size();j++){
      ofs << i << " " << j << " " << tab.at(i).at(j) << endl;}
  }
  ofs.close();
}
```

```
double getNfromC(double low, double high, double c) //Number of stars in mass
    interval from low to high
{
    return c/1.35*(pow(low,-1.35)-pow(high,-1.35));
}

double getc(double M) //Normalisation constant
{
    double a = (pow(startM,-0.35) - pow(endM,-0.35))/0.35;
    return M/a;
}



double getTfit(double m) //Temperatur from fit: low mass Andersen, high mass
    Martins
{
    double g = 11568, h = -1826, gm = 9848, hm = 4986;
    double mg = exp((hm-h)/(g-gm));
    if(m<mg) return g*log(m)+h;
    else return gm*log(m)+hm;
}

double getTMartins(double m)  //Logarithm over Martins 2005
{
    return 9850*log(m) + 4990;
}

double getTall(double m)  //Logarithm over Martins + Massey 2005
{
    return 4900*log(m)+24000;
}

double getT(double m)  //Enter chosen T
{
    return getTfit(m);
}


double getR(double m)//Logarithm over Martins 2005. Anderssen 1991, Massey 2005
{
    return 4.6*log(m)-5.5; //R_sol
}


double getLVit2007(double m) //Vitrichenko 2007
{
    return 19*pow(m,2.76);
}
```

```
double getLNR2005(double m, double Z) // Nadyozhin & Razinkova 2005
{
  double mu = 1/(2*(1-Z-Ys)+0.75*Ys+0.5*Z);
    //double mu = 0.618; //solar value
    cout << mu << endl;
  double mu2m = pow(mu,2)*m;
  //cout << mu2m << endl;
  double lmu2m = log10(mu2m);
  double l = 1;
  if(mu2m <= 2.4) l = 0.00157*pow(mu2m,3);
  else if (mu2m < 100) l = pow(10,-2.907029 + 3.552793*lmu2m - 0.7717945*pow(
   lmu2m,2) + 0.078623*pow(lmu2m,3));
  else l = mu2m*(1-4.5/sqrt(mu2m));

  return l/(1.5426e-5 *pow(mu,2)*(1+1-Z-Ys));
    //return l/(1.5426e-5 *pow(mu,2)*(1+1-0.02-Ys));
}

double getLfit(double m) //Fit over Andersen 1992 for low masses, Martins 2005
    for high masses
{
  double c = 257, d = 1.948, c2 = 9, d2 = 2.97;
  double mg = pow(c/c2,1/(d2-d));
  if(m<mg) return c2*pow(m,d2);
  else return c*pow(m,d);
}

double getL(double m, double Z)  //Enter chosen L
{
  return getLfit(m);
}

double getVinf(double m, double Z) //in m/s, Castor 1975
{
    double R = getR(m)*6.96342e8;
    double Ledd = 3.2e4*m; //Lsol
    double gamma = getL(m,Z)/Ledd;
    //cout << "R= " << R << endl;
    double corr = pow(Z/0.02,0.15);
    if(gamma<1) return a*sqrt(2*G*m/R*(1-gamma))*corr;
    else
    {
        cout << "rumms" << endl;
        return 1;
    }
}


double getMassLossRateVink(double m, double Z)
{
```

```
    double L = getL(m,Z);
    double T = getT(m);

    double se; //Thomson cross-section, Lamers & Leitherer 1993
    if(T>35000) se = 0.34;
    else if(T>30000) se = 0.32;
    else se = 0.31;

    double gammae = 7.66e-5*se*L*1/m; //vink 2000
    double logrho = -13.636+0.889*log10(Z/0.0142) + 3.2*gammae; //for T_jump, Vink 2001
    double Tjump = (61.2 + 2.59*logrho)*1000;
  //cout << "tjump " << Tjump << endl;

  double lM = 0;
    //if(log10(L) > 5.2) //weak winds if correction available
    {
        if(T > Tjump) // Vink 2001
        {
            lM = -6.697 + 2.194*(log10(L)-5) - 1.313*log10(m/30) - 1.226*log10(2.6/2) + 0.933*log10(T/40000) - 10.92*pow(log10(T/40000),2) + 0.85*log10(Z/0.0142);
        }
        else
        {
            lM = -6.688 + 2.210*(log10(L)-5) - 1.339*log10(m/30) - 1.601*log10(1.3/2) + 1.07*log10(T/20000) + 0.85*log10(Z/0.0142);
        }
        return pow(10,lM);
    }
    return pow(10,lM);
}

double getMassLossRateAlt(double m, double Z) //Castor 1975
{
    double corr = pow(Z/0.019,0.69);
    double L = getL(m,Z);
    double mSI = L*Lsol*corr/(getVinf(m,Z)*c); //kg/s

    return mSI*365.25*24*3600/1.889e30;     //Msol/yr
}

double getMassLossRateV(double m, double Z) //Vanbeveren 1998, p.70 top
{
  double corr = pow(Z/0.019,0.69);
  double T = getT(m), L = getL(m,Z);
  double Mdot = (pow(L,1.67)*pow(T,-1.55)*pow(10,-8.29));
  return Mdot*corr;
}
```

```
double getMassLossRate(double m, double Z) //Msol/yr
{
    return getMassLossRateVink(m, Z);
}



int findLine(double t0, vector<vector<double>> SFH) //Line belonging to t0 in
    SFH of one region
                            //Returns 12345, if t0 too close or distant for SFH
{                                                    //t0 in Myr
  double l = log10(t0)+6;

    if(l<6.6 || l > 10.05) return 12345;

  for(uint_fast8_t i=0;i<SFH.size();i++)
  {
    if(SFH.at(i).at(4) <= l && l <= SFH.at(i).at(5)) return i;
  }

  cout << "Fehler bei Zeitfindung" << endl;
    exit(0);
  return 0;
}

bool notdead(double m, double t, double Z) //t in Myr, true if star still alive
    after time t
{
  if(Z==0.004 && t<107.294/(m-5.53797)+1.91115) return true;
  else if (t<103.077/(m-5.73654)+1.83122) return true;
  else return false;
}

double simStars(uint_fast8_t t0, vector<vector<double>> SFH, double mlow, double
     mhigh, bool Z004, uint_fast8_t what)
{ //Iterates over time and mass and new star generation starting from t0 for
    area given by SFH, "what" determines whether to use Nhigh(8), Nlow(7) or
    Nexpect(6)
  double dt = 0.1; //Myr, time step width
  double dm = 1;   //Msol, mass bin width
    double line0 = findLine(t0, SFH); //line to start
    if(line0 == 12345) exit(0);       //if not in SFH: either too young (no
    stars) or too old to be relevant
    double Z = 0.008;
    if(Z004) Z = 0.004; //wanted metallicity
    double energy = 0;
    double tstart = 10; //time since when energy output gets counted

  vector<vector<vector<double>>> all; //collects data: all.at(timestep).at(star
    group).at(details)
```

```
vector<vector<double>> init;
for(int i=0; i*dm+mlow<mhigh; i++)
{
      double Nexpect = getNfromC(i*dm+mlow, (i+1)*dm+mlow, getc(SFH.at(line0).
  at(6+3*Z004)));
      double Nlow = getNfromC(i*dm+mlow, (i+1)*dm+mlow, getc(SFH.at(line0).at
  (7+3*Z004)));
      double Nhigh = getNfromC(i*dm+mlow, (i+1)*dm+mlow, getc(SFH.at(line0).at
  (8+3*Z004)));
      double vinf = getVinf(i*dm+mlow,Z);
  double L = getL(i*dm+mlow,Z);

  vector<double> massakt;
  massakt.push_back(t0);          //time of formation 0
  massakt.push_back(i*dm+mlow);   //lower mass limit 1
  massakt.push_back(0.);          //lost mass (total) 2
  massakt.push_back(0.);          //lost mass (step) 3
  massakt.push_back(vinf);        //vinf at this mass 4
      massakt.push_back(L);         //L at this mass 5
  massakt.push_back(Nexpect*dt);  //expected N 6
  massakt.push_back(Nlow*dt);     //lowest N 7
  massakt.push_back(Nhigh*dt);    //highest N 8
  init.push_back(massakt);
      //cout << "initialisiert" << endl;
}
all.push_back(init);


for(int i=1; i<t0/dt; i++) //time steps
{
  vector<vector<double>> neuZeile;
  double t = t0-i*dt;
  //cout << "t = " << t0-i*dt << endl;
  for(uint_fast16_t j=0;j<all.at(i-1).size();j++) //mass loss of all
  preexisting stars
  {
    double m = all.at(i-1).at(j).at(1)-all.at(i-1).at(j).at(2); //mass atm
    double massl4 = getMassLossRate(m,Z);
    double vinf = getVinf(m,Z);
    double L = getL(m,Z);
          if(notdead(m,all.at(i-1).at(j).at(0)-(t0-i*dt),Z)) //only if stars
  still alive
          {
              neuZeile.push_back(all.at(i-1).at(j));
              int ende = neuZeile.size()-1;
              neuZeile.at(ende).at(2) += massl4*dt*1e6;
              neuZeile.at(ende).at(3) = massl4;
              neuZeile.at(ende).at(4) = vinf;
              neuZeile.at(ende).at(5) = L;
```

```
                if(t<tstart) //remove if all energy generated since t0 relevant
                {                    //units: Msol(mdot)  dt        number
                    energy += 0.5*massl4*vinf*vinf*dt*1.9889e30*1e6*neuZeile.at(ende).at(what); //Joule, yr(dt)/yr(mdot) vanishes
                }
                //cout << neuZeile.at(ende).at(0) << " " << neuZeile.at(ende).at(1) << endl;
            }
    }

        double line = findLine(t0-(i*dt), SFH); //get relevant line
    if(line != 12345)            //if exists in SFH
        {

            for(int j=0; j*dm+mlow<mhigh; j++) //New stars
            {
                double Nexpect = getNfromC(j*dm+mlow, (j+1)*dm+mlow, getc(SFH.at(line).at(6+3*Z004)));
                double Nlow = getNfromC(j*dm+mlow, (j+1)*dm+mlow, getc(SFH.at(line).at(7+3*Z004)));
                double Nhigh = getNfromC(j*dm+mlow, (j+1)*dm+mlow, getc(SFH.at(line).at(8+3*Z004)));

                if((Nexpect != 0 && what==6)||(Nlow != 0 && what==7)||(Nhigh != 0 && what==8)) //to accelerate, remove this if whole table is returned
        {
          double vinf = getVinf(j*dm+mlow,Z);
          double L = getL(j*dm+mlow,Z);

          vector<double> massakt;          //200g Kokosraspeln
          massakt.push_back(t0-(i*dt));    //100-150g Puderzucker
          massakt.push_back(j*dm+mlow);    //2 Eiweiss
          massakt.push_back(0);            //etwas Vanille(aroma)
          massakt.push_back(0);            //mischen, kleine Kugeln formen
          massakt.push_back(vinf);         //5-10min bei 160 Grad backen
          massakt.push_back(L);
          massakt.push_back(Nexpect*dt);
          massakt.push_back(Nlow*dt);
          massakt.push_back(Nhigh*dt);
          neuZeile.push_back(massakt);
        }
            }
        }

    all.push_back(neuZeile);
  }

  cout << "energy: " << energy << endl;
    return energy; //total energy output
    //if more details necessary: return all
```

```
}


void plotLline(string name)
{
    double mlow = 3, mhigh = 100;
    vector<vector<double>> dat;

    for(int i=0; i<mhigh-mlow; i++)
    {
        vector<double> zeile;
        zeile.push_back(mlow + i);
        zeile.push_back(getLNR2005(mlow + i, 0.008));
        dat.push_back(zeile);
    }

    ofstream ofs(name);
    ofs << "# M, L(Nad/Raz)" << endl;
    for(uint_fast8_t i=0;i<dat.size();i++)
    {
    for(uint_fast8_t j=0;j<dat.at(i).size();j++){
      ofs << dat.at(i).at(j) << " ";}
    ofs << endl;
  }
  ofs.close();
}

vector<vector<double>> NperTmap(double m, double dM, double line, bool Z004,
   uint_fast8_t what)
//1. letter to T (RA), 2. letter to W (DEC)
//returns: line RA, column DEC, entry SFR in 1/Myr
//"what" determines whether to use Nhigh(8), Nlow(7) or Nexpect(6)
{
  vector<vector<double>> tab(20);


    #pragma omp parallel for
    for(char r='A'; r<'U'; r++)
    {
        vector<double> newr;
        for(char d='A'; d<'X'; d++)
        {
            stringstream ss;
            string s; //area
            ss << r << d;
            ss >> s;
            vector<vector<double>> SFH = readdat(s);
            //cout << s << endl;
            double NZ004 = SFH.at(line).at(what+2); //currently just add all
   metallicities
```

```
                double NZ008 = SFH.at(line).at(what);
                NZ004 = getNfromC(m, m+dM, getc(NZ004));
                NZ008 = getNfromC(m, m+dM, getc(NZ008));
                newr.push_back(NZ008+NZ004);
                /*if(Z004)  //use this if metallicity important
                {
                    double NZ004 = SFH.at(line).at(9);
                    NZ004 = getNfromC(m, m+dM, getc(NZ004));
                    newr.push_back(NZ004);
                }   //Jordanbloecke zum Eigenwert 0 sind voll neben der Spur
                else
                {
                    double NZ008 = SFH.at(line).at(6);
                    NZ008 = getNfromC(m, m+dM, getc(NZ008));
                    newr.push_back(NZ008);
                }*/
            }
            tab.at((int)r-65) = newr;
        }
        if(Z004) printtable("./map/NperT/line="+to_string((int)line)+"m="+to_string(
    m)+"what"+to_string(what), "#N per Myr",0, tab, true);
        else printtable("./map/NperT/line="+to_string((int)line)+"m="+to_string(m)+"
    what"+to_string(what), "#N per Myr",0, tab, true);

        return tab;
}

vector<vector<double>> energyMap(double mlow, double mhigh, uint_fast8_t t0,
    bool Z004, uint_fast8_t what)
//1. letter to T (RA), 2. letter to W (DEC)
//returns: line RA, column DEC, entry energy emission in erg
//"what" determines whether to use Nhigh(8), Nlow(7) or Nexpect(6)
{
  vector<vector<double>> tab(20);

        //Was ist gelb, gekruemmt und vollstaendig? Ein Bananachraum
        #pragma omp parallel for
        for(char r='A'; r<'U'; r++)
        {
            vector<double> newr;
            for(char d='A'; d<'X'; d++)
            {
                stringstream ss;
                string s;       //area
                ss << r << d;
                ss >> s;
                vector<vector<double>> SFH = readdat(s);
                cout << s << endl;
                double eZ004 = simStars(t0, SFH, mlow, mhigh, true, what); //
    currently just add all metallicities
```

```
            double eZ008 = simStars(t0, SFH, mlow, mhigh, false, what); //given
    in Joule, but we want erg
            newr.push_back((eZ008+eZ004)*1e7);
            /*if(Z004)  //use this if metallicity important
            {
                double eZ004 = simStars(15, SFH, 10, 100, true);
                newr.push_back(eZ004*1e7);
            }
            else
            {
                double eZ008 = simStars(15, SFH, 10, 100, false);
                newr.push_back(eZ008*1e7);
            }*/
        }
        tab.at((int)r-65) = newr;
    }
    //if(Z004) printtable("./map/energy/mlow="+to_string((int)mlow)+"mhigh="+
    to_string((int)mhigh)+"t0="+to_string(t0)+"what"+to_string(what), "#energy
    output by stars mlow<m<mhigh since t0 Myr in erg",0, tab, true);
    //else printtable("./map/energy/mlow="+to_string((int)mlow)+"mhigh="+
    to_string((int)mhigh)+"t0="+to_string(t0)+"what"+to_string(what), "#energy
    output by stars mlow<m<mhigh since t0 Myr in erg",0, tab, true);

    printLatextableFlipped("./map/energy/mlow="+to_string((int)mlow)+"mhigh="+
    to_string((int)mhigh)+"t0="+to_string(t0)+"ts=10what"+to_string(what)+"latex"
    , tab);
    return tab;
}

double regionVal(char r, char d,vector<vector<double>> map) //value of map at
    given region
{
  cout << "region " << r << r-'A' << " " << d << d-'A' << endl;
  return map.at(r-'A').at(d-'A');
}



string areaFromCoord(double r, double d) //area identifier nearest to given d[
    deg], r[min]
{
  double rcomp = 99999, dcomp = 99999;
  char rbest = 'A', dbest = 'A';
  for(char i='A'; i<'U'; i++)
  {
    for(char j='A'; j<'X'; j++)
    {
      double rakt = getRekt(i-'A');
      double dakt = getDec(j-'A');
      if(abs(rakt-r)<rcomp)
```

```
      {
        rbest = i;
        rcomp = abs(rakt-r);
      }
      if(abs(dakt-d)<dcomp)
      {
        dbest = j;
        dcomp = abs(dakt-d);
      }
    }
  }
  stringstream ss;
    string s;       //area
    ss << rbest << dbest;
    ss >> s;
  return s;
}


void plotMdot(string name)
{
    double mlow = 3, mhigh = 100;
    vector<vector<double>> dat;

    for(int i=0; i<mhigh-mlow; i++)
    {
        vector<double> zeile;
        zeile.push_back(mlow + i);
        zeile.push_back(getMassLossRateVink(mlow + i,0.004));
        zeile.push_back(getMassLossRateAlt(mlow + i,0.004));
        zeile.push_back(getMassLossRateV(mlow+i,0.004));
        dat.push_back(zeile);
    }

    ofstream ofs(name);
    ofs << "# M, Mdot(Vink), Mdot(Castor), Mdot(Vanbeveren)" << endl;
    for(uint_fast8_t i=0;i<dat.size();i++)
    {
    for(uint_fast8_t j=0;j<dat.at(i).size();j++){
      ofs << dat.at(i).at(j) << " ";}
    ofs << endl;
  }
  ofs.close();
}

void LatexBinToCoord() //Prints a Latex-table with conversion from letter/number
    of bin to coordinates
{
    ofstream ofs("./map/umrechnungTabRA.dat");
    for(char r='A'; r<'U'; r++)
```

```
    {
            stringstream ss;
            string s;       //area
            ss << r << 'A';
            ss >> s;
            vector<vector<double>> SFH = readdat(s);
            ofs << r << "&" << (int)(r-'A')+1 << "&" << SFH.at(0).at(0) << "h" << SFH.at(0).at(1) << "m" << "\\\\" << endl;
    }
    ofs.close();

    ofstream ofs2("./map/umrechnungTabDE.dat");
    for(char d='A'; d<'X'; d++)
    {
            stringstream ss;
            string s;       //area
            ss << 'A' << d;
            ss >> s;
            vector<vector<double>> SFH = readdat(s);
            ofs2 << d << "&" << ((int)(d-'A')+1) << "&" << SFH.at(0).at(2) << "$^\\circ$" << SFH.at(0).at(3) << "'" << "\\\\" << endl;
    }
    ofs2.close();


}






int main(int argc, char* argv[]) //Enter Region, some lower number, some higher number. Use in code as necessary. Program crashes if you don't.
{
  cout << "start" << endl;
  chrono::steady_clock::time_point begin = chrono::steady_clock::now(); // Measure duration (for fun)

  string area = argv[1];
    double lowM = stod(argv[2]);
    double highM = stod(argv[3]);


    //Write here whatever wanted

    for(int j=0; j<18; j++)
    {

            vector<vector<double>> tab = NperTmap(10,90,j,true,6);
```

```
    }/**/

    //cout << simStars(5,readdat(area),10, 100, false , 6) << endl;

    //regioncont(energyMap(lowM,highM,4,false,6));
    //LatexBinToCoord();

    /*vector<vector<double>> tab = energyMap(lowM, highM, 29, false , 6);
    tab = energyMap(lowM, highM, 20, false , 6);
    tab = energyMap(lowM, highM, 15, false , 6);
    tab = energyMap(lowM, highM, 10, false , 6);
    tab = energyMap(lowM, highM, 7, false , 6);
    tab = energyMap(lowM, highM, 4, false , 6);
    */
    /*tab = energyMap(lowM, highM, 29, false , 7);
    tab = energyMap(lowM, highM, 20, false , 7);
    tab = energyMap(lowM, highM, 15, false , 7);
    tab = energyMap(lowM, highM, 10, false , 7);
    tab = energyMap(lowM, highM, 7, false , 7);
    tab = energyMap(lowM, highM, 4, false , 7);
    */
    /*tab = energyMap(lowM, highM, 29, false , 8);
    tab = energyMap(lowM, highM, 20, false , 8);
    tab = energyMap(lowM, highM, 15, false , 8);
    tab = energyMap(lowM, highM, 10, false , 8);
    tab = energyMap(lowM, highM, 7, false , 8);
    tab = energyMap(lowM, highM, 4, false , 8);
    */
    //vector<vector<double>> npert = NperTmap(10,90,12,true,6);

    //plotLline("./plots/LNadRaz.dat");
    //smcds9();




    chrono::steady_clock::time_point end = chrono::steady_clock::now();
    cout << "Time difference = " << chrono::duration_cast<chrono::microseconds>(
   end - begin).count()/1e6 <<endl;
  cout << "ende" << endl;
}




/* Table Header:
#Title: The Star Formation History of the Small Magellanic Cloud
#Authors: Harris J., Zaritsky D.
#Table: SFH of the SMC
#===============================================================================
```

```
#Byte-by-byte Description of file: datafile2.txt
#------------------------------------------------------------------------------
#   Bytes Format Units          Label     Explanations
#------------------------------------------------------------------------------
#      1-  2  A2     ---              Region    Region identification
# 0        5  I1     h                RAh       Hour of right ascension (J2000)
# 1    7-  8  I2     min              RAm       Minute of right ascension (J2000)
#         10  A1     ---              DE-       Sign of the declination (J2000)
# 2   11- 12  I2     deg              DEd       Degree of declination (J2000)
# 3   14- 15  I2     arcmin           DEm       Arcminute of declination (J2000)
# 4   17- 21  F5.3   [yr]             Y-Age     Age bin's young boundary
# 5   23- 28  F6.3   [yr]             O-Age     Age bin's old boundary
# 6   30- 34  I5     solMass/Myr      SFR8      Best SFR with Z=0.008
# 7   36- 40  I5     solMass/Myr    e_SFR8      Lower limit on SFR8
# 8   42- 46  I5     solMass/Myr    E_SFR8      Upper limit on SFR8
# 9   48- 53  I6     solMass/Myr      SFR4      Best SFR with Z=0.004
#10   55- 60  I6     solMass/Myr    e_SFR4      Lower limit on SFR4
#11   62- 67  I6     solMass/Myr    E_SFR4      Upper limit on SFR4
#  69- 73  I5     solMass/Myr    SFR1      ? Best SFR with Z=0.001
#  75- 79  I5     solMass/Myr  e_SFR1      ? Lower limit on SFR1
#  81- 85  I5     solMass/Myr  E_SFR1      ? Upper limit on SFR1
#------------------------------------------------------------------------------

    */
```

B. Energy tables

Letter	Number	RA
A	1	0h25m
B	2	0h28m
C	3	0h31m
D	4	0h33m
E	5	0h36m
F	6	0h39m
G	7	0h41m
H	8	0h44m
I	9	0h47m
J	10	0h49m
K	11	0h52m
L	12	0h55m
M	13	0h58m
N	14	1h0m
O	15	1h3m
P	16	1h6m
Q	17	1h8m
R	18	1h11m
S	19	1h14m
T	20	1h16m

Letter	Number	DEC
A	1	-74°57’
B	2	-74°45’
C	3	-74°32’
D	4	-74°20’
E	5	-74°8’
F	6	-73°57’
G	7	-73°45’
H	8	-73°32’
I	9	-73°20’
J	10	-73°8’
K	11	-72°57’
L	12	-72°45’
M	13	-72°32’
N	14	-72°20’
O	15	-72°8’
P	16	-71°57’
Q	17	-71°45’
R	18	-71°32’
S	19	-71°20’
T	20	-71°8’
U	21	-70°57’
V	22	-70°45’
W	23	-70°32’

Table 1: Letter in Harris and Zaritsky (2004) area declaration, number in table and RA/DEC of center of bins.

	20	19	18	17	16	15	14	13	12	11	10	9	8	7	6	5	4	3	2	1
23	0.00e+00	0.00e+00	5.69e+49	0.00e+00	0.00e+00	0.00e+00	0.00e+00	0.00e+00	0.00e+00	0.00e+00	0.00e+00	0.00e+00	0.00e+00	0.00e+00	0.00e+00	0.00e+00	0.00e+00	0.00e+00	0.00e+00	0.00e+00
22	0.00e+00	0.00e+00	0.00e+00	0.00e+00	0.00e+00	0.00e+00	0.00e+00	0.00e+00	0.00e+00	0.00e+00	0.00e+00	0.00e+00	0.00e+00	0.00e+00	0.00e+00	0.00e+00	0.00e+00	0.00e+00	0.00e+00	0.00e+00
21	0.00e+00	0.00e+00	0.00e+00	0.00e+00	0.00e+00	0.00e+00	0.00e+00	0.00e+00	0.00e+00	0.00e+00	0.00e+00	0.00e+00	0.00e+00	0.00e+00	0.00e+00	4.28e+49	4.28e+49	0.00e+00	0.00e+00	0.00e+00
20	0.00e+00	0.00e+00	0.00e+00	0.00e+00	7.85e+47	0.00e+00	0.00e+00	0.00e+00	0.00e+00	0.00e+00	0.00e+00	0.00e+00	0.00e+00	0.00e+00	0.00e+00	4.28e+49	4.28e+49	0.00e+00	0.00e+00	0.00e+00
19	0.00e+00	0.00e+00	0.00e+00	8.44e+49	0.00e+00	0.00e+00	0.00e+00	0.00e+00	0.00e+00	0.00e+00	0.00e+00	0.00e+00	0.00e+00	0.00e+00	0.00e+00	0.00e+00	0.00e+00	0.00e+00	0.00e+00	0.00e+00
18	8.70e+49	3.16e+50	3.08e+50	1.34e+51	0.00e+00	0.00e+00	0.00e+00	0.00e+00	0.00e+00	0.00e+00	0.00e+00	0.00e+00	0.00e+00	0.00e+00	0.00e+00	0.00e+00	0.00e+00	0.00e+00	0.00e+00	0.00e+00
17	0.00e+00	0.00e+00	0.00e+00	1.32e+47	0.00e+00	2.63e+47	0.00e+00	0.00e+00	0.00e+00	1.54e+51	0.00e+00	0.00e+00	1.04e+50	0.00e+00	0.00e+00	0.00e+00	0.00e+00	0.00e+00	0.00e+00	0.00e+00
16	0.00e+00	0.00e+00	9.35e+50	1.11e+51	0.00e+00	0.00e+00	0.00e+00	0.00e+00	0.00e+00	0.00e+00	1.61e+51	0.00e+00	0.00e+00	0.00e+00	0.00e+00	1.32e+47	1.32e+47	0.00e+00	0.00e+00	0.00e+00
15	1.92e+50	0.00e+00	0.00e+00	0.00e+00	0.00e+00	5.54e+51	4.39e+51	0.00e+00	0.00e+00	0.00e+00	0.00e+00	1.18e+51	0.00e+00	0.00e+00	0.00e+00	0.00e+00	0.00e+00	0.00e+00	0.00e+00	0.00e+00
14	0.00e+00	0.00e+00	0.00e+00	0.00e+00	0.00e+00	0.00e+00	0.00e+00	0.00e+00	0.00e+00	0.00e+00	0.00e+00	0.00e+00	1.32e+47	2.82e+50	3.95e+47	0.00e+00	0.00e+00	0.00e+00	0.00e+00	0.00e+00
13	0.00e+00	0.00e+00	3.23e+50	0.00e+00	0.00e+00	0.00e+00	0.00e+00	0.00e+00	0.00e+00	0.00e+00	0.00e+00	0.00e+00	0.00e+00	0.00e+00	1.09e+50	0.00e+00	0.00e+00	0.00e+00	0.00e+00	0.00e+00
12	0.00e+00	0.00e+00	0.00e+00	0.00e+00	0.00e+00	0.00e+00	0.00e+00	0.00e+00	0.00e+00	7.39e+51	0.00e+00	0.00e+00	0.00e+00	0.00e+00	0.00e+00	0.00e+00	0.00e+00	0.00e+00	0.00e+00	0.00e+00
11	1.32e+47	0.00e+00	0.00e+00	0.00e+00	0.00e+00	0.00e+00	0.00e+00	0.00e+00	0.00e+00	0.00e+00	0.00e+00	0.00e+00	0.00e+00	0.00e+00	0.00e+00	0.00e+00	0.00e+00	0.00e+00	0.00e+00	0.00e+00
10	0.00e+00	0.00e+00	0.00e+00	0.00e+00	0.00e+00	0.00e+00	0.00e+00	0.00e+00	0.00e+00	0.00e+00	0.00e+00	0.00e+00	0.00e+00	3.54e+51	0.00e+00	0.00e+00	6.95e+50	0.00e+00	0.00e+00	0.00e+00
9	0.00e+00	0.00e+00	0.00e+00	0.00e+00	0.00e+00	0.00e+00	0.00e+00	0.00e+00	0.00e+00	0.00e+00	0.00e+00	0.00e+00	0.00e+00	0.00e+00	0.00e+00	0.00e+00	9.56e+50	0.00e+00	0.00e+00	0.00e+00
8	0.00e+00	0.00e+00	0.00e+00	0.00e+00	0.00e+00	0.00e+00	0.00e+00	0.00e+00	0.00e+00	0.00e+00	3.51e+50	1.42e+51	0.00e+00	0.00e+00	0.00e+00	0.00e+00	0.00e+00	0.00e+00	0.00e+00	0.00e+00
7	0.00e+00	0.00e+00	0.00e+00	0.00e+00	0.00e+00	0.00e+00	0.00e+00	0.00e+00	0.00e+00	0.00e+00	0.00e+00	0.00e+00	0.00e+00	0.00e+00	0.00e+00	0.00e+00	0.00e+00	0.00e+00	0.00e+00	0.00e+00
6	0.00e+00	0.00e+00	0.00e+00	0.00e+00	0.00e+00	0.00e+00	0.00e+00	0.00e+00	0.00e+00	0.00e+00	0.00e+00	0.00e+00	0.00e+00	0.00e+00	0.00e+00	0.00e+00	0.00e+00	0.00e+00	0.00e+00	0.00e+00
5	0.00e+00	0.00e+00	0.00e+00	0.00e+00	0.00e+00	0.00e+00	0.00e+00	0.00e+00	6.70e+49	0.00e+00	0.00e+00	0.00e+00	0.00e+00	0.00e+00	0.00e+00	0.00e+00	0.00e+00	0.00e+00	9.29e+49	6.54e+46
4	0.00e+00	0.00e+00	0.00e+00	0.00e+00	0.00e+00	0.00e+00	0.00e+00	0.00e+00	0.00e+00	0.00e+00	0.00e+00	0.00e+00	2.15e+50	6.54e+46	0.00e+00	0.00e+00	2.62e+50	2.11e+48	0.00e+00	0.00e+00
3	0.00e+00	0.00e+00	0.00e+00	0.00e+00	0.00e+00	0.00e+00	0.00e+00	0.00e+00	0.00e+00	0.00e+00	0.00e+00	0.00e+00	0.00e+00	0.00e+00	0.00e+00	0.00e+00	7.06e+48	0.00e+00	0.00e+00	0.00e+00
2	0.00e+00	0.00e+00	0.00e+00	0.00e+00	1.12e+50	0.00e+00	0.00e+00	0.00e+00	0.00e+00	0.00e+00	0.00e+00	0.00e+00	0.00e+00	0.00e+00	9.73e+49	0.00e+00	0.00e+00	0.00e+00	0.00e+00	0.00e+00
1	0.00e+00	0.00e+00	0.00e+00	0.00e+00	1.12e+50	0.00e+00	0.00e+00	0.00e+00	0.00e+00	0.00e+00	0.00e+00	0.00e+00	0.00e+00	0.00e+00	9.73e+49	0.00e+00	0.00e+00	0.00e+00	0.00e+00	0.00e+00

Table 2: Expected energy emission in erg by stars formed in the last 4 Myrs. Rows: DEC-Bin, Columns: RA-Bin (as in images), binsize $12' \times 12'$, conversion to coordinates in table 1.

	20	19	18	17	16	15	14	13	12	11	10	9	8	7	6	5	4	3	2	1
23	0.00e+00	0.00e+00	8.38e+50	0.00e+00	0.00e+00	0.00e+00	2.26e+50	0.00e+00	0.00e+00	0.00e+00	0.00e+00	0.00e+00	0.00e+00	0.00e+00	0.00e+00	0.00e+00	0.00e+00	0.00e+00	0.00e+00	0.00e+00
22	0.00e+00	0.00e+00	1.69e+51	0.00e+00	0.00e+00	0.00e+00	0.00e+00	0.00e+00	0.00e+00	0.00e+00	0.00e+00	0.00e+00	0.00e+00	0.00e+00	0.00e+00	0.00e+00	0.00e+00	0.00e+00	0.00e+00	0.00e+00
21	0.00e+00	0.00e+00	0.00e+00	0.00e+00	0.00e+00	0.00e+00	0.00e+00	0.00e+00	0.00e+00	0.00e+00	0.00e+00	0.00e+00	0.00e+00	0.00e+00	0.00e+00	6.30e+50	6.30e+50	0.00e+00	0.00e+00	0.00e+00
20	0.00e+00	0.00e+00	0.00e+00	0.00e+00	1.40e+50	0.00e+00	0.00e+00	4.33e+51	0.00e+00	0.00e+00	0.00e+00	5.10e+50	5.10e+50	0.00e+00	0.00e+00	6.30e+50	6.30e+50	0.00e+00	0.00e+00	0.00e+00
19	0.00e+00	0.00e+00	0.00e+00	1.24e+51	8.53e+50	0.00e+00	0.00e+00	0.00e+00	0.00e+00	0.00e+00	0.00e+00	0.00e+00	0.00e+00	1.49e+49	1.49e+49	9.55e+50	9.55e+50	0.00e+00	0.00e+00	0.00e+00
18	1.28e+51	4.65e+51	4.54e+51	1.98e+52	0.00e+00	0.00e+00	0.00e+00	0.00e+00	0.00e+00	0.00e+00	1.63e+51	0.00e+00	0.00e+00	0.00e+00	0.00e+00	9.55e+50	9.55e+50	0.00e+00	0.00e+00	0.00e+00
17	3.91e+50	2.89e+51	9.40e+51	1.94e+48	0.00e+00	6.64e+51	0.00e+00	0.00e+00	0.00e+00	2.27e+52	0.00e+00	9.94e+49	1.53e+51	0.00e+00	0.00e+00	0.00e+00	0.00e+00	0.00e+00	0.00e+00	0.00e+00
16	0.00e+00	0.00e+00	1.38e+52	1.63e+52	2.76e+51	2.49e+48	0.00e+00	0.00e+00	0.00e+00	0.00e+00	2.36e+52	0.00e+00	0.00e+00	0.00e+00	0.00e+00	1.94e+48	1.94e+48	0.00e+00	0.00e+00	0.00e+00
15	2.82e+51	0.00e+00	0.00e+00	0.00e+00	3.18e+51	1.03e+53	6.46e+52	0.00e+00	0.00e+00	0.00e+00	0.00e+00	1.74e+52	0.00e+00	0.00e+00	0.00e+00	0.00e+00	0.00e+00	0.00e+00	0.00e+00	0.00e+00
14	2.39e+51	1.07e+51	2.61e+52	0.00e+00	0.00e+00	2.51e+52	0.00e+00	0.00e+00	0.00e+00	0.00e+00	0.00e+00	0.00e+00	8.95e+51	4.15e+51	2.74e+51	0.00e+00	0.00e+00	0.00e+00	0.00e+00	0.00e+00
13	0.00e+00	0.00e+00	4.76e+51	0.00e+00	0.00e+00	7.58e+51	0.00e+00	0.00e+00	0.00e+00	0.00e+00	0.00e+00	0.00e+00	7.06e+51	2.39e+51	1.62e+51	0.00e+00	0.00e+00	0.00e+00	0.00e+00	0.00e+00
12	0.00e+00	0.00e+00	0.00e+00	0.00e+00	0.00e+00	0.00e+00	0.00e+00	0.00e+00	0.00e+00	1.09e+53	0.00e+00	0.00e+00	0.00e+00	0.00e+00	0.00e+00	0.00e+00	0.00e+00	0.00e+00	0.00e+00	0.00e+00
11	4.42e+48	0.00e+00	0.00e+00	0.00e+00	0.00e+00	0.00e+00	0.00e+00	0.00e+00	0.00e+00	0.00e+00	0.00e+00	0.00e+00	0.00e+00	0.00e+00	0.00e+00	0.00e+00	0.00e+00	0.00e+00	0.00e+00	0.00e+00
10	0.00e+00	0.00e+00	0.00e+00	0.00e+00	0.00e+00	0.00e+00	0.00e+00	0.00e+00	0.00e+00	0.00e+00	4.28e+52	9.62e+52	0.00e+00	5.22e+52	0.00e+00	0.00e+00	1.02e+52	0.00e+00	0.00e+00	1.21e+51
9	0.00e+00	0.00e+00	0.00e+00	0.00e+00	0.00e+00	0.00e+00	0.00e+00	0.00e+00	0.00e+00	0.00e+00	8.83e+51	0.00e+00	0.00e+00	0.00e+00	0.00e+00	0.00e+00	1.41e+52	0.00e+00	0.00e+00	1.21e+51
8	0.00e+00	0.00e+00	0.00e+00	0.00e+00	0.00e+00	0.00e+00	0.00e+00	0.00e+00	0.00e+00	0.00e+00	5.17e+51	2.09e+52	0.00e+00	0.00e+00	0.00e+00	0.00e+00	0.00e+00	0.00e+00	0.00e+00	0.00e+00
7	0.00e+00	0.00e+00	0.00e+00	0.00e+00	0.00e+00	9.72e+51	6.44e+51	0.00e+00	0.00e+00	0.00e+00	0.00e+00	0.00e+00	0.00e+00	0.00e+00	0.00e+00	0.00e+00	0.00e+00	0.00e+00	0.00e+00	0.00e+00
6	3.49e+50	0.00e+00	0.00e+00	0.00e+00	0.00e+00	0.00e+00	2.78e+51	0.00e+00	0.00e+00	0.00e+00	0.00e+00	0.00e+00	1.05e+52	0.00e+00	0.00e+00	0.00e+00	0.00e+00	0.00e+00	0.00e+00	0.00e+00
5	3.49e+50	0.00e+00	0.00e+00	0.00e+00	0.00e+00	0.00e+00	0.00e+00	0.00e+00	9.87e+50	0.00e+00	6.76e+50	2.59e+51	0.00e+00	0.00e+00	2.49e+48	0.00e+00	0.00e+00	0.00e+00	1.73e+51	1.29e+51
4	3.28e+51	3.28e+51	1.75e+51	3.58e+50	0.00e+00	3.98e+49	0.00e+00	1.04e+50	0.00e+00	0.00e+00	0.00e+00	1.02e+51	3.16e+51	9.63e+47	0.00e+00	4.08e+51	3.86e+51	7.80e+50	8.79e+50	0.00e+00
3	3.28e+51	3.28e+51	1.75e+51	3.58e+50	0.00e+00	0.00e+00	0.00e+00	0.00e+00	0.00e+00	0.00e+00	0.00e+00	0.00e+00	0.00e+00	8.23e+50	0.00e+00	6.43e+50	1.04e+50	0.00e+00	8.15e+50	0.00e+00
2	1.99e+50	1.99e+50	0.00e+00	0.00e+00	1.73e+51	0.00e+00	0.00e+00	0.00e+00	5.69e+50	0.00e+00	0.00e+00	1.14e+50	0.00e+00	0.00e+00	1.68e+51	0.00e+00	0.00e+00	0.00e+00	1.11e+51	0.00e+00
1	1.99e+50	1.99e+50	0.00e+00	0.00e+00	1.73e+51	0.00e+00	0.00e+00	0.00e+00	5.69e+50	0.00e+00	0.00e+00	1.14e+50	0.00e+00	0.00e+00	1.68e+51	0.00e+00	0.00e+00	0.00e+00	1.11e+51	0.00e+00

Table 3: Expected energy emission in erg by stars formed in the last 7 Myrs. Rows: DEC-Bin, Columns: RA-Bin (as in images), binsize $12' \times 12'$, conversion to coordinates in table 1.

	20	19	18	17	16	15	14	13	12	11	10	9	8	7	6	5	4	3	2	1
23	0.00e+00	0.00e+00	8.38e+50	0.00e+00	0.00e+00	0.00e+00	5.11e+50	0.00e+00	0.00e+00	0.00e+00	0.00e+00	0.00e+00	0.00e+00	1.20e+49	1.20e+49	0.00e+00	0.00e+00	0.00e+00	0.00e+00	0.00e+00
22	0.00e+00	0.00e+00	3.11e+51	0.00e+00	0.00e+00	0.00e+00	0.00e+00	0.00e+00	0.00e+00	0.00e+00	0.00e+00	0.00e+00	0.00e+00	1.20e+49	1.20e+49	0.00e+00	0.00e+00	0.00e+00	0.00e+00	0.00e+00
21	0.00e+00	0.00e+00	2.30e+50	0.00e+00	0.00e+00	0.00e+00	0.00e+00	0.00e+00	0.00e+00	0.00e+00	0.00e+00	0.00e+00	0.00e+00	0.00e+00	0.00e+00	6.30e+50	6.30e+50	0.00e+00	0.00e+00	0.00e+00
20	0.00e+00	4.67e+50	0.00e+00	0.00e+00	2.48e+50	0.00e+00	0.00e+00	7.95e+51	0.00e+00	0.00e+00	0.00e+00	9.37e+50	9.37e+50	0.00e+00	0.00e+00	6.30e+50	6.30e+50	0.00e+00	0.00e+00	0.00e+00
19	7.37e+50	0.00e+00	0.00e+00	1.24e+51	1.57e+51	0.00e+00	0.00e+00	5.86e+51	0.00e+00	0.00e+00	0.00e+00	0.00e+00	0.00e+00	2.74e+49	2.74e+49	1.75e+51	1.75e+51	0.00e+00	0.00e+00	0.00e+00
18	1.28e+51	4.65e+51	4.54e+51	1.98e+52	0.00e+00	0.00e+00	2.87e+52	0.00e+00	0.00e+00	0.00e+00	3.00e+51	8.47e+50	8.47e+50	4.79e+48	4.79e+48	1.75e+51	1.75e+51	0.00e+00	0.00e+00	0.00e+00
17	7.18e+50	5.32e+51	1.73e+52	1.20e+52	1.42e+52	1.22e+52	1.51e+52	1.19e+52	1.92e+52	2.27e+52	6.56e+51	1.83e+50	1.53e+51	0.00e+00	0.00e+00	0.00e+00	0.00e+00	0.00e+00	0.00e+00	0.00e+00
16	0.00e+00	0.00e+00	1.89e+52	1.76e+52	4.27e+52	2.28e+51	0.00e+00	0.00e+00	0.00e+00	0.00e+00	2.36e+52	0.00e+00	0.00e+00	0.00e+00	0.00e+00	1.94e+48	1.94e+48	0.00e+00	0.00e+00	0.00e+00
15	2.82e+51	6.90e+49	0.00e+00	1.96e+52	2.61e+52	1.21e+53	6.46e+52	0.00e+00	0.00e+00	1.16e+52	8.88e+51	1.74e+52	0.00e+00	0.00e+00	0.00e+00	0.00e+00	0.00e+00	0.00e+00	0.00e+00	0.00e+00
14	4.39e+51	2.62e+51	5.37e+52	0.00e+00	0.00e+00	4.61e+52	0.00e+00	0.00e+00	0.00e+00	0.00e+00	1.54e+52	0.00e+00	1.64e+52	4.15e+51	5.09e+51	1.84e+51	1.84e+51	0.00e+00	0.00e+00	0.00e+00
13	0.00e+00	7.99e+52	1.41e+52	0.00e+00	0.00e+00	2.05e+52	0.00e+00	0.00e+00	0.00e+00	0.00e+00	0.00e+00	0.00e+00	1.30e+52	4.39e+51	1.62e+51	0.00e+00	0.00e+00	0.00e+00	0.00e+00	0.00e+00
12	0.00e+00	0.00e+00	2.92e+52	1.04e+52	0.00e+00	0.00e+00	1.81e+52	0.00e+00	0.00e+00	1.09e+53	0.00e+00	0.00e+00	0.00e+00	0.00e+00	1.65e+51	0.00e+00	0.00e+00	0.00e+00	0.00e+00	0.00e+00
11	6.51e+48	0.00e+00	1.70e+52	2.87e+51	5.91e+51	0.00e+00	0.00e+00	0.00e+00	0.00e+00	0.00e+00	0.00e+00	0.00e+00	0.00e+00	0.00e+00	0.00e+00	0.00e+00	5.09e+50	0.00e+00	3.83e+49	3.83e+49
10	3.09e+52	3.59e+52	2.02e+52	1.97e+52	5.43e+51	0.00e+00	0.00e+00	0.00e+00	0.00e+00	0.00e+00	7.86e+52	1.77e+53	0.00e+00	5.22e+52	0.00e+00	0.00e+00	1.02e+52	0.00e+00	0.00e+00	2.22e+51
9	3.35e+52	4.36e+52	2.18e+52	2.38e+52	8.64e+51	7.64e+51	0.00e+00	0.00e+00	0.00e+00	0.00e+00	2.27e+52	7.09e+51	0.00e+00	0.00e+00	7.83e+51	2.15e+51	1.41e+52	1.56e+51	1.29e+50	2.22e+51
8	0.00e+00	0.00e+00	0.00e+00	0.00e+00	0.00e+00	0.00e+00	8.95e+51	7.95e+51	0.00e+00	0.00e+00	5.17e+51	2.09e+52	0.00e+00	0.00e+00	0.00e+00	0.00e+00	0.00e+00	0.00e+00	2.39e+48	1.54e+51
7	0.00e+00	0.00e+00	0.00e+00	0.00e+00	8.23e+51	1.79e+52	1.18e+52	0.00e+00	0.00e+00	0.00e+00	0.00e+00	0.00e+00	0.00e+00	0.00e+00	0.00e+00	1.16e+52	0.00e+00	0.00e+00	0.00e+00	0.00e+00
6	6.41e+50	0.00e+00	0.00e+00	0.00e+00	0.00e+00	0.00e+00	5.12e+51	3.23e+51	1.10e+51	0.00e+00	4.40e+51	0.00e+00	1.92e+52	0.00e+00	0.00e+00	0.00e+00	0.00e+00	0.00e+00	0.00e+00	0.00e+00
5	6.41e+50	0.00e+00	0.00e+00	0.00e+00	0.00e+00	0.00e+00	0.00e+00	1.71e+51	9.87e+50	0.00e+00	1.24e+51	4.75e+51	3.02e+51	0.00e+00	3.71e+51	3.31e+50	0.00e+00	0.00e+00	2.03e+51	2.37e+51
4	6.03e+51	6.03e+51	3.22e+51	6.58e+50	0.00e+00	7.31e+49	0.00e+00	1.91e+50	0.00e+00	0.00e+00	1.07e+51	1.88e+51	3.16e+51	1.02e+51	0.00e+00	7.49e+51	3.86e+51	1.41e+51	1.62e+51	1.22e+51
3	6.03e+51	6.03e+51	3.22e+51	6.58e+50	0.00e+00	0.00e+00	0.00e+00	0.00e+00	0.00e+00	0.00e+00	0.00e+00	0.00e+00	0.00e+00	1.51e+51	0.00e+00	1.18e+51	1.04e+50	0.00e+00	1.50e+51	0.00e+00
2	3.66e+50	3.66e+50	0.00e+00	0.00e+00	1.80e+51	0.00e+00	0.00e+00	0.00e+00	1.05e+51	0.00e+00	0.00e+00	2.10e+50	2.75e+50	0.00e+00	1.88e+51	0.00e+00	0.00e+00	0.00e+00	2.04e+51	0.00e+00
1	3.66e+50	3.66e+50	0.00e+00	0.00e+00	1.80e+51	0.00e+00	0.00e+00	0.00e+00	1.05e+51	0.00e+00	0.00e+00	2.10e+50	2.75e+50	0.00e+00	1.88e+51	0.00e+00	0.00e+00	0.00e+00	2.04e+51	0.00e+00

Table 4: Expected energy emission in erg by stars formed in the last 10 Myrs. Rows: DEC-Bin, Columns: RA-Bin (as in images), binsize $12' \times 12'$, conversion to coordinates in table 1.

	20	19	18	17	16	15	14	13	12	11	10	9	8	7	6	5	4	3	2	1
23	0.00e+00	0.00e+00	8.38e+50	0.00e+00	0.00e+00	0.00e+00	7.08e+50	8.95e+49	5.47e+50	5.91e+50	5.91e+50	0.00e+00	0.00e+00	1.19e+50	1.19e+50	0.00e+00	0.00e+00	0.00e+00	0.00e+00	0.00e+00
22	0.00e+00	0.00e+00	3.17e+51	8.80e+50	0.00e+00	0.00e+00	0.00e+00	0.00e+00	0.00e+00	5.91e+50	5.91e+50	0.00e+00	0.00e+00	1.19e+50	1.19e+50	0.00e+00	0.00e+00	0.00e+00	0.00e+00	0.00e+00
21	0.00e+00	0.00e+00	7.05e+50	8.26e+49	0.00e+00	0.00e+00	0.00e+00	0.00e+00	0.00e+00	0.00e+00	0.00e+00	0.00e+00	0.00e+00	0.00e+00	0.00e+00	6.30e+50	6.30e+50	0.00e+00	0.00e+00	0.00e+00
20	0.00e+00	1.43e+51	0.00e+00	0.00e+00	2.48e+50	0.00e+00	0.00e+00	7.95e+51	3.32e+49	0.00e+00	0.00e+00	9.37e+50	9.37e+50	0.00e+00	0.00e+00	6.30e+50	6.30e+50	0.00e+00	0.00e+00	0.00e+00
19	2.26e+51	0.00e+00	1.98e+51	1.24e+51	4.97e+51	3.30e+51	0.00e+00	1.80e+52	1.66e+51	0.00e+00	0.00e+00	7.65e+50	7.65e+50	2.74e+49	2.74e+49	1.75e+51	1.75e+51	0.00e+00	0.00e+00	0.00e+00
18	1.28e+51	4.66e+51	4.54e+51	1.98e+52	6.01e+51	7.08e+51	8.82e+52	9.46e+51	6.19e+51	1.05e+51	3.00e+51	2.86e+51	2.86e+51	3.63e+50	3.63e+50	1.75e+51	1.75e+51	0.00e+00	0.00e+00	0.00e+00
17	7.18e+50	5.32e+51	1.73e+52	3.68e+52	4.35e+52	1.22e+52	4.64e+52	3.67e+52	5.89e+52	2.88e+52	2.01e+52	2.45e+51	1.53e+51	2.71e+50	2.71e+50	0.00e+00	0.00e+00	0.00e+00	0.00e+00	0.00e+00
16	2.38e+51	0.00e+00	2.96e+52	2.57e+52	1.20e+53	9.48e+51	0.00e+00	0.00e+00	0.00e+00	1.90e+52	2.36e+52	0.00e+00	0.00e+00	1.94e+50	0.00e+00	1.94e+48	1.94e+48	0.00e+00	0.00e+00	0.00e+00
15	2.82e+51	2.12e+50	1.02e+52	6.03e+52	8.03e+52	1.21e+53	6.46e+52	0.00e+00	0.00e+00	3.56e+52	4.29e+52	1.74e+52	0.00e+00	0.00e+00	3.71e+50	0.00e+00	0.00e+00	0.00e+00	0.00e+00	0.00e+00
14	4.39e+51	4.19e+51	6.55e+52	1.14e+51	0.00e+00	6.37e+52	0.00e+00	0.00e+00	0.00e+00	0.00e+00	4.72e+52	8.72e+51	1.64e+52	4.15e+51	5.21e+51	5.64e+51	5.64e+51	0.00e+00	0.00e+00	0.00e+00
13	2.48e+51	2.45e+53	3.35e+52	0.00e+00	0.00e+00	6.21e+52	2.17e+51	0.00e+00	0.00e+00	0.00e+00	0.00e+00	7.90e+51	1.30e+52	4.39e+51	1.62e+51	1.22e+51	1.22e+51	4.32e+50	4.32e+50	4.32e+50
12	4.22e+51	8.62e+51	8.97e+52	4.08e+52	0.00e+00	0.00e+00	6.51e+52	0.00e+00	2.76e+52	1.09e+53	0.00e+00	0.00e+00	0.00e+00	0.00e+00	5.08e+51	0.00e+00	4.81e+50	0.00e+00	0.00e+00	0.00e+00
11	2.50e+51	1.07e+52	5.23e+52	1.55e+52	2.97e+52	0.00e+00	0.00e+00	0.00e+00	0.00e+00	0.00e+00	0.00e+00	0.00e+00	0.00e+00	0.00e+00	0.00e+00	7.42e+51	1.56e+51	0.00e+00	3.78e+50	3.78e+50
10	9.48e+52	1.10e+53	6.19e+52	6.05e+52	1.67e+52	0.00e+00	0.00e+00	0.00e+00	0.00e+00	0.00e+00	7.86e+52	1.77e+53	3.22e+52	5.22e+52	7.98e+51	8.39e+51	1.02e+52	0.00e+00	0.00e+00	2.22e+51
9	1.10e+53	1.34e+53	6.70e+52	7.30e+52	2.65e+52	2.34e+52	0.00e+00	0.00e+00	2.84e+51	6.32e+51	4.72e+52	2.18e+52	0.00e+00	0.00e+00	2.40e+52	6.61e+51	1.41e+52	4.79e+51	3.94e+50	2.22e+51
8	5.73e+51	0.00e+00	5.55e+51	1.22e+51	7.44e+51	9.39e+51	2.75e+52	2.44e+52	1.27e+52	0.00e+00	5.17e+51	2.09e+52	0.00e+00	0.00e+00	0.00e+00	9.72e+51	1.17e+52	1.04e+51	4.34e+50	4.71e+51
7	0.00e+00	3.38e+51	2.00e+51	3.89e+51	2.53e+52	1.79e+52	1.18e+52	4.17e+51	5.19e+51	2.97e+51	0.00e+00	0.00e+00	0.00e+00	0.00e+00	0.00e+00	3.57e+52	3.68e+51	3.81e+51	1.21e+51	0.00e+00
6	6.81e+50	9.80e+50	1.73e+51	0.00e+00	0.00e+00	0.00e+00	5.12e+51	9.92e+51	3.38e+51	0.00e+00	1.35e+52	5.75e+51	1.96e+52	6.68e+51	8.36e+51	1.08e+51	6.62e+51	8.49e+50	4.96e+51	6.80e+50
5	6.81e+50	9.80e+50	1.73e+51	0.00e+00	0.00e+00	0.00e+00	0.00e+00	5.24e+51	9.87e+50	0.00e+00	1.24e+51	4.75e+51	9.26e+51	0.00e+00	1.14e+52	1.02e+51	0.00e+00	0.00e+00	2.03e+51	3.41e+51
4	6.03e+51	6.03e+51	3.22e+51	6.58e+50	0.00e+00	7.31e+49	0.00e+00	1.91e+50	0.00e+00	0.00e+00	3.30e+51	1.88e+51	3.16e+51	3.13e+51	0.00e+00	7.49e+51	3.86e+51	1.41e+51	1.62e+51	4.80e+51
3	6.03e+51	6.03e+51	3.22e+51	6.58e+50	0.00e+00	0.00e+00	0.00e+00	0.00e+00	0.00e+00	0.00e+00	0.00e+00	2.99e+50	0.00e+00	1.51e+51	0.00e+00	1.18e+51	1.04e+50	0.00e+00	1.50e+51	2.59e+50
2	3.66e+50	3.66e+50	0.00e+00	0.00e+00	1.80e+51	0.00e+00	0.00e+00	0.00e+00	1.05e+51	0.00e+00	0.00e+00	2.10e+50	8.73e+50	0.00e+00	1.88e+51	0.00e+00	0.00e+00	0.00e+00	2.28e+51	1.84e+50
1	3.66e+50	3.66e+50	0.00e+00	0.00e+00	1.80e+51	0.00e+00	0.00e+00	0.00e+00	1.05e+51	0.00e+00	0.00e+00	2.10e+50	8.73e+50	0.00e+00	1.88e+51	0.00e+00	0.00e+00	0.00e+00	2.28e+51	1.84e+50

Table 5: Expected energy emission in erg by stars formed in the last 15 Myrs. Rows: DEC-Bin, Columns: RA-Bin (as in images), binsize $12' \times 12'$, conversion to coordinates in table 1.

	20	19	18	17	16	15	14	13	12	11	10	9	8	7	6	5	4	3	2	1
23	0.00e+00	0.00e+00	8.38e+50	0.00e+00	0.00e+00	0.00e+00	7.08e+50	3.53e+50	2.16e+51	2.33e+51	2.33e+51	0.00e+00	0.00e+00	3.60e+50	3.60e+50	0.00e+00	0.00e+00	0.00e+00	0.00e+00	0.00e+00
22	0.00e+00	0.00e+00	3.35e+51	3.47e+51	0.00e+00	0.00e+00	0.00e+00	0.00e+00	0.00e+00	2.33e+51	2.33e+51	0.00e+00	0.00e+00	3.60e+50	3.60e+50	0.00e+00	0.00e+00	0.00e+00	0.00e+00	0.00e+00
21	0.00e+00	0.00e+00	7.05e+50	3.25e+50	0.00e+00	0.00e+00	0.00e+00	0.00e+00	0.00e+00	0.00e+00	0.00e+00	0.00e+00	0.00e+00	0.00e+00	0.00e+00	6.30e+50	6.30e+50	0.00e+00	0.00e+00	0.00e+00
20	0.00e+00	1.43e+51	0.00e+00	0.00e+00	2.48e+50	0.00e+00	0.00e+00	7.95e+51	1.31e+50	0.00e+00	0.00e+00	9.37e+50	9.37e+50	0.00e+00	0.00e+00	6.30e+50	6.30e+50	0.00e+00	0.00e+00	0.00e+00
19	2.26e+51	0.00e+00	7.82e+51	1.24e+51	1.50e+52	1.30e+52	0.00e+00	1.80e+52	6.54e+51	0.00e+00	0.00e+00	3.02e+51	3.02e+51	2.74e+49	2.74e+49	1.75e+51	1.75e+51	0.00e+00	0.00e+00	0.00e+00
18	1.28e+51	4.66e+51	4.54e+51	1.98e+52	2.37e+52	2.80e+52	8.82e+52	3.73e+52	2.44e+52	4.14e+51	3.00e+51	3.63e+51	3.63e+51	1.39e+51	1.39e+51	1.75e+51	1.75e+51	0.00e+00	0.00e+00	0.00e+00
17	7.18e+50	5.32e+51	1.73e+52	3.68e+52	4.35e+52	1.22e+52	4.64e+52	3.67e+52	5.89e+52	4.67e+52	2.01e+52	9.14e+51	1.53e+51	1.07e+51	1.07e+51	0.00e+00	0.00e+00	0.00e+00	0.00e+00	0.00e+00
16	9.40e+51	0.00e+00	2.96e+52	4.23e+52	1.20e+53	1.68e+52	0.00e+00	0.00e+00	0.00e+00	7.50e+52	2.36e+52	0.00e+00	0.00e+00	7.67e+50	0.00e+00	1.94e+48	1.94e+48	0.00e+00	0.00e+00	0.00e+00
15	2.82e+51	2.12e+50	4.04e+52	6.03e+52	1.16e+53	1.21e+53	6.46e+52	0.00e+00	0.00e+00	3.56e+52	8.88e+52	1.74e+52	0.00e+00	0.00e+00	1.46e+51	0.00e+00	0.00e+00	0.00e+00	0.00e+00	0.00e+00
14	4.39e+51	4.82e+51	6.55e+52	4.50e+51	0.00e+00	1.15e+53	0.00e+00	0.00e+00	0.00e+00	0.00e+00	4.72e+52	3.44e+52	1.64e+52	4.15e+51	5.21e+51	5.64e+51	5.64e+51	0.00e+00	0.00e+00	0.00e+00
13	9.80e+51	2.45e+53	3.35e+52	0.00e+00	0.00e+00	1.45e+53	8.57e+51	0.00e+00	0.00e+00	0.00e+00	0.00e+00	3.12e+52	1.30e+52	4.39e+51	1.62e+51	4.81e+51	4.81e+51	1.71e+51	1.71e+51	1.71e+51
12	1.67e+52	3.40e+52	8.97e+52	6.68e+52	0.00e+00	0.00e+00	9.34e+52	0.00e+00	1.09e+53	1.09e+53	0.00e+00	0.00e+00	0.00e+00	0.00e+00	5.08e+51	0.00e+00	1.90e+51	0.00e+00	0.00e+00	0.00e+00
11	9.85e+51	4.21e+52	5.23e+52	3.53e+52	6.38e+52	0.00e+00	0.00e+00	0.00e+00	0.00e+00	0.00e+00	0.00e+00	0.00e+00	0.00e+00	0.00e+00	0.00e+00	2.93e+52	1.56e+51	0.00e+00	1.15e+51	1.15e+51
10	9.48e+52	1.10e+53	6.19e+52	6.05e+52	1.67e+52	0.00e+00	0.00e+00	0.00e+00	0.00e+00	0.00e+00	7.86e+52	1.77e+53	1.27e+53	5.22e+52	3.15e+52	3.31e+52	1.02e+52	0.00e+00	0.00e+00	2.22e+51
9	1.32e+53	1.36e+53	6.70e+52	7.30e+52	2.65e+52	2.34e+52	0.00e+00	0.00e+00	1.12e+52	2.49e+52	7.98e+52	2.18e+52	0.00e+00	0.00e+00	2.40e+52	6.61e+51	1.41e+52	4.79e+51	3.94e+50	2.22e+51
8	2.26e+52	0.00e+00	2.19e+52	4.80e+51	2.94e+52	3.70e+52	2.75e+52	2.44e+52	5.03e+52	0.00e+00	5.17e+51	2.09e+52	0.00e+00	0.00e+00	0.00e+00	3.83e+52	4.63e+52	4.10e+51	1.69e+51	4.71e+51
7	0.00e+00	1.33e+52	7.90e+51	1.53e+52	2.53e+52	1.79e+52	1.18e+52	1.64e+52	2.05e+52	1.17e+52	0.00e+00	0.00e+00	0.00e+00	0.00e+00	0.00e+00	3.57e+52	1.45e+52	1.50e+52	4.77e+51	0.00e+00
6	8.01e+50	3.87e+51	6.84e+51	0.00e+00	0.00e+00	0.00e+00	5.12e+51	9.92e+51	3.38e+51	0.00e+00	1.35e+52	2.27e+52	2.06e+52	2.63e+52	3.30e+52	4.27e+51	2.61e+52	3.35e+51	1.96e+52	2.68e+51
5	8.01e+50	3.87e+51	6.84e+51	0.00e+00	0.00e+00	0.00e+00	0.00e+00	5.24e+51	9.87e+50	0.00e+00	1.24e+51	4.75e+51	9.26e+51	0.00e+00	1.14e+52	1.02e+51	0.00e+00	0.00e+00	2.03e+51	6.49e+51
4	6.03e+51	6.03e+51	3.22e+51	6.58e+50	0.00e+00	7.31e+49	0.00e+00	1.91e+50	0.00e+00	0.00e+00	3.30e+51	1.88e+51	3.16e+51	3.13e+51	0.00e+00	7.49e+51	3.86e+51	1.41e+51	1.62e+51	7.95e+51
3	6.03e+51	6.03e+51	3.22e+51	6.58e+50	0.00e+00	0.00e+00	0.00e+00	0.00e+00	0.00e+00	0.00e+00	0.00e+00	1.18e+51	0.00e+00	1.51e+51	0.00e+00	1.18e+51	1.04e+50	0.00e+00	1.50e+51	1.02e+51
2	3.66e+50	3.66e+50	0.00e+00	0.00e+00	1.80e+51	0.00e+00	0.00e+00	0.00e+00	1.05e+51	0.00e+00	0.00e+00	2.10e+50	9.56e+50	0.00e+00	1.88e+51	0.00e+00	0.00e+00	0.00e+00	2.98e+51	7.26e+50
1	3.66e+50	3.66e+50	0.00e+00	0.00e+00	1.80e+51	0.00e+00	0.00e+00	0.00e+00	1.05e+51	0.00e+00	0.00e+00	2.10e+50	9.56e+50	0.00e+00	1.88e+51	0.00e+00	0.00e+00	0.00e+00	2.98e+51	7.26e+50

Table 6: Expected energy emission in erg by stars formed in the last 20 Myrs. Rows: DEC-Bin, Columns: RA-Bin (as in images), binsize $12' \times 12'$, conversion to coordinates in table 1.

	20	19	18	17	16	15	14	13	12	11	10	9	8	7	6	5	4	3	2	1
23	0.00e+00	0.00e+00	8.38e+50	0.00e+00	0.00e+00	1.90e+51	1.32e+51	4.11e+50	2.51e+51	2.71e+51	2.71e+51	0.00e+00	0.00e+00	4.13e+50	4.13e+50	0.00e+00	0.00e+00	1.79e+50	1.79e+50	0.00e+00
22	0.00e+00	0.00e+00	3.39e+51	4.04e+51	0.00e+00	0.00e+00	0.00e+00	3.50e+51	0.00e+00	2.71e+51	2.71e+51	0.00e+00	0.00e+00	4.13e+50	4.13e+50	0.00e+00	0.00e+00	1.79e+50	1.79e+50	0.00e+00
21	0.00e+00	0.00e+00	7.05e+50	3.79e+50	0.00e+00	0.00e+00	0.00e+00	0.00e+00	2.91e+51	0.00e+00	0.00e+00	0.00e+00	0.00e+00	0.00e+00	0.00e+00	6.30e+50	6.30e+50	1.00e+51	1.00e+51	0.00e+00
20	0.00e+00	1.43e+51	0.00e+00	0.00e+00	3.68e+51	2.38e+51	1.47e+51	7.95e+51	1.53e+50	0.00e+00	0.00e+00	9.37e+50	9.37e+50	0.00e+00	0.00e+00	6.30e+50	6.30e+50	1.00e+51	1.00e+51	0.00e+00
19	2.26e+51	0.00e+00	9.11e+51	1.36e+51	1.72e+52	1.52e+52	0.00e+00	1.80e+52	7.61e+51	0.00e+00	0.00e+00	3.51e+51	3.51e+51	2.74e+49	2.74e+49	1.75e+51	1.75e+51	1.00e+51	1.00e+51	0.00e+00
18	1.28e+51	4.66e+51	4.54e+51	1.98e+52	2.76e+52	3.25e+52	8.82e+52	4.35e+52	2.84e+52	4.82e+51	3.00e+51	3.80e+51	3.80e+51	1.61e+51	1.61e+51	1.75e+51	1.75e+51	0.00e+00	0.00e+00	0.00e+00
17	7.24e+50	5.32e+51	1.73e+52	3.68e+52	4.35e+52	2.84e+52	8.67e+52	6.05e+52	5.89e+52	5.06e+52	2.01e+52	1.06e+52	1.53e+51	1.25e+51	1.25e+51	0.00e+00	0.00e+00	0.00e+00	0.00e+00	0.00e+00
16	1.09e+52	4.33e+51	2.96e+52	4.60e+52	1.23e+53	1.84e+52	7.57e+51	0.00e+00	0.00e+00	8.73e+52	2.36e+52	1.53e+52	0.00e+00	8.93e+50	0.00e+00	1.94e+48	1.94e+48	0.00e+00	0.00e+00	0.00e+00
15	2.82e+51	1.12e+52	4.70e+52	8.35e+52	1.52e+53	1.21e+53	6.46e+52	5.30e+52	0.00e+00	1.02e+53	9.89e+52	1.74e+52	8.01e+51	0.00e+00	1.70e+51	0.00e+00	0.00e+00	0.00e+00	0.00e+00	0.00e+00
14	4.39e+51	5.22e+51	6.55e+52	5.24e+51	1.02e+52	1.84e+53	0.00e+00	0.00e+00	0.00e+00	0.00e+00	4.72e+52	4.01e+52	1.64e+52	4.15e+51	5.21e+51	5.64e+51	5.64e+51	0.00e+00	0.00e+00	0.00e+00
13	1.14e+52	2.61e+53	3.35e+52	4.11e+51	7.80e+51	2.55e+53	9.98e+51	0.00e+00	1.99e+53	0.00e+00	0.00e+00	3.63e+52	1.30e+52	4.39e+51	1.62e+51	5.61e+51	5.61e+51	1.99e+51	1.99e+51	1.99e+51
12	1.94e+52	3.96e+52	8.97e+52	7.25e+52	0.00e+00	0.00e+00	9.96e+52	0.00e+00	1.27e+53	2.96e+53	0.00e+00	0.00e+00	0.00e+00	0.00e+00	5.08e+51	0.00e+00	2.21e+51	0.00e+00	0.00e+00	0.00e+00
11	1.45e+52	4.90e+52	5.23e+52	3.96e+52	7.13e+52	2.47e+51	0.00e+00	0.00e+00	0.00e+00	1.26e+53	0.00e+00	0.00e+00	0.00e+00	0.00e+00	0.00e+00	3.41e+52	1.56e+51	0.00e+00	1.32e+51	1.32e+51
10	1.07e+53	1.10e+53	6.19e+52	6.05e+52	4.17e+52	0.00e+00	0.00e+00	0.00e+00	0.00e+00	1.22e+53	2.34e+53	2.48e+53	1.48e+53	5.22e+52	3.67e+52	3.85e+52	1.02e+52	0.00e+00	3.13e+51	2.22e+51
9	1.37e+53	1.36e+53	6.70e+52	7.30e+52	2.65e+52	2.34e+52	0.00e+00	0.00e+00	1.30e+52	2.90e+52	1.54e+53	2.18e+52	1.77e+52	0.00e+00	2.40e+52	1.87e+52	1.41e+52	4.79e+51	3.94e+50	2.22e+51
8	2.63e+52	0.00e+00	2.55e+52	1.84e+52	3.42e+52	4.31e+52	2.75e+52	2.44e+52	5.85e+52	0.00e+00	1.32e+52	2.09e+52	0.00e+00	5.37e+51	0.00e+00	4.47e+52	5.39e+52	4.77e+51	1.97e+51	4.71e+51
7	0.00e+00	1.69e+52	9.20e+51	1.79e+52	2.53e+52	1.79e+52	1.18e+52	1.92e+52	2.39e+52	1.36e+52	0.00e+00	3.79e+51	0.00e+00	0.00e+00	0.00e+00	3.57e+52	1.69e+52	1.75e+52	5.93e+51	0.00e+00
6	2.43e+51	4.50e+51	7.96e+51	2.77e+51	3.39e+51	0.00e+00	5.12e+51	9.92e+51	3.38e+51	7.71e+51	1.35e+52	2.64e+52	2.08e+52	3.07e+52	3.84e+52	4.97e+51	3.04e+52	3.90e+51	2.28e+52	4.33e+51
5	2.43e+51	4.50e+51	7.96e+51	2.77e+51	0.00e+00	7.50e+50	0.00e+00	5.24e+51	9.87e+50	0.00e+00	1.24e+51	4.75e+51	9.26e+51	0.00e+00	1.14e+52	1.02e+51	0.00e+00	8.09e+51	2.07e+51	7.17e+51
4	6.03e+51	6.03e+51	3.22e+51	6.58e+50	0.00e+00	7.31e+49	0.00e+00	1.91e+50	0.00e+00	0.00e+00	3.30e+51	1.88e+51	3.16e+51	3.13e+51	3.47e+51	7.49e+51	3.86e+51	1.41e+51	1.62e+51	8.65e+51
3	6.03e+51	6.03e+51	3.22e+51	6.58e+50	0.00e+00	0.00e+00	0.00e+00	0.00e+00	0.00e+00	0.00e+00	0.00e+00	1.37e+51	0.00e+00	1.51e+51	0.00e+00	1.18e+51	1.04e+50	0.00e+00	4.62e+51	1.19e+51
2	3.66e+50	3.66e+50	0.00e+00	0.00e+00	1.80e+51	0.00e+00	0.00e+00	0.00e+00	1.05e+51	0.00e+00	0.00e+00	2.10e+50	9.74e+50	0.00e+00	1.88e+51	0.00e+00	0.00e+00	0.00e+00	3.13e+51	8.45e+50
1	3.66e+50	3.66e+50	0.00e+00	0.00e+00	1.80e+51	0.00e+00	0.00e+00	0.00e+00	1.05e+51	0.00e+00	0.00e+00	2.10e+50	9.74e+50	0.00e+00	1.88e+51	0.00e+00	0.00e+00	0.00e+00	3.13e+51	8.45e+50

Table 7: Expected energy emission in erg by stars formed in the last 29 Myrs. Rows: DEC-Bin, Columns: RA-Bin (as in images), binsize $12' \times 12'$, conversion to coordinates in table 1.

	20	19	18	17	16	15	14	13	12	11	10	9	8	7	6	5	4	3	2	1
23	0.00e+00	0.00e+00	0.00e+00	0.00e+00	0.00e+00	0.00e+00	0.00e+00	0.00e+00	0.00e+00	0.00e+00	0.00e+00	0.00e+00	0.00e+00	0.00e+00	0.00e+00	0.00e+00	0.00e+00	0.00e+00	0.00e+00	0.00e+00
22	0.00e+00	0.00e+00	0.00e+00	0.00e+00	0.00e+00	0.00e+00	0.00e+00	0.00e+00	0.00e+00	0.00e+00	0.00e+00	0.00e+00	0.00e+00	0.00e+00	0.00e+00	0.00e+00	0.00e+00	0.00e+00	0.00e+00	0.00e+00
21	0.00e+00	0.00e+00	0.00e+00	0.00e+00	0.00e+00	0.00e+00	0.00e+00	0.00e+00	0.00e+00	0.00e+00	0.00e+00	0.00e+00	0.00e+00	0.00e+00	0.00e+00	0.00e+00	0.00e+00	0.00e+00	0.00e+00	0.00e+00
20	0.00e+00	0.00e+00	0.00e+00	0.00e+00	0.00e+00	0.00e+00	0.00e+00	0.00e+00	0.00e+00	0.00e+00	0.00e+00	0.00e+00	0.00e+00	0.00e+00	0.00e+00	0.00e+00	0.00e+00	0.00e+00	0.00e+00	0.00e+00
19	0.00e+00	0.00e+00	0.00e+00	0.00e+00	0.00e+00	0.00e+00	0.00e+00	0.00e+00	0.00e+00	0.00e+00	0.00e+00	0.00e+00	0.00e+00	0.00e+00	0.00e+00	0.00e+00	0.00e+00	0.00e+00	0.00e+00	0.00e+00
18	1.96e+48	1.96e+48	6.54e+47	2.63e+49	0.00e+00	0.00e+00	0.00e+00	0.00e+00	0.00e+00	0.00e+00	0.00e+00	0.00e+00	0.00e+00	0.00e+00	0.00e+00	0.00e+00	0.00e+00	0.00e+00	0.00e+00	0.00e+00
17	0.00e+00	0.00e+00	0.00e+00	0.00e+00	0.00e+00	0.00e+00	0.00e+00	0.00e+00	0.00e+00	5.40e+50	0.00e+00	0.00e+00	0.00e+00	0.00e+00	0.00e+00	0.00e+00	0.00e+00	0.00e+00	0.00e+00	0.00e+00
16	0.00e+00	0.00e+00	0.00e+00	3.95e+48	0.00e+00	0.00e+00	0.00e+00	0.00e+00	0.00e+00	0.00e+00	7.37e+50	0.00e+00	0.00e+00	0.00e+00	0.00e+00	0.00e+00	0.00e+00	0.00e+00	0.00e+00	0.00e+00
15	1.96e+48	0.00e+00	0.00e+00	0.00e+00	0.00e+00	2.25e+51	1.08e+50	0.00e+00	0.00e+00	0.00e+00	0.00e+00	3.78e+50	0.00e+00	0.00e+00	0.00e+00	0.00e+00	0.00e+00	0.00e+00	0.00e+00	0.00e+00
14	0.00e+00	0.00e+00	0.00e+00	0.00e+00	0.00e+00	0.00e+00	0.00e+00	0.00e+00	0.00e+00	0.00e+00	0.00e+00	0.00e+00	0.00e+00	5.27e+48	0.00e+00	0.00e+00	0.00e+00	0.00e+00	0.00e+00	0.00e+00
13	0.00e+00	0.00e+00	0.00e+00	0.00e+00	0.00e+00	0.00e+00	0.00e+00	0.00e+00	0.00e+00	0.00e+00	0.00e+00	0.00e+00	0.00e+00	0.00e+00	1.32e+47	0.00e+00	0.00e+00	0.00e+00	0.00e+00	0.00e+00
12	0.00e+00	0.00e+00	0.00e+00	0.00e+00	0.00e+00	0.00e+00	0.00e+00	0.00e+00	0.00e+00	4.77e+51	0.00e+00	0.00e+00	0.00e+00	0.00e+00	0.00e+00	0.00e+00	0.00e+00	0.00e+00	0.00e+00	0.00e+00
11	0.00e+00	0.00e+00	0.00e+00	0.00e+00	0.00e+00	0.00e+00	0.00e+00	0.00e+00	0.00e+00	0.00e+00	0.00e+00	0.00e+00	0.00e+00	0.00e+00	0.00e+00	0.00e+00	0.00e+00	0.00e+00	0.00e+00	0.00e+00
10	0.00e+00	0.00e+00	0.00e+00	0.00e+00	0.00e+00	0.00e+00	0.00e+00	0.00e+00	0.00e+00	0.00e+00	0.00e+00	0.00e+00	0.00e+00	1.32e+51	0.00e+00	0.00e+00	8.95e+49	0.00e+00	0.00e+00	0.00e+00
9	0.00e+00	0.00e+00	0.00e+00	0.00e+00	0.00e+00	0.00e+00	0.00e+00	0.00e+00	0.00e+00	0.00e+00	0.00e+00	0.00e+00	0.00e+00	0.00e+00	0.00e+00	0.00e+00	2.05e+50	0.00e+00	0.00e+00	0.00e+00
8	0.00e+00	0.00e+00	0.00e+00	0.00e+00	0.00e+00	0.00e+00	0.00e+00	0.00e+00	0.00e+00	0.00e+00	0.00e+00	0.00e+00	0.00e+00	0.00e+00	0.00e+00	0.00e+00	0.00e+00	0.00e+00	0.00e+00	0.00e+00
7	0.00e+00	0.00e+00	0.00e+00	0.00e+00	0.00e+00	0.00e+00	0.00e+00	0.00e+00	0.00e+00	0.00e+00	0.00e+00	0.00e+00	0.00e+00	0.00e+00	0.00e+00	0.00e+00	0.00e+00	0.00e+00	0.00e+00	0.00e+00
6	0.00e+00	0.00e+00	0.00e+00	0.00e+00	0.00e+00	0.00e+00	0.00e+00	0.00e+00	0.00e+00	0.00e+00	0.00e+00	0.00e+00	0.00e+00	0.00e+00	0.00e+00	0.00e+00	0.00e+00	0.00e+00	0.00e+00	0.00e+00
5	0.00e+00	0.00e+00	0.00e+00	0.00e+00	0.00e+00	0.00e+00	0.00e+00	0.00e+00	0.00e+00	0.00e+00	0.00e+00	0.00e+00	0.00e+00	0.00e+00	0.00e+00	0.00e+00	0.00e+00	0.00e+00	1.31e+48	0.00e+00
4	0.00e+00	0.00e+00	0.00e+00	0.00e+00	0.00e+00	0.00e+00	0.00e+00	0.00e+00	0.00e+00	0.00e+00	0.00e+00	0.00e+00	3.95e+48	0.00e+00	0.00e+00	0.00e+00	0.00e+00	1.32e+47	0.00e+00	0.00e+00
3	0.00e+00	0.00e+00	0.00e+00	0.00e+00	0.00e+00	0.00e+00	0.00e+00	0.00e+00	0.00e+00	0.00e+00	0.00e+00	0.00e+00	0.00e+00	0.00e+00	0.00e+00	0.00e+00	0.00e+00	0.00e+00	0.00e+00	0.00e+00
2	0.00e+00	0.00e+00	0.00e+00	0.00e+00	0.00e+00	0.00e+00	0.00e+00	0.00e+00	0.00e+00	0.00e+00	0.00e+00	0.00e+00	0.00e+00	0.00e+00	0.00e+00	0.00e+00	0.00e+00	0.00e+00	0.00e+00	0.00e+00
1	0.00e+00	0.00e+00	0.00e+00	0.00e+00	0.00e+00	0.00e+00	0.00e+00	0.00e+00	0.00e+00	0.00e+00	0.00e+00	0.00e+00	0.00e+00	0.00e+00	0.00e+00	0.00e+00	0.00e+00	0.00e+00	0.00e+00	0.00e+00

Table 8: Lower limit energy emission in erg by stars formed in the last 4 Myrs. Rows: DEC-Bin, Columns: RA-Bin (as in images), binsize $12' \times 12'$, conversion to coordinates in table 1.

	20	19	18	17	16	15	14	13	12	11	10	9	8	7	6	5	4	3	2	1
23	0.00e+00	0.00e+00	0.00e+00	0.00e+00	0.00e+00	0.00e+00	3.71e+48	0.00e+00	0.00e+00	0.00e+00	0.00e+00	0.00e+00	0.00e+00	0.00e+00	0.00e+00	0.00e+00	0.00e+00	0.00e+00	0.00e+00	0.00e+00
22	0.00e+00	0.00e+00	0.00e+00	0.00e+00	0.00e+00	0.00e+00	0.00e+00	0.00e+00	0.00e+00	0.00e+00	0.00e+00	0.00e+00	0.00e+00	0.00e+00	0.00e+00	0.00e+00	0.00e+00	0.00e+00	0.00e+00	0.00e+00
21	0.00e+00	0.00e+00	0.00e+00	0.00e+00	0.00e+00	0.00e+00	0.00e+00	0.00e+00	0.00e+00	0.00e+00	0.00e+00	0.00e+00	0.00e+00	0.00e+00	0.00e+00	0.00e+00	0.00e+00	0.00e+00	0.00e+00	0.00e+00
20	0.00e+00	0.00e+00	0.00e+00	0.00e+00	4.95e+48	0.00e+00	0.00e+00	9.94e+49	0.00e+00	0.00e+00	0.00e+00	1.24e+49	1.24e+49	0.00e+00	0.00e+00	0.00e+00	0.00e+00	0.00e+00	0.00e+00	0.00e+00
19	0.00e+00	0.00e+00	0.00e+00	0.00e+00	7.46e+48	0.00e+00	0.00e+00	0.00e+00	0.00e+00	0.00e+00	0.00e+00	0.00e+00	0.00e+00	0.00e+00	0.00e+00	9.94e+48	9.94e+48	0.00e+00	0.00e+00	0.00e+00
18	2.89e+49	2.89e+49	9.63e+48	3.88e+50	0.00e+00	0.00e+00	0.00e+00	0.00e+00	0.00e+00	0.00e+00	0.00e+00	0.00e+00	0.00e+00	0.00e+00	0.00e+00	9.94e+48	9.94e+48	0.00e+00	0.00e+00	0.00e+00
17	0.00e+00	4.95e+49	0.00e+00	0.00e+00	0.00e+00	0.00e+00	0.00e+00	0.00e+00	0.00e+00	7.95e+51	0.00e+00	0.00e+00	0.00e+00	0.00e+00	0.00e+00	0.00e+00	0.00e+00	0.00e+00	0.00e+00	0.00e+00
16	0.00e+00	0.00e+00	0.00e+00	5.81e+49	2.49e+49	0.00e+00	0.00e+00	0.00e+00	0.00e+00	0.00e+00	1.09e+52	0.00e+00	0.00e+00	0.00e+00	0.00e+00	0.00e+00	0.00e+00	0.00e+00	0.00e+00	0.00e+00
15	2.89e+49	0.00e+00	0.00e+00	0.00e+00	0.00e+00	3.31e+52	1.59e+51	0.00e+00	0.00e+00	0.00e+00	0.00e+00	5.56e+51	0.00e+00	0.00e+00	0.00e+00	0.00e+00	0.00e+00	0.00e+00	0.00e+00	0.00e+00
14	3.71e+49	0.00e+00	9.45e+51	0.00e+00	0.00e+00	9.02e+51	0.00e+00	0.00e+00	0.00e+00	0.00e+00	0.00e+00	0.00e+00	1.24e+51	7.75e+49	0.00e+00	0.00e+00	0.00e+00	0.00e+00	0.00e+00	0.00e+00
13	0.00e+00	0.00e+00	0.00e+00	0.00e+00	0.00e+00	3.71e+49	0.00e+00	0.00e+00	0.00e+00	0.00e+00	0.00e+00	0.00e+00	9.94e+49	3.71e+49	1.94e+48	0.00e+00	0.00e+00	0.00e+00	0.00e+00	0.00e+00
12	0.00e+00	0.00e+00	0.00e+00	0.00e+00	0.00e+00	0.00e+00	0.00e+00	0.00e+00	0.00e+00	7.03e+52	0.00e+00	0.00e+00	0.00e+00	0.00e+00	0.00e+00	0.00e+00	0.00e+00	0.00e+00	0.00e+00	0.00e+00
11	0.00e+00	0.00e+00	0.00e+00	0.00e+00	0.00e+00	0.00e+00	0.00e+00	0.00e+00	0.00e+00	0.00e+00	0.00e+00	0.00e+00	0.00e+00	0.00e+00	0.00e+00	0.00e+00	0.00e+00	0.00e+00	0.00e+00	0.00e+00
10	0.00e+00	0.00e+00	0.00e+00	0.00e+00	0.00e+00	0.00e+00	0.00e+00	0.00e+00	0.00e+00	0.00e+00	4.97e+50	4.65e+52	0.00e+00	1.95e+52	0.00e+00	0.00e+00	1.32e+51	0.00e+00	0.00e+00	0.00e+00
9	0.00e+00	0.00e+00	0.00e+00	0.00e+00	0.00e+00	0.00e+00	0.00e+00	0.00e+00	0.00e+00	0.00e+00	1.24e+50	0.00e+00	0.00e+00	0.00e+00	0.00e+00	0.00e+00	3.02e+51	0.00e+00	0.00e+00	0.00e+00
8	0.00e+00	0.00e+00	0.00e+00	0.00e+00	0.00e+00	0.00e+00	0.00e+00	0.00e+00	0.00e+00	0.00e+00	0.00e+00	0.00e+00	0.00e+00	0.00e+00	0.00e+00	0.00e+00	0.00e+00	0.00e+00	0.00e+00	0.00e+00
7	0.00e+00	0.00e+00	0.00e+00	0.00e+00	0.00e+00	2.49e+49	0.00e+00	0.00e+00	0.00e+00	0.00e+00	0.00e+00	0.00e+00	0.00e+00	0.00e+00	0.00e+00	0.00e+00	0.00e+00	0.00e+00	0.00e+00	0.00e+00
6	2.47e+48	0.00e+00	0.00e+00	0.00e+00	0.00e+00	0.00e+00	4.97e+49	0.00e+00	0.00e+00	0.00e+00	0.00e+00	0.00e+00	1.27e+51	0.00e+00	0.00e+00	0.00e+00	0.00e+00	0.00e+00	0.00e+00	0.00e+00
5	2.47e+48	0.00e+00	0.00e+00	0.00e+00	0.00e+00	0.00e+00	0.00e+00	0.00e+00	0.00e+00	0.00e+00	4.97e+48	9.94e+49	0.00e+00	0.00e+00	0.00e+00	0.00e+00	0.00e+00	0.00e+00	2.17e+49	4.95e+49
4	4.97e+49	4.97e+49	1.24e+49	9.94e+48	0.00e+00	0.00e+00	0.00e+00	0.00e+00	0.00e+00	0.00e+00	0.00e+00	2.49e+48	5.81e+49	0.00e+00	0.00e+00	9.94e+49	0.00e+00	4.41e+48	1.24e+48	0.00e+00
3	4.97e+49	4.97e+49	1.24e+49	9.94e+48	0.00e+00	0.00e+00	0.00e+00	0.00e+00	0.00e+00	0.00e+00	0.00e+00	0.00e+00	0.00e+00	2.49e+48	0.00e+00	0.00e+00	0.00e+00	0.00e+00	0.00e+00	0.00e+00
2	0.00e+00	0.00e+00	0.00e+00	0.00e+00	0.00e+00	0.00e+00	0.00e+00	0.00e+00	0.00e+00	0.00e+00	0.00e+00	0.00e+00	0.00e+00	0.00e+00	0.00e+00	0.00e+00	0.00e+00	0.00e+00	0.00e+00	0.00e+00
1	0.00e+00	0.00e+00	0.00e+00	0.00e+00	0.00e+00	0.00e+00	0.00e+00	0.00e+00	0.00e+00	0.00e+00	0.00e+00	0.00e+00	0.00e+00	0.00e+00	0.00e+00	0.00e+00	0.00e+00	0.00e+00	0.00e+00	0.00e+00

Table 9: Lower limit energy emission in erg by stars formed in the last 7 Myrs. Rows: DEC-Bin, Columns: RA-Bin (as in images), binsize $12' \times 12'$, conversion to coordinates in table 1.

	20	19	18	17	16	15	14	13	12	11	10	9	8	7	6	5	4	3	2	1
23	0.00e+00	0.00e+00	0.00e+00	0.00e+00	0.00e+00	0.00e+00	6.82e+48	0.00e+00	0.00e+00	0.00e+00	0.00e+00	0.00e+00	0.00e+00	0.00e+00	0.00e+00	0.00e+00	0.00e+00	0.00e+00	0.00e+00	0.00e+00
22	0.00e+00	0.00e+00	0.00e+00	0.00e+00	0.00e+00	0.00e+00	0.00e+00	0.00e+00	0.00e+00	0.00e+00	0.00e+00	0.00e+00	0.00e+00	0.00e+00	0.00e+00	0.00e+00	0.00e+00	0.00e+00	0.00e+00	0.00e+00
21	0.00e+00	0.00e+00	3.57e+48	0.00e+00	0.00e+00	0.00e+00	0.00e+00	0.00e+00	0.00e+00	0.00e+00	0.00e+00	0.00e+00	0.00e+00	0.00e+00	0.00e+00	0.00e+00	0.00e+00	0.00e+00	0.00e+00	0.00e+00
20	0.00e+00	2.38e+48	0.00e+00	0.00e+00	9.09e+48	0.00e+00	0.00e+00	1.83e+50	0.00e+00	0.00e+00	0.00e+00	2.28e+49	2.28e+49	0.00e+00	0.00e+00	0.00e+00	0.00e+00	0.00e+00	0.00e+00	0.00e+00
19	0.00e+00	0.00e+00	0.00e+00	0.00e+00	1.37e+49	0.00e+00	0.00e+00	0.00e+00	0.00e+00	0.00e+00	0.00e+00	0.00e+00	0.00e+00	0.00e+00	0.00e+00	1.83e+49	1.83e+49	0.00e+00	0.00e+00	0.00e+00
18	2.89e+49	2.89e+49	9.63e+48	3.88e+50	0.00e+00	0.00e+00	2.08e+52	0.00e+00	0.00e+00	0.00e+00	0.00e+00	9.57e+48	9.57e+48	0.00e+00	0.00e+00	1.83e+49	1.83e+49	0.00e+00	0.00e+00	0.00e+00
17	0.00e+00	9.09e+49	0.00e+00	3.85e+51	5.31e+51	0.00e+00	4.81e+51	4.55e+50	1.03e+52	7.95e+51	9.57e+49	0.00e+00	0.00e+00	0.00e+00	0.00e+00	0.00e+00	0.00e+00	0.00e+00	0.00e+00	0.00e+00
16	0.00e+00	0.00e+00	0.00e+00	6.53e+49	2.49e+52	0.00e+00	0.00e+00	0.00e+00	0.00e+00	0.00e+00	1.09e+52	0.00e+00	0.00e+00	0.00e+00	0.00e+00	0.00e+00	0.00e+00	0.00e+00	0.00e+00	0.00e+00
15	2.89e+49	0.00e+00	0.00e+00	9.81e+51	3.28e+51	3.31e+52	1.59e+51	0.00e+00	0.00e+00	0.00e+00	2.39e+49	5.56e+51	0.00e+00	0.00e+00	0.00e+00	0.00e+00	0.00e+00	0.00e+00	0.00e+00	0.00e+00
14	6.82e+49	0.00e+00	1.74e+52	0.00e+00	0.00e+00	1.66e+52	0.00e+00	0.00e+00	0.00e+00	0.00e+00	3.64e+51	0.00e+00	2.28e+51	7.75e+49	0.00e+00	0.00e+00	0.00e+00	0.00e+00	0.00e+00	0.00e+00
13	0.00e+00	6.61e+52	1.46e+51	0.00e+00	0.00e+00	1.16e+50	0.00e+00	0.00e+00	0.00e+00	0.00e+00	0.00e+00	0.00e+00	1.83e+50	6.82e+49	1.94e+48	0.00e+00	0.00e+00	0.00e+00	0.00e+00	0.00e+00
12	0.00e+00	0.00e+00	1.94e+52	0.00e+00	0.00e+00	0.00e+00	3.83e+50	0.00e+00	0.00e+00	7.03e+52	0.00e+00	0.00e+00	0.00e+00	0.00e+00	0.00e+00	0.00e+00	0.00e+00	0.00e+00	0.00e+00	0.00e+00
11	0.00e+00	0.00e+00	8.43e+51	0.00e+00	0.00e+00	0.00e+00	0.00e+00	0.00e+00	0.00e+00	0.00e+00	0.00e+00	0.00e+00	0.00e+00	0.00e+00	0.00e+00	0.00e+00	0.00e+00	0.00e+00	0.00e+00	0.00e+00
10	2.25e+52	2.87e+52	1.35e+52	1.06e+52	0.00e+00	0.00e+00	0.00e+00	0.00e+00	0.00e+00	0.00e+00	9.14e+50	8.54e+52	0.00e+00	1.95e+52	0.00e+00	0.00e+00	1.32e+51	0.00e+00	0.00e+00	0.00e+00
9	2.54e+52	3.18e+52	1.46e+52	1.52e+52	2.39e+49	0.00e+00	0.00e+00	0.00e+00	0.00e+00	0.00e+00	2.52e+50	0.00e+00	0.00e+00	0.00e+00	0.00e+00	0.00e+00	3.02e+51	1.19e+49	0.00e+00	0.00e+00
8	0.00e+00	0.00e+00	0.00e+00	0.00e+00	0.00e+00	0.00e+00	9.57e+49	4.79e+49	0.00e+00	0.00e+00	0.00e+00	0.00e+00	0.00e+00	0.00e+00	0.00e+00	0.00e+00	0.00e+00	0.00e+00	0.00e+00	0.00e+00
7	0.00e+00	0.00e+00	0.00e+00	0.00e+00	2.01e+51	4.57e+49	0.00e+00	0.00e+00	0.00e+00	0.00e+00	0.00e+00	0.00e+00	0.00e+00	0.00e+00	0.00e+00	3.49e+51	0.00e+00	0.00e+00	0.00e+00	0.00e+00
6	4.54e+48	0.00e+00	0.00e+00	0.00e+00	0.00e+00	0.00e+00	9.14e+49	1.20e+50	4.76e+48	0.00e+00	9.57e+49	0.00e+00	2.33e+51	0.00e+00	0.00e+00	0.00e+00	0.00e+00	0.00e+00	0.00e+00	0.00e+00
5	4.54e+48	0.00e+00	0.00e+00	0.00e+00	0.00e+00	0.00e+00	0.00e+00	7.18e+48	0.00e+00	0.00e+00	9.14e+48	1.83e+50	0.00e+00	0.00e+00	1.20e+50	0.00e+00	0.00e+00	0.00e+00	2.38e+49	9.09e+49
4	9.14e+49	9.14e+49	2.28e+49	1.83e+49	0.00e+00	0.00e+00	0.00e+00	0.00e+00	0.00e+00	0.00e+00	0.00e+00	4.57e+48	5.81e+49	0.00e+00	0.00e+00	1.83e+50	0.00e+00	6.48e+48	2.27e+48	0.00e+00
3	9.14e+49	9.14e+49	2.28e+49	1.83e+49	0.00e+00	0.00e+00	0.00e+00	0.00e+00	0.00e+00	0.00e+00	0.00e+00	0.00e+00	0.00e+00	4.57e+48	0.00e+00	0.00e+00	0.00e+00	0.00e+00	0.00e+00	0.00e+00
2	0.00e+00	0.00e+00	0.00e+00	0.00e+00	0.00e+00	0.00e+00	0.00e+00	0.00e+00	0.00e+00	0.00e+00	0.00e+00	0.00e+00	0.00e+00	0.00e+00	0.00e+00	0.00e+00	0.00e+00	0.00e+00	0.00e+00	0.00e+00
1	0.00e+00	0.00e+00	0.00e+00	0.00e+00	0.00e+00	0.00e+00	0.00e+00	0.00e+00	0.00e+00	0.00e+00	0.00e+00	0.00e+00	0.00e+00	0.00e+00	0.00e+00	0.00e+00	0.00e+00	0.00e+00	0.00e+00	0.00e+00

Table 10: Lower limit energy emission in erg by stars formed in the last 10 Myrs. Rows: DEC-Bin, Columns: RA-Bin (as in images), binsize $12' \times 12'$, conversion to coordinates in table 1.

	20	19	18	17	16	15	14	13	12	11	10	9	8	7	6	5	4	3	2	1
23	0.00e+00	0.00e+00	0.00e+00	0.00e+00	0.00e+00	0.00e+00	6.82e+48	0.00e+00	1.27e+48	2.56e+48	2.56e+48	0.00e+00	0.00e+00	0.00e+00	0.00e+00	0.00e+00	0.00e+00	0.00e+00	0.00e+00	0.00e+00
22	0.00e+00	0.00e+00	0.00e+00	1.02e+49	0.00e+00	0.00e+00	0.00e+00	0.00e+00	0.00e+00	2.56e+48	2.56e+48	0.00e+00	0.00e+00	0.00e+00	0.00e+00	0.00e+00	0.00e+00	0.00e+00	0.00e+00	0.00e+00
21	0.00e+00	0.00e+00	1.10e+49	0.00e+00	0.00e+00	0.00e+00	0.00e+00	0.00e+00	0.00e+00	0.00e+00	0.00e+00	0.00e+00	0.00e+00	0.00e+00	0.00e+00	0.00e+00	0.00e+00	0.00e+00	0.00e+00	0.00e+00
20	0.00e+00	7.31e+48	0.00e+00	0.00e+00	9.09e+48	0.00e+00	0.00e+00	1.83e+50	0.00e+00	0.00e+00	0.00e+00	2.28e+49	2.28e+49	0.00e+00	0.00e+00	0.00e+00	0.00e+00	0.00e+00	0.00e+00	0.00e+00
19	0.00e+00	0.00e+00	1.28e+49	0.00e+00	9.04e+49	0.00e+00	0.00e+00	0.00e+00	0.00e+00	0.00e+00	0.00e+00	0.00e+00	0.00e+00	0.00e+00	0.00e+00	1.83e+49	1.83e+49	0.00e+00	0.00e+00	0.00e+00
18	2.89e+49	2.89e+49	9.63e+48	3.88e+50	8.95e+50	1.79e+50	6.39e+52	4.86e+51	2.35e+51	0.00e+00	0.00e+00	3.45e+49	3.45e+49	0.00e+00	0.00e+00	1.83e+49	1.83e+49	0.00e+00	0.00e+00	0.00e+00
17	0.00e+00	9.09e+49	0.00e+00	1.18e+52	1.63e+52	0.00e+00	1.48e+52	1.40e+51	3.17e+52	8.92e+51	2.94e+50	0.00e+00	0.00e+00	0.00e+00	0.00e+00	0.00e+00	0.00e+00	0.00e+00	0.00e+00	0.00e+00
16	2.56e+48	0.00e+00	0.00e+00	8.02e+49	7.65e+52	1.02e+49	0.00e+00	0.00e+00	0.00e+00	1.18e+52	1.09e+52	0.00e+00	0.00e+00	0.00e+00	0.00e+00	0.00e+00	0.00e+00	0.00e+00	0.00e+00	0.00e+00
15	2.89e+49	0.00e+00	5.12e+51	3.01e+52	1.01e+52	3.31e+52	1.59e+51	0.00e+00	0.00e+00	0.00e+00	9.79e+51	5.56e+51	0.00e+00	0.00e+00	0.00e+00	0.00e+00	0.00e+00	0.00e+00	0.00e+00	0.00e+00
14	6.82e+49	0.00e+00	1.74e+52	0.00e+00	0.00e+00	1.98e+52	0.00e+00	0.00e+00	0.00e+00	0.00e+00	1.12e+52	4.12e+51	2.28e+51	7.75e+49	0.00e+00	0.00e+00	0.00e+00	0.00e+00	0.00e+00	0.00e+00
13	2.56e+48	2.03e+53	4.48e+51	0.00e+00	0.00e+00	1.33e+52	0.00e+00	0.00e+00	0.00e+00	0.00e+00	0.00e+00	2.30e+50	1.83e+50	6.82e+49	1.94e+48	0.00e+00	0.00e+00	0.00e+00	0.00e+00	0.00e+00
12	0.00e+00	3.50e+51	5.95e+52	6.14e+50	0.00e+00	0.00e+00	1.18e+51	0.00e+00	1.61e+52	7.03e+52	0.00e+00	0.00e+00	0.00e+00	0.00e+00	0.00e+00	0.00e+00	0.00e+00	0.00e+00	0.00e+00	0.00e+00
11	7.67e+48	5.55e+51	2.59e+52	5.12e+49	2.61e+51	0.00e+00	0.00e+00	0.00e+00	0.00e+00	0.00e+00	0.00e+00	0.00e+00	0.00e+00	0.00e+00	0.00e+00	3.84e+51	0.00e+00	0.00e+00	5.12e+48	5.12e+48
10	6.91e+52	8.82e+52	4.14e+52	3.26e+52	0.00e+00	0.00e+00	0.00e+00	0.00e+00	0.00e+00	0.00e+00	9.14e+50	8.54e+52	1.41e+52	1.95e+52	5.12e+49	4.30e+51	1.32e+51	0.00e+00	0.00e+00	0.00e+00
9	7.97e+52	9.77e+52	4.50e+52	4.66e+52	7.35e+49	0.00e+00	0.00e+00	0.00e+00	2.56e+49	0.00e+00	3.79e+50	0.00e+00	0.00e+00	0.00e+00	0.00e+00	0.00e+00	3.02e+51	3.65e+49	0.00e+00	0.00e+00
8	8.70e+50	0.00e+00	0.00e+00	0.00e+00	2.56e+49	3.50e+51	2.94e+50	1.47e+50	2.51e+51	0.00e+00	0.00e+00	0.00e+00	0.00e+00	0.00e+00	0.00e+00	4.60e+51	7.14e+51	0.00e+00	0.00e+00	0.00e+00
7	0.00e+00	5.12e+49	7.67e+48	5.12e+49	6.17e+51	4.57e+49	0.00e+00	7.67e+49	7.67e+49	0.00e+00	0.00e+00	0.00e+00	0.00e+00	0.00e+00	0.00e+00	1.07e+52	1.02e+50	0.00e+00	7.67e+48	0.00e+00
6	4.54e+48	7.67e+48	2.56e+48	0.00e+00	0.00e+00	0.00e+00	9.14e+49	3.67e+50	1.46e+49	0.00e+00	2.94e+50	1.66e+51	2.33e+51	2.58e+51	3.25e+51	7.67e+48	2.30e+50	5.12e+48	1.02e+50	0.00e+00
5	4.54e+48	7.67e+48	2.56e+48	0.00e+00	0.00e+00	0.00e+00	0.00e+00	2.20e+49	0.00e+00	0.00e+00	9.14e+48	1.83e+50	0.00e+00	0.00e+00	3.67e+50	0.00e+00	0.00e+00	0.00e+00	2.38e+49	9.47e+49
4	9.14e+49	9.14e+49	2.28e+49	1.83e+49	0.00e+00	0.00e+00	0.00e+00	0.00e+00	0.00e+00	0.00e+00	0.00e+00	4.57e+48	5.81e+49	0.00e+00	0.00e+00	1.83e+50	0.00e+00	6.48e+48	2.27e+48	0.00e+00
3	9.14e+49	9.14e+49	2.28e+49	1.83e+49	0.00e+00	0.00e+00	0.00e+00	0.00e+00	0.00e+00	0.00e+00	0.00e+00	0.00e+00	0.00e+00	4.57e+48	0.00e+00	0.00e+00	0.00e+00	0.00e+00	0.00e+00	5.08e+48
2	0.00e+00	0.00e+00	0.00e+00	0.00e+00	0.00e+00	0.00e+00	0.00e+00	0.00e+00	0.00e+00	0.00e+00	0.00e+00	0.00e+00	0.00e+00	0.00e+00	0.00e+00	0.00e+00	0.00e+00	0.00e+00	0.00e+00	6.35e+48
1	0.00e+00	0.00e+00	0.00e+00	0.00e+00	0.00e+00	0.00e+00	0.00e+00	0.00e+00	0.00e+00	0.00e+00	0.00e+00	0.00e+00	0.00e+00	0.00e+00	0.00e+00	0.00e+00	0.00e+00	0.00e+00	0.00e+00	6.35e+48

Table 11: Lower limit energy emission in erg by stars formed in the last 15 Myrs. Rows: DEC-Bin, Columns: RA-Bin (as in images), binsize $12' \times 12'$, conversion to coordinates in table 1.

	20	19	18	17	16	15	14	13	12	11	10	9	8	7	6	5	4	3	2	1
23	0.00e+00	0.00e+00	0.00e+00	0.00e+00	0.00e+00	0.00e+00	6.82e+48	0.00e+00	5.01e+48	1.01e+49	1.01e+49	0.00e+00	0.00e+00	0.00e+00	0.00e+00	0.00e+00	0.00e+00	0.00e+00	0.00e+00	0.00e+00
22	0.00e+00	0.00e+00	0.00e+00	4.04e+49	0.00e+00	0.00e+00	0.00e+00	0.00e+00	0.00e+00	1.01e+49	1.01e+49	0.00e+00	0.00e+00	0.00e+00	0.00e+00	0.00e+00	0.00e+00	0.00e+00	0.00e+00	0.00e+00
21	0.00e+00	0.00e+00	1.10e+49	0.00e+00	0.00e+00	0.00e+00	0.00e+00	0.00e+00	0.00e+00	0.00e+00	0.00e+00	0.00e+00	0.00e+00	0.00e+00	0.00e+00	0.00e+00	0.00e+00	0.00e+00	0.00e+00	0.00e+00
20	0.00e+00	7.31e+48	0.00e+00	0.00e+00	9.09e+48	0.00e+00	0.00e+00	1.83e+50	0.00e+00	0.00e+00	0.00e+00	2.28e+49	2.28e+49	0.00e+00	0.00e+00	0.00e+00	0.00e+00	0.00e+00	0.00e+00	0.00e+00
19	0.00e+00	0.00e+00	5.05e+49	0.00e+00	3.16e+50	0.00e+00	0.00e+00	0.00e+00	0.00e+00	0.00e+00	0.00e+00	0.00e+00	0.00e+00	0.00e+00	0.00e+00	1.83e+49	1.83e+49	0.00e+00	0.00e+00	0.00e+00
18	2.89e+49	2.89e+49	9.63e+48	3.88e+50	3.53e+51	7.06e+50	6.39e+52	1.92e+52	9.28e+51	0.00e+00	0.00e+00	4.96e+49	4.96e+49	0.00e+00	0.00e+00	1.83e+49	1.83e+49	0.00e+00	0.00e+00	0.00e+00
17	0.00e+00	9.09e+49	0.00e+00	1.18e+52	1.63e+52	0.00e+00	1.48e+52	1.40e+51	3.17e+52	1.18e+52	2.94e+50	0.00e+00	0.00e+00	0.00e+00	0.00e+00	0.00e+00	0.00e+00	0.00e+00	0.00e+00	0.00e+00
16	1.01e+49	0.00e+00	0.00e+00	8.02e+49	7.65e+52	4.04e+49	0.00e+00	0.00e+00	0.00e+00	4.67e+52	1.09e+52	0.00e+00	0.00e+00	0.00e+00	0.00e+00	0.00e+00	0.00e+00	0.00e+00	0.00e+00	0.00e+00
15	2.89e+49	0.00e+00	2.02e+52	3.01e+52	1.01e+52	3.31e+52	1.59e+51	0.00e+00	0.00e+00	0.00e+00	3.84e+52	5.56e+51	0.00e+00	0.00e+00	0.00e+00	0.00e+00	0.00e+00	0.00e+00	0.00e+00	0.00e+00
14	6.82e+49	0.00e+00	1.74e+52	0.00e+00	0.00e+00	2.94e+52	0.00e+00	0.00e+00	0.00e+00	0.00e+00	1.12e+52	1.62e+52	2.28e+51	7.75e+49	0.00e+00	0.00e+00	0.00e+00	0.00e+00	0.00e+00	0.00e+00
13	1.01e+49	2.03e+53	4.48e+51	0.00e+00	0.00e+00	5.17e+52	0.00e+00	0.00e+00	0.00e+00	0.00e+00	0.00e+00	9.08e+50	1.83e+50	6.82e+49	1.94e+48	0.00e+00	0.00e+00	0.00e+00	0.00e+00	0.00e+00
12	0.00e+00	1.38e+52	5.95e+52	2.42e+51	0.00e+00	0.00e+00	1.18e+51	0.00e+00	6.36e+52	7.03e+52	0.00e+00	0.00e+00	0.00e+00	0.00e+00	0.00e+00	0.00e+00	0.00e+00	0.00e+00	0.00e+00	0.00e+00
11	3.03e+49	2.19e+52	2.59e+52	2.02e+50	1.03e+52	0.00e+00	0.00e+00	0.00e+00	0.00e+00	0.00e+00	0.00e+00	0.00e+00	0.00e+00	0.00e+00	0.00e+00	1.51e+52	0.00e+00	0.00e+00	2.02e+49	2.02e+49
10	6.91e+52	8.82e+52	4.14e+52	3.26e+52	0.00e+00	0.00e+00	0.00e+00	0.00e+00	0.00e+00	0.00e+00	9.14e+50	8.54e+52	5.55e+52	1.95e+52	2.02e+50	1.70e+52	1.32e+51	0.00e+00	0.00e+00	0.00e+00
9	8.51e+52	9.77e+52	4.50e+52	4.66e+52	7.35e+49	0.00e+00	0.00e+00	0.00e+00	1.01e+50	0.00e+00	6.05e+50	0.00e+00	0.00e+00	0.00e+00	0.00e+00	0.00e+00	3.02e+51	3.65e+49	0.00e+00	0.00e+00
8	3.43e+51	0.00e+00	0.00e+00	0.00e+00	1.01e+50	1.38e+52	2.94e+50	1.47e+50	9.89e+51	0.00e+00	0.00e+00	0.00e+00	0.00e+00	0.00e+00	0.00e+00	1.82e+52	2.82e+52	0.00e+00	0.00e+00	0.00e+00
7	0.00e+00	2.02e+50	3.03e+49	2.02e+50	6.17e+51	4.57e+49	0.00e+00	3.03e+50	3.03e+50	0.00e+00	0.00e+00	0.00e+00	0.00e+00	0.00e+00	0.00e+00	1.07e+52	4.04e+50	0.00e+00	3.03e+49	0.00e+00
6	4.54e+48	3.03e+49	1.01e+49	0.00e+00	0.00e+00	0.00e+00	9.14e+49	3.67e+50	1.46e+49	0.00e+00	2.94e+50	6.56e+51	2.34e+51	1.02e+52	1.28e+52	3.03e+49	9.08e+50	2.02e+49	4.04e+50	0.00e+00
5	4.54e+48	3.03e+49	1.01e+49	0.00e+00	0.00e+00	0.00e+00	0.00e+00	2.20e+49	0.00e+00	0.00e+00	9.14e+48	1.83e+50	0.00e+00	0.00e+00	3.67e+50	0.00e+00	0.00e+00	0.00e+00	2.38e+49	1.06e+50
4	9.14e+49	9.14e+49	2.28e+49	1.83e+49	0.00e+00	0.00e+00	0.00e+00	0.00e+00	0.00e+00	0.00e+00	0.00e+00	4.57e+48	5.81e+49	0.00e+00	0.00e+00	1.83e+50	0.00e+00	6.48e+48	2.27e+48	0.00e+00
3	9.14e+49	9.14e+49	2.28e+49	1.83e+49	0.00e+00	0.00e+00	0.00e+00	0.00e+00	0.00e+00	0.00e+00	0.00e+00	0.00e+00	0.00e+00	4.57e+48	0.00e+00	0.00e+00	0.00e+00	0.00e+00	0.00e+00	2.00e+49
2	0.00e+00	0.00e+00	0.00e+00	0.00e+00	0.00e+00	0.00e+00	0.00e+00	0.00e+00	0.00e+00	0.00e+00	0.00e+00	0.00e+00	0.00e+00	0.00e+00	0.00e+00	0.00e+00	0.00e+00	0.00e+00	0.00e+00	2.50e+49
1	0.00e+00	0.00e+00	0.00e+00	0.00e+00	0.00e+00	0.00e+00	0.00e+00	0.00e+00	0.00e+00	0.00e+00	0.00e+00	0.00e+00	0.00e+00	0.00e+00	0.00e+00	0.00e+00	0.00e+00	0.00e+00	0.00e+00	2.50e+49

Table 12: Lower limit energy emission in erg by stars formed in the last 20 Myrs. Rows: DEC-Bin, Columns: RA-Bin (as in images), binsize $12' \times 12'$, conversion to coordinates in table 1.

	20	19	18	17	16	15	14	13	12	11	10	9	8	7	6	5	4	3	2	1
23	0.00e+00	0.00e+00	0.00e+00	0.00e+00	0.00e+00	0.00e+00	2.45e+49	0.00e+00	5.83e+48	1.18e+49	1.18e+49	0.00e+00	0.00e+00	0.00e+00	0.00e+00	0.00e+00	0.00e+00	0.00e+00	0.00e+00	0.00e+00
22	0.00e+00	0.00e+00	0.00e+00	4.70e+49	0.00e+00	0.00e+00	0.00e+00	1.77e+49	0.00e+00	1.18e+49	1.18e+49	0.00e+00	0.00e+00	0.00e+00	0.00e+00	0.00e+00	0.00e+00	0.00e+00	0.00e+00	0.00e+00
21	0.00e+00	0.00e+00	1.10e+49	0.00e+00	0.00e+00	0.00e+00	0.00e+00	0.00e+00	1.18e+49	0.00e+00	0.00e+00	0.00e+00	0.00e+00	0.00e+00	0.00e+00	0.00e+00	0.00e+00	0.00e+00	0.00e+00	0.00e+00
20	0.00e+00	7.31e+48	0.00e+00	0.00e+00	1.50e+49	1.77e+49	0.00e+00	1.83e+50	0.00e+00	0.00e+00	0.00e+00	2.28e+49	2.28e+49	0.00e+00	0.00e+00	0.00e+00	0.00e+00	0.00e+00	0.00e+00	0.00e+00
19	0.00e+00	0.00e+00	5.88e+49	0.00e+00	3.66e+50	0.00e+00	0.00e+00	0.00e+00	0.00e+00	0.00e+00	0.00e+00	0.00e+00	0.00e+00	0.00e+00	0.00e+00	1.83e+49	1.83e+49	0.00e+00	0.00e+00	0.00e+00
18	2.89e+49	2.89e+49	9.63e+48	3.88e+50	4.11e+51	8.23e+50	6.39e+52	2.23e+52	1.08e+52	0.00e+00	0.00e+00	5.29e+49	5.29e+49	0.00e+00	0.00e+00	1.83e+49	1.83e+49	0.00e+00	0.00e+00	0.00e+00
17	0.00e+00	9.09e+49	0.00e+00	1.18e+52	1.63e+52	0.00e+00	3.36e+52	2.59e+51	3.17e+52	1.24e+52	2.94e+50	0.00e+00	0.00e+00	0.00e+00	0.00e+00	0.00e+00	0.00e+00	0.00e+00	0.00e+00	0.00e+00
16	1.18e+49	1.77e+49	0.00e+00	8.02e+49	7.65e+52	4.70e+49	4.77e+49	0.00e+00	0.00e+00	5.44e+52	1.09e+52	6.21e+51	0.00e+00	0.00e+00	0.00e+00	0.00e+00	0.00e+00	0.00e+00	0.00e+00	0.00e+00
15	2.89e+49	2.36e+49	2.35e+52	3.31e+52	1.04e+52	3.31e+52	1.59e+51	2.67e+52	0.00e+00	3.84e+52	4.47e+52	5.56e+51	1.19e+49	0.00e+00	0.00e+00	0.00e+00	0.00e+00	0.00e+00	0.00e+00	0.00e+00
14	6.82e+49	0.00e+00	1.74e+52	0.00e+00	0.00e+00	6.94e+52	0.00e+00	0.00e+00	0.00e+00	0.00e+00	1.12e+52	1.89e+52	2.28e+51	7.75e+49	0.00e+00	0.00e+00	0.00e+00	0.00e+00	0.00e+00	0.00e+00
13	1.18e+49	2.03e+53	4.48e+51	4.77e+49	4.77e+49	8.10e+52	0.00e+00	0.00e+00	1.61e+53	0.00e+00	0.00e+00	1.06e+51	1.83e+50	6.82e+49	1.94e+48	0.00e+00	0.00e+00	0.00e+00	0.00e+00	0.00e+00
12	0.00e+00	1.61e+52	5.95e+52	2.82e+51	0.00e+00	0.00e+00	1.18e+51	0.00e+00	7.40e+52	2.00e+53	0.00e+00	0.00e+00	0.00e+00	0.00e+00	0.00e+00	0.00e+00	0.00e+00	0.00e+00	0.00e+00	0.00e+00
11	5.89e+49	2.55e+52	2.59e+52	2.35e+50	1.20e+52	0.00e+00	0.00e+00	0.00e+00	0.00e+00	6.09e+52	0.00e+00	0.00e+00	0.00e+00	0.00e+00	0.00e+00	1.76e+52	0.00e+00	0.00e+00	2.35e+49	2.35e+49
10	6.92e+52	8.82e+52	4.14e+52	3.26e+52	0.00e+00	0.00e+00	0.00e+00	0.00e+00	0.00e+00	6.80e+52	9.52e+52	8.54e+52	6.46e+52	1.95e+52	2.35e+50	1.97e+52	1.32e+51	0.00e+00	2.39e+49	0.00e+00
9	8.62e+52	9.77e+52	4.50e+52	4.66e+52	7.35e+49	0.00e+00	0.00e+00	0.00e+00	1.18e+50	0.00e+00	6.54e+50	0.00e+00	0.00e+00	0.00e+00	0.00e+00	1.19e+50	3.02e+51	3.65e+49	0.00e+00	0.00e+00
8	4.00e+51	0.00e+00	0.00e+00	0.00e+00	1.18e+50	1.61e+52	2.94e+50	1.47e+50	1.15e+52	0.00e+00	0.00e+00	0.00e+00	0.00e+00	0.00e+00	0.00e+00	2.12e+52	3.28e+52	0.00e+00	0.00e+00	0.00e+00
7	0.00e+00	2.83e+50	3.53e+49	2.35e+50	6.17e+51	4.57e+49	0.00e+00	3.53e+50	3.53e+50	0.00e+00	0.00e+00	0.00e+00	0.00e+00	0.00e+00	0.00e+00	1.07e+52	4.70e+50	0.00e+00	3.53e+49	0.00e+00
6	1.05e+49	3.53e+49	1.18e+49	0.00e+00	2.36e+49	0.00e+00	9.14e+49	3.67e+50	1.46e+49	0.00e+00	2.94e+50	7.64e+51	2.34e+51	1.19e+52	1.49e+52	3.53e+49	1.06e+51	2.35e+49	4.70e+50	2.36e+49
5	1.05e+49	3.53e+49	1.18e+49	0.00e+00	0.00e+00	0.00e+00	0.00e+00	2.20e+49	0.00e+00	0.00e+00	9.14e+48	1.83e+50	0.00e+00	0.00e+00	3.67e+50	0.00e+00	0.00e+00	3.01e+51	2.38e+49	1.08e+50
4	9.14e+49	9.14e+49	2.28e+49	1.83e+49	0.00e+00	0.00e+00	0.00e+00	0.00e+00	0.00e+00	0.00e+00	0.00e+00	4.57e+48	5.81e+49	0.00e+00	1.19e+49	1.83e+50	0.00e+00	6.48e+48	2.27e+48	0.00e+00
3	9.14e+49	9.14e+49	2.28e+49	1.83e+49	0.00e+00	0.00e+00	0.00e+00	0.00e+00	0.00e+00	0.00e+00	0.00e+00	0.00e+00	0.00e+00	4.57e+48	0.00e+00	0.00e+00	0.00e+00	0.00e+00	2.36e+49	2.33e+49
2	0.00e+00	0.00e+00	0.00e+00	0.00e+00	0.00e+00	0.00e+00	0.00e+00	0.00e+00	0.00e+00	0.00e+00	0.00e+00	0.00e+00	0.00e+00	0.00e+00	0.00e+00	0.00e+00	0.00e+00	0.00e+00	0.00e+00	2.91e+49
1	0.00e+00	0.00e+00	0.00e+00	0.00e+00	0.00e+00	0.00e+00	0.00e+00	0.00e+00	0.00e+00	0.00e+00	0.00e+00	0.00e+00	0.00e+00	0.00e+00	0.00e+00	0.00e+00	0.00e+00	0.00e+00	0.00e+00	2.91e+49

Table 13: Lower limit energy emission in erg by stars formed in the last 29 Myrs. Rows: DEC-Bin, Columns: RA-Bin (as in images), binsize $12' \times 12'$, conversion to coordinates in table 1.

	20	19	18	17	16	15	14	13	12	11	10	9	8	7	6	5	4	3	2	1
23	3.28e+50	3.28e+50	4.31e+50	4.20e+50	3.55e+50	4.79e+50	5.19e+50	4.53e+50	4.01e+50	5.39e+50	5.39e+50	4.27e+50	4.27e+50	4.01e+50	4.01e+50	3.68e+50	3.68e+50	3.09e+50	3.09e+50	0.00e+00
22	3.02e+50	4.07e+50	4.99e+50	5.19e+50	0.00e+00	0.00e+00	0.00e+00	7.95e+50	5.19e+50	5.39e+50	5.39e+50	4.27e+50	4.27e+50	4.01e+50	4.01e+50	3.68e+50	3.68e+50	3.09e+50	3.09e+50	0.00e+00
21	3.09e+50	7.23e+50	5.85e+50	1.06e+51	0.00e+00	0.00e+00	0.00e+00	6.83e+50	6.24e+50	0.00e+00	0.00e+00	3.74e+50	3.74e+50	4.47e+50	4.47e+50	4.63e+50	4.63e+50	4.07e+50	4.07e+50	0.00e+00
20	5.12e+50	7.42e+50	1.04e+51	1.53e+51	1.68e+51	1.00e+51	8.28e+50	9.00e+50	6.57e+50	0.00e+00	0.00e+00	3.94e+50	3.94e+50	4.47e+50	4.47e+50	4.63e+50	4.63e+50	4.07e+50	4.07e+50	0.00e+00
19	8.15e+50	1.23e+51	1.89e+51	1.81e+51	1.43e+51	1.27e+51	1.25e+51	1.24e+51	8.80e+50	0.00e+00	0.00e+00	5.19e+50	5.19e+50	4.01e+50	4.01e+50	4.66e+50	4.66e+50	4.07e+50	4.07e+50	0.00e+00
18	1.10e+51	2.13e+51	2.13e+51	2.99e+51	1.73e+51	1.47e+51	1.53e+51	1.57e+51	1.29e+51	1.12e+51	6.31e+50	6.04e+50	6.04e+50	4.40e+50	4.40e+50	4.66e+50	4.66e+50	0.00e+00	0.00e+00	0.00e+00
17	1.39e+51	1.66e+51	1.29e+51	1.71e+51	2.48e+51	2.04e+51	2.17e+51	2.17e+51	1.85e+51	3.03e+51	9.46e+50	7.69e+50	5.83e+50	4.93e+50	4.93e+50	4.20e+50	4.20e+50	0.00e+00	0.00e+00	0.00e+00
16	1.00e+51	1.21e+51	2.42e+51	4.00e+51	3.22e+51	1.87e+51	1.45e+51	1.03e+51	1.05e+51	1.92e+51	2.86e+51	1.03e+51	6.04e+50	4.66e+50	4.07e+50	4.34e+50	4.34e+50	0.00e+00	0.00e+00	0.00e+00
15	1.20e+51	1.55e+51	1.66e+51	1.97e+51	3.42e+51	9.62e+51	8.20e+51	1.96e+51	2.63e+51	2.76e+51	1.81e+51	2.31e+51	9.66e+50	6.70e+50	4.60e+50	4.27e+50	4.27e+50	0.00e+00	0.00e+00	0.00e+00
14	1.30e+51	1.51e+51	1.94e+51	1.30e+51	1.27e+51	4.01e+51	2.69e+51	2.20e+51	2.23e+51	1.87e+51	1.94e+51	1.46e+51	1.06e+51	9.85e+50	6.77e+50	5.65e+50	5.65e+50	0.00e+00	0.00e+00	0.00e+00
13	1.29e+51	2.43e+51	2.04e+51	1.13e+51	1.28e+51	4.86e+51	1.31e+51	2.02e+51	3.09e+51	2.83e+51	2.30e+51	1.84e+51	1.05e+51	1.08e+51	7.99e+50	6.31e+50	6.31e+50	5.52e+50	5.52e+50	5.52e+50
12	1.54e+51	1.82e+51	1.91e+51	2.69e+51	9.07e+50	1.48e+51	3.09e+51	1.86e+51	3.29e+51	1.48e+52	2.63e+51	2.30e+51	2.30e+51	1.47e+51	1.15e+51	6.90e+50	5.65e+50	4.73e+50	4.66e+50	4.66e+50
11	1.31e+51	1.77e+51	1.80e+51	2.43e+51	2.50e+51	1.05e+51	8.67e+50	9.33e+50	2.83e+51	5.91e+51	4.01e+51	3.29e+51	2.56e+51	1.85e+51	1.66e+51	1.29e+51	6.50e+50	5.39e+50	6.04e+50	6.04e+50
10	1.65e+51	1.43e+51	1.31e+51	1.79e+51	2.37e+51	1.01e+51	9.92e+50	1.09e+51	3.29e+51	4.53e+51	6.05e+51	6.04e+51	3.48e+51	6.83e+51	1.82e+51	1.33e+51	1.57e+51	7.82e+50	6.83e+50	8.21e+50
9	1.77e+51	1.87e+51	1.50e+51	1.68e+51	1.90e+51	2.30e+51	1.04e+51	9.86e+50	1.65e+51	2.89e+51	4.47e+51	3.09e+51	2.56e+51	8.41e+50	2.17e+51	1.36e+51	2.05e+51	1.12e+51	9.72e+50	8.21e+50
8	1.24e+51	1.22e+51	1.47e+51	2.17e+51	1.66e+51	1.78e+51	1.92e+51	2.30e+51	2.43e+51	1.01e+51	3.31e+51	6.02e+51	2.10e+51	1.21e+51	2.17e+51	1.49e+51	1.36e+51	1.18e+51	1.10e+51	9.26e+50
7	1.16e+51	1.23e+51	1.45e+51	1.43e+51	1.35e+51	1.41e+51	1.36e+51	1.33e+51	1.58e+51	1.94e+51	9.53e+50	9.53e+50	7.88e+50	9.99e+50	8.15e+50	1.64e+51	1.55e+51	1.28e+51	1.25e+51	1.22e+51
6	1.12e+51	1.19e+51	1.39e+51	1.35e+51	1.20e+51	1.06e+51	9.46e+50	9.07e+50	1.33e+51	1.20e+51	1.13e+51	1.33e+51	1.22e+51	1.26e+51	1.52e+51	1.52e+51	1.59e+51	1.45e+51	1.40e+51	1.25e+51
5	1.12e+51	1.19e+51	1.39e+51	1.35e+51	9.79e+50	8.41e+50	7.55e+50	8.21e+50	8.29e+50	6.90e+50	7.62e+50	8.67e+50	9.07e+50	1.21e+51	1.08e+51	1.32e+51	1.18e+51	1.00e+51	1.21e+51	1.68e+51
4	8.80e+50	8.80e+50	8.15e+50	7.75e+50	1.05e+51	7.29e+50	6.44e+50	7.75e+50	6.90e+50	5.12e+50	6.37e+50	6.44e+50	8.72e+50	8.41e+50	8.15e+50	7.29e+50	1.04e+51	7.58e+50	9.26e+50	9.52e+50
3	8.80e+50	8.80e+50	8.15e+50	7.75e+50	1.05e+51	6.24e+50	6.63e+50	5.85e+50	5.58e+50	6.24e+50	5.71e+50	6.31e+50	6.04e+50	5.71e+50	5.26e+50	5.85e+50	7.23e+50	5.78e+50	8.01e+50	8.60e+50
2	6.24e+50	6.24e+50	7.16e+50	7.16e+50	7.75e+50	6.44e+50	6.57e+50	7.23e+50	6.04e+50	5.85e+50	5.71e+50	5.52e+50	4.86e+50	5.06e+50	7.08e+50	4.53e+50	5.52e+50	4.53e+50	4.79e+50	5.32e+50
1	6.24e+50	6.24e+50	7.16e+50	7.16e+50	7.75e+50	6.44e+50	6.57e+50	7.23e+50	6.04e+50	5.85e+50	5.71e+50	5.52e+50	4.86e+50	5.06e+50	7.08e+50	4.53e+50	5.52e+50	4.53e+50	4.79e+50	5.32e+50

Table 14: Upper limit energy emission in erg by stars formed in the last 4 Myrs. Rows: DEC-Bin, Columns: RA-Bin (as in images), binsize $12' \times 12'$, conversion to coordinates in table 1.

	20	19	18	17	16	15	14	13	12	11	10	9	8	7	6	5	4	3	2	1
23	8.25e+51	8.15e+51	1.02e+52	1.04e+52	8.92e+51	1.20e+52	1.32e+52	1.14e+52	1.01e+52	1.35e+52	1.35e+52	1.08e+52	1.08e+52	9.99e+51	9.99e+51	9.26e+51	9.26e+51	7.83e+51	7.83e+51	0.00e+00
22	7.51e+51	1.01e+52	1.43e+52	1.30e+52	0.00e+00	0.00e+00	0.00e+00	2.01e+52	1.30e+52	1.35e+52	1.35e+52	1.08e+52	1.08e+52	9.99e+51	9.99e+51	9.26e+51	9.26e+51	7.83e+51	7.83e+51	0.00e+00
21	7.75e+51	1.82e+52	1.44e+52	2.49e+52	0.00e+00	0.00e+00	0.00e+00	1.71e+52	1.56e+52	0.00e+00	0.00e+00	9.48e+51	9.48e+51	1.12e+52	1.12e+52	1.12e+52	1.12e+52	1.05e+52	1.05e+52	0.00e+00
20	1.29e+52	1.86e+52	2.62e+52	3.84e+52	4.24e+52	2.52e+52	2.06e+52	2.70e+52	1.65e+52	0.00e+00	0.00e+00	1.04e+52	1.04e+52	1.12e+52	1.12e+52	1.12e+52	1.12e+52	1.05e+52	1.05e+52	0.00e+00
19	2.03e+52	3.09e+52	4.73e+52	4.35e+52	3.63e+52	3.19e+52	3.13e+52	3.06e+52	2.20e+52	0.00e+00	0.00e+00	1.30e+52	1.30e+52	1.00e+52	1.00e+52	1.27e+52	1.27e+52	1.05e+52	1.05e+52	0.00e+00
18	2.66e+52	5.02e+52	4.94e+52	6.09e+52	4.34e+52	3.73e+52	3.94e+52	3.99e+52	3.27e+52	2.76e+52	1.74e+52	1.52e+52	1.52e+52	1.09e+52	1.09e+52	1.27e+52	1.27e+52	0.00e+00	0.00e+00	0.00e+00
17	3.53e+52	4.51e+52	4.21e+52	4.36e+52	5.67e+52	5.82e+52	5.49e+52	5.56e+52	4.70e+52	6.04e+52	2.41e+52	1.96e+52	1.34e+52	1.22e+52	1.22e+52	1.07e+52	1.07e+52	0.00e+00	0.00e+00	0.00e+00
16	2.51e+52	3.06e+52	5.10e+52	7.99e+52	7.99e+52	4.72e+52	3.49e+52	2.60e+52	2.69e+52	4.86e+52	5.58e+52	2.64e+52	1.52e+52	1.17e+52	1.01e+52	1.09e+52	1.09e+52	0.00e+00	0.00e+00	0.00e+00
15	2.80e+52	3.70e+52	4.20e+52	5.11e+52	8.81e+52	2.05e+53	1.75e+53	4.82e+52	6.60e+52	6.97e+52	4.60e+52	4.59e+52	2.48e+52	1.67e+52	1.16e+52	1.08e+52	1.08e+52	0.00e+00	0.00e+00	0.00e+00
14	3.34e+52	3.92e+52	7.56e+52	3.37e+52	3.26e+52	1.32e+53	6.90e+52	5.64e+52	5.78e+52	4.90e+52	5.06e+52	3.70e+52	3.56e+52	2.18e+52	1.95e+52	1.43e+52	1.43e+52	0.00e+00	0.00e+00	0.00e+00
13	3.29e+52	6.42e+52	4.81e+52	2.92e+52	3.16e+52	1.28e+53	3.34e+52	5.23e+52	8.11e+52	7.39e+52	5.92e+52	4.49e+52	3.37e+52	2.94e+52	1.88e+52	1.56e+52	1.56e+52	1.38e+52	1.38e+52	1.38e+52
12	3.61e+52	4.58e+52	4.87e+52	6.57e+52	2.30e+52	3.67e+52	7.98e+52	4.92e+52	8.47e+52	2.78e+53	6.84e+52	5.99e+52	5.77e+52	3.73e+52	2.91e+52	1.72e+52	1.40e+52	1.18e+52	1.17e+52	1.17e+52
11	3.25e+52	4.42e+52	4.50e+52	5.81e+52	6.23e+52	2.68e+52	2.18e+52	2.39e+52	7.36e+52	1.40e+53	1.00e+53	8.19e+52	6.56e+52	4.78e+52	4.25e+52	3.26e+52	1.64e+52	1.35e+52	1.52e+52	1.52e+52
10	4.20e+52	3.61e+52	3.33e+52	4.60e+52	6.03e+52	2.53e+52	2.49e+52	2.77e+52	8.37e+52	1.15e+53	1.96e+53	2.39e+53	8.85e+52	1.33e+53	4.59e+52	3.37e+52	3.24e+52	1.96e+52	1.71e+52	2.19e+52
9	4.50e+52	4.74e+52	3.74e+52	4.27e+52	4.83e+52	5.78e+52	2.63e+52	2.52e+52	3.95e+52	7.16e+52	1.18e+53	7.86e+52	6.61e+52	2.16e+52	5.47e+52	3.48e+52	4.18e+52	2.83e+52	2.55e+52	2.19e+52
8	3.13e+52	3.10e+52	3.48e+52	5.03e+52	4.18e+52	4.58e+52	4.96e+52	5.80e+52	6.38e+52	2.57e+52	7.86e+52	1.33e+53	5.57e+52	3.17e+52	5.62e+52	3.88e+52	3.55e+52	3.04e+52	2.77e+52	2.32e+52
7	2.97e+52	3.05e+52	3.49e+52	3.62e+52	3.39e+52	4.52e+52	4.09e+52	3.38e+52	4.08e+52	4.76e+52	2.42e+52	2.44e+52	2.02e+52	2.53e+52	2.07e+52	4.25e+52	3.97e+52	3.28e+52	3.10e+52	2.98e+52
6	2.83e+52	2.93e+52	3.47e+52	3.58e+52	3.05e+52	2.70e+52	2.66e+52	2.30e+52	3.37e+52	3.07e+52	2.87e+52	3.39e+52	4.19e+52	3.26e+52	3.90e+52	3.87e+52	3.87e+52	3.63e+52	3.51e+52	3.10e+52
5	2.83e+52	2.93e+52	3.47e+52	3.58e+52	2.47e+52	2.11e+52	1.89e+52	2.07e+52	1.99e+52	1.71e+52	1.98e+52	2.43e+52	2.29e+52	3.05e+52	2.71e+52	3.31e+52	2.99e+52	2.52e+52	2.97e+52	3.85e+52
4	2.54e+52	2.54e+52	2.22e+52	1.96e+52	2.63e+52	1.82e+52	1.61e+52	1.92e+52	1.71e+52	1.26e+52	1.60e+52	1.73e+52	1.97e+52	2.09e+52	2.03e+52	2.23e+52	2.32e+52	1.96e+52	2.41e+52	2.38e+52
3	2.54e+52	2.54e+52	2.22e+52	1.96e+52	2.63e+52	1.55e+52	1.65e+52	1.46e+52	1.38e+52	1.55e+52	1.41e+52	1.57e+52	1.49e+52	1.49e+52	1.29e+52	1.53e+52	1.80e+52	1.45e+52	2.09e+52	2.15e+52
2	1.57e+52	1.57e+52	1.79e+52	1.79e+52	1.82e+52	1.59e+52	1.61e+52	1.81e+52	1.54e+52	1.46e+52	1.44e+52	1.38e+52	1.20e+52	1.27e+52	1.70e+52	1.11e+52	1.37e+52	1.11e+52	1.30e+52	1.32e+52
1	1.57e+52	1.57e+52	1.79e+52	1.79e+52	1.82e+52	1.59e+52	1.61e+52	1.81e+52	1.54e+52	1.46e+52	1.44e+52	1.38e+52	1.20e+52	1.27e+52	1.70e+52	1.11e+52	1.37e+52	1.11e+52	1.30e+52	1.32e+52

Table 15: Upper limit energy emission in erg by stars formed in the last 7 Myrs. Rows: DEC-Bin, Columns: RA-Bin (as in images), binsize $12' \times 12'$, conversion to coordinates in table 1.

	20	19	18	17	16	15	14	13	12	11	10	9	8	7	6	5	4	3	2	1
23	1.31e+52	1.29e+52	1.57e+52	1.65e+52	1.42e+52	1.92e+52	2.12e+52	1.82e+52	1.62e+52	2.17e+52	2.17e+52	1.71e+52	1.71e+52	1.59e+52	1.59e+52	1.48e+52	1.48e+52	1.25e+52	1.25e+52	0.00e+00
22	1.19e+52	1.60e+52	2.32e+52	2.07e+52	0.00e+00	0.00e+00	0.00e+00	3.22e+52	2.07e+52	2.17e+52	2.17e+52	1.71e+52	1.71e+52	1.59e+52	1.59e+52	1.48e+52	1.48e+52	1.25e+52	1.25e+52	0.00e+00
21	1.23e+52	2.92e+52	2.31e+52	3.80e+52	0.00e+00	0.00e+00	0.00e+00	2.75e+52	2.50e+52	0.00e+00	0.00e+00	1.52e+52	1.52e+52	1.78e+52	1.78e+52	1.74e+52	1.74e+52	1.68e+52	1.68e+52	0.00e+00
20	2.06e+52	3.02e+52	4.18e+52	6.16e+52	6.79e+52	4.04e+52	3.28e+52	4.43e+52	2.62e+52	0.00e+00	0.00e+00	1.68e+52	1.68e+52	1.78e+52	1.78e+52	1.74e+52	1.74e+52	1.68e+52	1.68e+52	0.00e+00
19	3.30e+52	4.95e+52	7.56e+52	6.81e+52	5.81e+52	5.12e+52	5.00e+52	5.41e+52	3.50e+52	0.00e+00	0.00e+00	2.07e+52	2.07e+52	1.59e+52	1.59e+52	2.04e+52	2.04e+52	1.68e+52	1.68e+52	0.00e+00
18	4.15e+52	7.79e+52	7.55e+52	8.55e+52	6.99e+52	6.02e+52	9.29e+52	6.42e+52	5.26e+52	4.36e+52	2.81e+52	2.52e+52	2.52e+52	1.74e+52	1.74e+52	2.04e+52	2.04e+52	0.00e+00	0.00e+00	0.00e+00
17	5.65e+52	7.33e+52	6.99e+52	8.26e+52	1.00e+53	9.56e+52	1.04e+53	1.02e+53	9.54e+52	8.33e+52	4.53e+52	3.14e+52	2.04e+52	1.94e+52	1.94e+52	1.69e+52	1.69e+52	0.00e+00	0.00e+00	0.00e+00
16	4.02e+52	4.92e+52	7.86e+52	1.12e+53	1.64e+53	7.87e+52	5.57e+52	4.25e+52	4.40e+52	7.89e+52	7.58e+52	4.24e+52	2.43e+52	1.86e+52	1.60e+52	1.72e+52	1.72e+52	0.00e+00	0.00e+00	0.00e+00
15	4.29e+52	5.79e+52	6.76e+52	1.03e+53	1.65e+53	2.86e+53	2.50e+53	7.78e+52	1.06e+53	1.23e+53	8.32e+52	6.35e+52	3.99e+52	2.66e+52	1.85e+52	1.71e+52	1.71e+52	0.00e+00	0.00e+00	0.00e+00
14	5.26e+52	6.36e+52	1.34e+53	5.58e+52	5.38e+52	2.20e+53	1.12e+53	9.27e+52	9.57e+52	8.10e+52	9.90e+52	5.99e+52	5.91e+52	3.24e+52	3.17e+52	2.46e+52	2.46e+52	0.00e+00	0.00e+00	0.00e+00
13	5.32e+52	1.87e+53	8.40e+52	4.81e+52	5.08e+52	2.10e+53	5.47e+52	8.60e+52	1.34e+53	1.22e+53	9.63e+52	7.25e+52	5.60e+52	4.77e+52	2.91e+52	2.49e+52	2.49e+52	2.21e+52	2.21e+52	2.21e+52
12	5.59e+52	7.34e+52	1.09e+53	1.14e+53	3.77e+52	5.93e+52	1.47e+53	8.22e+52	1.38e+53	3.63e+53	1.12e+53	9.82e+52	9.23e+52	6.03e+52	4.83e+52	2.73e+52	2.23e+52	1.88e+52	1.87e+52	1.87e+52
11	5.20e+52	7.09e+52	8.96e+52	9.33e+52	1.06e+53	4.36e+52	3.56e+52	3.94e+52	1.21e+53	2.23e+53	1.61e+53	1.31e+53	1.06e+53	7.78e+52	6.87e+52	5.24e+52	2.66e+52	2.15e+52	2.44e+52	2.44e+52
10	9.92e+52	9.40e+52	7.40e+52	9.47e+52	1.04e+53	4.12e+52	4.06e+52	4.54e+52	1.36e+53	1.87e+53	3.29e+53	3.99e+53	1.51e+53	1.92e+53	7.37e+52	5.45e+52	4.59e+52	3.12e+52	2.72e+52	3.53e+52
9	1.06e+53	1.21e+53	8.21e+52	9.34e+52	8.69e+52	1.00e+53	4.30e+52	4.14e+52	6.21e+52	1.14e+53	2.00e+53	1.33e+53	1.10e+53	3.55e+52	9.62e+52	5.85e+52	5.86e+52	4.72e+52	4.11e+52	3.53e+52
8	5.06e+52	5.01e+52	5.43e+52	7.73e+52	6.78e+52	7.52e+52	9.01e+52	1.02e+53	1.07e+53	4.24e+52	1.25e+53	2.01e+53	9.19e+52	5.22e+52	9.19e+52	6.40e+52	5.83e+52	4.95e+52	4.45e+52	3.85e+52
7	4.79e+52	4.84e+52	5.58e+52	5.85e+52	6.27e+52	7.56e+52	6.74e+52	5.48e+52	6.59e+52	7.80e+52	3.98e+52	4.10e+52	3.31e+52	4.08e+52	3.37e+52	8.12e+52	6.47e+52	5.31e+52	4.95e+52	4.73e+52
6	4.62e+52	4.66e+52	5.64e+52	5.86e+52	4.91e+52	4.32e+52	4.33e+52	4.05e+52	5.54e+52	4.98e+52	5.07e+52	5.51e+52	7.03e+52	5.33e+52	6.35e+52	6.23e+52	6.11e+52	5.85e+52	5.62e+52	4.95e+52
5	4.62e+52	4.66e+52	5.64e+52	5.86e+52	3.95e+52	3.37e+52	3.01e+52	3.47e+52	3.11e+52	2.71e+52	3.18e+52	3.94e+52	3.98e+52	4.89e+52	4.72e+52	5.35e+52	4.80e+52	4.03e+52	4.66e+52	5.87e+52
4	4.15e+52	4.15e+52	3.59e+52	3.13e+52	4.20e+52	2.90e+52	2.54e+52	3.03e+52	2.71e+52	2.00e+52	2.66e+52	2.80e+52	2.94e+52	3.44e+52	3.24e+52	3.65e+52	3.45e+52	3.13e+52	3.88e+52	3.92e+52
3	4.15e+52	4.15e+52	3.59e+52	3.13e+52	4.20e+52	2.46e+52	2.63e+52	2.31e+52	2.18e+52	2.46e+52	2.24e+52	2.51e+52	2.34e+52	2.38e+52	2.05e+52	2.45e+52	2.81e+52	2.30e+52	3.36e+52	3.44e+52
2	2.50e+52	2.50e+52	2.82e+52	2.82e+52	2.78e+52	2.53e+52	2.55e+52	2.89e+52	2.44e+52	2.31e+52	2.28e+52	2.19e+52	1.92e+52	2.01e+52	2.63e+52	1.76e+52	2.18e+52	1.76e+52	2.09e+52	2.09e+52
1	2.50e+52	2.50e+52	2.82e+52	2.82e+52	2.78e+52	2.53e+52	2.55e+52	2.89e+52	2.44e+52	2.31e+52	2.28e+52	2.19e+52	1.92e+52	2.01e+52	2.63e+52	1.76e+52	2.18e+52	1.76e+52	2.09e+52	2.09e+52

Table 16: Upper limit energy emission in erg by stars formed in the last 10 Myrs. Rows: DEC-Bin, Columns: RA-Bin (as in images), binsize $12' \times 12'$, conversion to coordinates in table 1.

	20	19	18	17	16	15	14	13	12	11	10	9	8	7	6	5	4	3	2	1
23	1.86e+52	1.84e+52	2.20e+52	2.35e+52	2.04e+52	2.74e+52	3.04e+52	2.62e+52	2.37e+52	3.19e+52	3.19e+52	2.43e+52	2.43e+52	2.29e+52	2.29e+52	2.13e+52	2.13e+52	1.79e+52	1.79e+52	0.00e+00
22	1.69e+52	2.28e+52	3.18e+52	3.07e+52	0.00e+00	0.00e+00	0.00e+00	4.67e+52	2.96e+52	3.19e+52	3.19e+52	2.43e+52	2.43e+52	2.29e+52	2.29e+52	2.13e+52	2.13e+52	1.79e+52	1.79e+52	0.00e+00
21	1.75e+52	4.21e+52	3.32e+52	5.34e+52	0.00e+00	0.00e+00	0.00e+00	3.96e+52	3.58e+52	0.00e+00	0.00e+00	2.18e+52	2.18e+52	2.55e+52	2.55e+52	2.44e+52	2.44e+52	2.40e+52	2.40e+52	0.00e+00
20	2.94e+52	4.40e+52	6.01e+52	8.93e+52	9.78e+52	5.81e+52	4.70e+52	6.00e+52	3.71e+52	0.00e+00	0.00e+00	2.36e+52	2.36e+52	2.55e+52	2.55e+52	2.44e+52	2.44e+52	2.40e+52	2.40e+52	0.00e+00
19	4.84e+52	7.13e+52	1.11e+53	9.78e+52	8.61e+52	7.73e+52	7.16e+52	8.68e+52	5.16e+52	0.00e+00	0.00e+00	3.03e+52	3.03e+52	2.26e+52	2.26e+52	2.82e+52	2.82e+52	2.40e+52	2.40e+52	0.00e+00
18	5.87e+52	1.11e+53	1.06e+53	1.14e+53	1.06e+53	9.39e+52	1.81e+53	1.01e+53	8.17e+52	6.32e+52	3.89e+52	3.77e+52	3.77e+52	2.50e+52	2.50e+52	2.82e+52	2.82e+52	0.00e+00	0.00e+00	0.00e+00
17	8.11e+52	1.03e+53	9.32e+52	1.39e+53	1.65e+53	1.37e+53	1.76e+53	1.68e+53	1.69e+53	1.16e+53	7.55e+52	4.72e+52	2.84e+52	2.80e+52	2.80e+52	2.39e+52	2.39e+52	0.00e+00	0.00e+00	0.00e+00
16	6.02e+52	7.10e+52	1.15e+53	1.56e+53	2.93e+53	1.22e+53	8.23e+52	6.33e+52	6.56e+52	1.35e+53	9.92e+52	6.08e+52	3.48e+52	2.68e+52	2.27e+52	2.44e+52	2.44e+52	0.00e+00	0.00e+00	0.00e+00
15	6.00e+52	8.53e+52	1.08e+53	1.82e+53	2.87e+53	3.59e+53	3.30e+53	1.16e+53	1.55e+53	1.97e+53	1.51e+53	8.39e+52	5.69e+52	3.81e+52	2.67e+52	2.45e+52	2.45e+52	0.00e+00	0.00e+00	0.00e+00
14	7.25e+52	9.22e+52	1.81e+53	8.52e+52	8.11e+52	3.07e+53	1.64e+53	1.38e+53	1.44e+53	1.20e+53	1.72e+53	9.55e+52	7.76e+52	4.43e+52	4.30e+52	3.81e+52	3.81e+52	0.00e+00	0.00e+00	0.00e+00
13	7.92e+52	4.03e+53	1.34e+53	7.20e+52	7.53e+52	3.35e+53	8.44e+52	1.28e+53	1.99e+53	1.81e+53	1.41e+53	1.14e+53	7.53e+52	6.66e+52	4.08e+52	3.70e+52	3.70e+52	3.20e+52	3.20e+52	3.20e+52
12	8.38e+52	1.13e+53	2.06e+53	1.91e+53	5.67e+52	8.85e+52	2.49e+53	1.23e+53	2.30e+53	4.64e+53	1.65e+53	1.44e+53	1.33e+53	8.71e+52	7.18e+52	3.88e+52	3.25e+52	2.69e+52	2.67e+52	2.67e+52
11	7.75e+52	1.12e+53	1.58e+53	1.44e+53	1.77e+53	6.49e+52	5.35e+52	5.93e+52	1.78e+53	3.32e+53	2.35e+53	1.89e+53	1.55e+53	1.13e+53	9.93e+52	8.22e+52	3.85e+52	3.07e+52	3.52e+52	3.52e+52
10	1.95e+53	1.93e+53	1.40e+53	1.70e+53	1.64e+53	6.16e+52	6.09e+52	6.80e+52	1.98e+53	2.76e+53	4.44e+53	4.97e+53	2.63e+53	2.71e+53	1.15e+53	8.71e+52	6.14e+52	4.46e+52	3.88e+52	4.97e+52
9	2.15e+53	2.49e+53	1.54e+53	1.75e+53	1.41e+53	1.57e+53	6.42e+52	6.22e+52	9.33e+52	1.74e+53	3.14e+53	2.08e+53	1.68e+53	5.36e+52	1.53e+53	8.85e+52	7.82e+52	7.03e+52	5.81e+52	4.97e+52
8	7.93e+52	7.26e+52	8.29e+52	1.10e+53	1.06e+53	1.19e+53	1.47e+53	1.61e+53	1.74e+53	6.41e+52	1.84e+53	2.83e+53	1.35e+53	7.78e+52	1.34e+53	1.04e+53	9.66e+52	7.29e+52	6.48e+52	5.77e+52
7	6.92e+52	7.27e+52	8.41e+52	8.88e+52	1.04e+53	1.03e+53	9.28e+52	8.40e+52	1.00e+53	1.19e+53	5.95e+52	6.24e+52	4.93e+52	5.99e+52	4.99e+52	1.37e+53	9.82e+52	8.11e+52	7.30e+52	6.86e+52
6	6.75e+52	6.85e+52	8.43e+52	8.42e+52	7.11e+52	6.23e+52	5.97e+52	6.38e+52	8.14e+52	7.19e+52	8.05e+52	8.54e+52	9.41e+52	8.42e+52	1.01e+53	9.12e+52	9.43e+52	8.62e+52	8.62e+52	7.20e+52
5	6.75e+52	6.85e+52	8.43e+52	8.42e+52	5.67e+52	4.85e+52	4.29e+52	5.23e+52	4.42e+52	3.85e+52	4.49e+52	5.45e+52	6.22e+52	7.04e+52	7.44e+52	7.76e+52	6.89e+52	5.78e+52	6.57e+52	8.31e+52
4	5.69e+52	5.69e+52	4.99e+52	4.47e+52	6.03e+52	4.15e+52	3.59e+52	4.27e+52	3.85e+52	2.83e+52	3.98e+52	3.90e+52	4.05e+52	5.08e+52	4.64e+52	4.89e+52	4.76e+52	4.41e+52	5.51e+52	5.94e+52
3	5.69e+52	5.69e+52	4.99e+52	4.47e+52	6.03e+52	3.51e+52	3.77e+52	3.28e+52	3.10e+52	3.52e+52	3.20e+52	3.62e+52	3.33e+52	3.32e+52	2.91e+52	3.43e+52	3.95e+52	3.26e+52	4.74e+52	4.97e+52
2	3.55e+52	3.55e+52	3.98e+52	3.98e+52	3.87e+52	3.61e+52	3.63e+52	4.13e+52	3.43e+52	3.29e+52	3.24e+52	3.10e+52	2.78e+52	2.85e+52	3.68e+52	2.51e+52	3.13e+52	2.51e+52	2.90e+52	2.99e+52
1	3.55e+52	3.55e+52	3.98e+52	3.98e+52	3.87e+52	3.61e+52	3.63e+52	4.13e+52	3.43e+52	3.29e+52	3.24e+52	3.10e+52	2.78e+52	2.85e+52	3.68e+52	2.51e+52	3.13e+52	2.51e+52	2.90e+52	2.99e+52

Table 17: Upper limit energy emission in erg by stars formed in the last 15 Myrs. Rows: DEC-Bin, Columns: RA-Bin (as in images), binsize $12' \times 12'$, conversion to coordinates in table 1.

	20	19	18	17	16	15	14	13	12	11	10	9	8	7	6	5	4	3	2	1
23	2.27e+52	2.23e+52	2.66e+52	2.86e+52	2.48e+52	3.34e+52	3.70e+52	3.23e+52	3.05e+52	4.07e+52	4.07e+52	2.95e+52	2.95e+52	2.81e+52	2.81e+52	2.60e+52	2.60e+52	2.18e+52	2.18e+52	0.00e+00
22	2.06e+52	2.78e+52	3.83e+52	3.99e+52	0.00e+00	0.00e+00	0.00e+00	5.87e+52	3.61e+52	4.07e+52	4.07e+52	2.95e+52	2.95e+52	2.81e+52	2.81e+52	2.60e+52	2.60e+52	2.18e+52	2.18e+52	0.00e+00
21	2.12e+52	5.17e+52	4.04e+52	6.53e+52	0.00e+00	0.00e+00	0.00e+00	4.85e+52	4.36e+52	0.00e+00	0.00e+00	2.65e+52	2.65e+52	3.11e+52	3.11e+52	2.96e+52	2.96e+52	2.92e+52	2.92e+52	0.00e+00
20	3.59e+52	5.33e+52	7.40e+52	1.10e+53	1.20e+53	7.09e+52	5.75e+52	7.12e+52	4.55e+52	0.00e+00	0.00e+00	2.85e+52	2.85e+52	3.11e+52	3.11e+52	2.96e+52	2.96e+52	2.92e+52	2.92e+52	0.00e+00
19	5.86e+52	8.74e+52	1.42e+53	1.21e+53	1.14e+53	1.04e+53	8.74e+52	1.02e+53	6.77e+52	0.00e+00	0.00e+00	3.91e+52	3.91e+52	2.74e+52	2.74e+52	3.39e+52	3.39e+52	2.92e+52	2.92e+52	0.00e+00
18	7.15e+52	1.36e+53	1.29e+53	1.34e+53	1.44e+53	1.34e+53	2.02e+53	1.48e+53	1.16e+53	7.95e+52	4.67e+52	4.59e+52	4.59e+52	3.13e+52	3.13e+52	3.39e+52	3.39e+52	0.00e+00	0.00e+00	0.00e+00
17	9.95e+52	1.24e+53	1.10e+53	1.63e+53	1.91e+53	1.73e+53	2.10e+53	1.98e+53	1.94e+53	1.53e+53	8.74e+52	6.36e+52	3.42e+52	3.49e+52	3.49e+52	2.90e+52	2.90e+52	0.00e+00	0.00e+00	0.00e+00
16	8.00e+52	8.71e+52	1.34e+53	2.00e+53	3.30e+53	1.57e+53	1.04e+53	8.02e+52	8.33e+52	2.18e+53	1.16e+53	7.43e+52	4.23e+52	3.31e+52	2.76e+52	2.97e+52	2.97e+52	0.00e+00	0.00e+00	0.00e+00
15	7.28e+52	1.11e+53	1.59e+53	2.11e+53	3.70e+53	4.07e+53	3.86e+53	1.46e+53	1.93e+53	2.34e+53	2.22e+53	9.82e+52	6.84e+52	4.65e+52	3.35e+52	2.98e+52	2.98e+52	0.00e+00	0.00e+00	0.00e+00
14	8.76e+52	1.14e+53	2.06e+53	1.12e+53	1.03e+53	4.11e+53	2.05e+53	1.75e+53	1.83e+53	1.51e+53	2.05e+53	1.40e+53	9.03e+52	5.25e+52	5.13e+52	4.53e+52	4.53e+52	0.00e+00	0.00e+00	0.00e+00
13	1.03e+53	4.40e+53	1.56e+53	9.16e+52	9.60e+52	4.87e+53	1.15e+53	1.62e+53	2.50e+53	2.28e+53	1.75e+53	1.61e+53	8.92e+52	7.94e+52	4.93e+52	4.86e+52	4.86e+52	4.02e+52	4.02e+52	4.02e+52
12	1.14e+53	1.60e+53	2.33e+53	2.51e+53	7.24e+52	1.13e+53	3.18e+53	1.55e+53	3.59e+53	5.42e+53	2.05e+53	1.78e+53	1.63e+53	1.06e+53	8.57e+52	4.70e+52	4.10e+52	3.27e+52	3.25e+52	3.25e+52
11	1.01e+53	1.65e+53	1.81e+53	1.93e+53	2.47e+53	8.21e+52	6.81e+52	7.59e+52	2.22e+53	4.17e+53	2.93e+53	2.32e+53	1.91e+53	1.40e+53	1.22e+53	1.19e+53	4.67e+52	3.74e+52	4.35e+52	4.35e+52
10	2.18e+53	2.10e+53	1.56e+53	1.96e+53	2.04e+53	7.85e+52	7.78e+52	8.64e+52	2.44e+53	3.46e+53	5.26e+53	5.76e+53	4.07e+53	3.10e+53	1.63e+53	1.28e+53	7.21e+52	5.41e+52	4.75e+52	6.02e+52
9	2.61e+53	2.76e+53	1.73e+53	1.97e+53	1.67e+53	1.89e+53	8.15e+52	7.92e+52	1.25e+53	2.37e+53	4.12e+53	2.64e+53	2.15e+53	6.90e+52	1.83e+53	1.08e+53	9.21e+52	8.39e+52	7.05e+52	6.02e+52
8	1.13e+53	8.95e+52	1.16e+53	1.37e+53	1.49e+53	1.71e+53	1.77e+53	1.90e+53	2.52e+53	8.21e+52	2.29e+53	3.41e+53	1.69e+53	9.92e+52	1.65e+53	1.53e+53	1.50e+53	9.25e+52	8.07e+52	7.01e+52
7	8.46e+52	9.84e+52	1.09e+53	1.20e+53	1.21e+53	1.21e+53	1.12e+53	1.14e+53	1.38e+53	1.53e+53	7.45e+52	7.82e+52	6.20e+52	7.53e+52	6.27e+52	1.60e+53	1.30e+53	1.10e+53	9.43e+52	8.48e+52
6	8.23e+52	8.79e+52	1.07e+53	1.03e+53	8.80e+52	7.69e+52	7.17e+52	7.55e+52	9.83e+52	8.77e+52	9.55e+52	1.19e+53	1.12e+53	1.20e+53	1.47e+53	1.15e+53	1.33e+53	1.08e+53	1.20e+53	9.02e+52
5	8.23e+52	8.79e+52	1.07e+53	1.03e+53	6.95e+52	5.91e+52	5.22e+52	6.24e+52	5.34e+52	4.66e+52	5.42e+52	6.56e+52	7.40e+52	8.54e+52	8.86e+52	9.41e+52	8.47e+52	7.10e+52	7.96e+52	1.03e+53
4	6.81e+52	6.81e+52	6.00e+52	5.44e+52	7.35e+52	5.05e+52	4.36e+52	5.18e+52	4.64e+52	3.42e+52	4.74e+52	4.68e+52	4.84e+52	6.10e+52	5.61e+52	5.78e+52	5.76e+52	5.34e+52	6.67e+52	7.49e+52
3	6.81e+52	6.81e+52	6.00e+52	5.44e+52	7.35e+52	4.26e+52	4.58e+52	4.00e+52	3.75e+52	4.29e+52	3.90e+52	4.50e+52	4.05e+52	4.01e+52	3.54e+52	4.16e+52	4.84e+52	3.97e+52	5.74e+52	6.13e+52
2	4.30e+52	4.30e+52	4.85e+52	4.85e+52	4.68e+52	4.41e+52	4.43e+52	5.03e+52	4.15e+52	4.01e+52	3.93e+52	3.77e+52	3.37e+52	3.45e+52	4.44e+52	3.06e+52	3.82e+52	3.05e+52	3.55e+52	3.68e+52
1	4.30e+52	4.30e+52	4.85e+52	4.85e+52	4.68e+52	4.41e+52	4.43e+52	5.03e+52	4.15e+52	4.01e+52	3.93e+52	3.77e+52	3.37e+52	3.45e+52	4.44e+52	3.06e+52	3.82e+52	3.05e+52	3.55e+52	3.68e+52

Table 18: Upper limit energy emission in erg by stars formed in the last 20 Myrs. Rows: DEC-Bin, Columns: RA-Bin (as in images), binsize $12' \times 12'$, conversion to coordinates in table 1.

	20	19	18	17	16	15	14	13	12	11	10	9	8	7	6	5	4	3	2	1
23	2.75e+52	2.71e+52	3.21e+52	3.48e+52	3.02e+52	4.27e+52	4.63e+52	3.95e+52	3.72e+52	4.98e+52	4.98e+52	3.58e+52	3.58e+52	3.42e+52	3.42e+52	3.17e+52	3.17e+52	2.67e+52	2.67e+52	0.00e+00
22	2.49e+52	3.39e+52	4.60e+52	4.85e+52	0.00e+00	0.00e+00	0.00e+00	7.54e+52	4.41e+52	4.98e+52	4.98e+52	3.58e+52	3.58e+52	3.42e+52	3.42e+52	3.17e+52	3.17e+52	2.67e+52	2.67e+52	0.00e+00
21	2.58e+52	6.34e+52	4.91e+52	7.97e+52	0.00e+00	0.00e+00	0.00e+00	5.94e+52	5.61e+52	0.00e+00	0.00e+00	3.21e+52	3.21e+52	3.79e+52	3.79e+52	3.58e+52	3.58e+52	3.65e+52	3.65e+52	0.00e+00
20	4.37e+52	6.50e+52	9.13e+52	1.37e+53	1.53e+53	8.97e+52	7.22e+52	8.54e+52	5.60e+52	0.00e+00	0.00e+00	3.44e+52	3.44e+52	3.79e+52	3.79e+52	3.58e+52	3.58e+52	3.65e+52	3.65e+52	0.00e+00
19	7.12e+52	1.08e+53	1.75e+53	1.50e+53	1.40e+53	1.27e+53	1.08e+53	1.21e+53	8.29e+52	0.00e+00	0.00e+00	4.75e+52	4.75e+52	3.32e+52	3.32e+52	4.08e+52	4.08e+52	3.65e+52	3.65e+52	0.00e+00
18	8.76e+52	1.72e+53	1.60e+53	1.59e+53	1.72e+53	1.60e+53	2.25e+53	1.76e+53	1.39e+53	9.67e+52	5.63e+52	5.52e+52	5.52e+52	3.80e+52	3.80e+52	4.08e+52	4.08e+52	0.00e+00	0.00e+00	0.00e+00
17	1.24e+53	1.53e+53	1.30e+53	1.91e+53	2.23e+53	2.30e+53	2.88e+53	2.61e+53	2.24e+53	1.81e+53	1.04e+53	7.71e+52	4.12e+52	4.25e+52	4.25e+52	3.52e+52	3.52e+52	0.00e+00	0.00e+00	0.00e+00
16	9.77e+52	1.12e+53	1.56e+53	2.37e+53	3.86e+53	1.98e+53	1.41e+53	1.04e+53	1.07e+53	2.66e+53	1.35e+53	1.05e+53	5.15e+52	4.02e+52	3.36e+52	3.61e+52	3.61e+52	0.00e+00	0.00e+00	0.00e+00
15	8.88e+52	1.48e+53	1.91e+53	2.69e+53	4.62e+53	4.69e+53	4.48e+53	2.40e+53	2.43e+53	3.46e+53	2.64e+53	1.15e+53	8.96e+52	5.68e+52	4.07e+52	3.63e+52	3.63e+52	0.00e+00	0.00e+00	0.00e+00
14	1.08e+53	1.40e+53	2.37e+53	1.44e+53	1.45e+53	5.43e+53	2.57e+53	2.25e+53	2.36e+53	1.93e+53	2.43e+53	1.68e+53	1.06e+53	6.23e+52	6.15e+52	5.39e+52	5.39e+52	0.00e+00	0.00e+00	0.00e+00
13	1.26e+53	5.02e+53	1.82e+53	1.23e+53	1.33e+53	6.77e+53	1.47e+53	2.08e+53	5.15e+53	2.89e+53	2.19e+53	2.03e+53	1.06e+53	9.39e+52	5.97e+52	5.91e+52	5.91e+52	4.91e+52	4.91e+52	4.91e+52
12	1.39e+53	1.89e+53	2.65e+53	3.10e+53	9.55e+52	1.47e+53	3.77e+53	1.98e+53	4.37e+53	8.30e+53	2.58e+53	2.22e+53	2.01e+53	1.31e+53	1.02e+53	5.67e+52	5.00e+52	3.98e+52	3.96e+52	3.96e+52
11	1.26e+53	1.96e+53	2.08e+53	2.36e+53	3.07e+53	1.09e+53	9.05e+52	1.00e+53	2.77e+53	6.49e+53	3.72e+53	2.91e+53	2.38e+53	1.72e+53	1.49e+53	1.41e+53	5.65e+52	4.55e+52	5.29e+52	5.29e+52
10	2.58e+53	2.28e+53	1.75e+53	2.28e+53	2.73e+53	1.03e+53	1.03e+53	1.14e+53	3.03e+53	5.58e+53	7.84e+53	7.40e+53	4.89e+53	3.58e+53	2.06e+53	1.54e+53	8.49e+52	6.54e+52	6.12e+52	7.32e+52
9	2.95e+53	3.07e+53	1.95e+53	2.25e+53	2.02e+53	2.31e+53	1.07e+53	1.05e+53	1.62e+53	3.09e+53	5.72e+53	3.32e+53	3.17e+53	9.29e+52	2.22e+53	1.44e+53	1.09e+53	9.92e+52	8.62e+52	7.32e+52
8	1.38e+53	1.11e+53	1.41e+53	1.80e+53	1.80e+53	2.07e+53	2.15e+53	2.26e+53	3.13e+53	1.09e+53	2.98e+53	4.14e+53	2.11e+53	1.36e+53	2.04e+53	1.85e+53	1.80e+53	1.14e+53	9.93e+52	8.52e+52
7	1.03e+53	1.22e+53	1.36e+53	1.47e+53	1.42e+53	1.44e+53	1.36e+53	1.39e+53	1.76e+53	1.89e+53	9.87e+52	1.04e+53	8.06e+52	9.52e+52	8.10e+52	1.89e+53	1.59e+53	1.36e+53	1.16e+53	1.05e+53
6	1.02e+53	1.08e+53	1.32e+53	1.28e+53	1.12e+53	9.49e+52	8.65e+52	8.98e+52	1.18e+53	1.14e+53	1.14e+53	1.43e+53	1.33e+53	1.44e+53	1.79e+53	1.41e+53	1.61e+53	1.32e+53	1.49e+53	1.13e+53
5	1.02e+53	1.08e+53	1.32e+53	1.28e+53	8.62e+52	7.31e+52	6.36e+52	7.43e+52	6.44e+52	5.63e+52	6.51e+52	7.88e+52	8.80e+52	1.03e+53	1.06e+53	1.14e+53	1.05e+53	9.57e+52	9.75e+52	1.23e+53
4	8.19e+52	8.19e+52	7.24e+52	6.61e+52	8.98e+52	6.15e+52	5.30e+52	6.25e+52	5.59e+52	4.12e+52	5.63e+52	5.62e+52	5.77e+52	7.30e+52	7.10e+52	6.86e+52	6.96e+52	6.48e+52	8.14e+52	9.07e+52
3	8.19e+52	8.19e+52	7.24e+52	6.61e+52	8.98e+52	5.18e+52	5.58e+52	4.86e+52	4.52e+52	5.21e+52	4.75e+52	5.48e+52	4.93e+52	4.85e+52	4.30e+52	5.05e+52	5.80e+52	4.84e+52	7.30e+52	7.51e+52
2	5.21e+52	5.21e+52	5.91e+52	5.91e+52	5.67e+52	5.37e+52	5.41e+52	6.13e+52	5.03e+52	4.88e+52	4.78e+52	4.57e+52	4.08e+52	4.19e+52	5.35e+52	3.72e+52	4.66e+52	3.72e+52	4.26e+52	4.48e+52
1	5.21e+52	5.21e+52	5.91e+52	5.91e+52	5.67e+52	5.37e+52	5.41e+52	6.13e+52	5.03e+52	4.88e+52	4.78e+52	4.57e+52	4.08e+52	4.19e+52	5.35e+52	3.72e+52	4.66e+52	3.72e+52	4.26e+52	4.48e+52

Table 19: Upper limit energy emission in erg by stars formed in the last 29 Myrs. Rows: DEC-Bin, Columns: RA-Bin (as in images), binsize $12' \times 12'$, conversion to coordinates in table 1.

	20	19	18	17	16	15	14	13	12	11	10	9	8	7	6	5	4	3	2	1
23	0.00e+00	0.00e+00	0.00e+00	0.00e+00	0.00e+00	0.00e+00	6.82e+48	0.00e+00	1.94e+47	4.10e+47	4.10e+47	0.00e+00	0.00e+00	0.00e+00	0.00e+00	0.00e+00	0.00e+00	0.00e+00	0.00e+00	0.00e+00
22	0.00e+00	0.00e+00	0.00e+00	1.64e+48	0.00e+00	0.00e+00	0.00e+00	0.00e+00	0.00e+00	4.10e+47	4.10e+47	0.00e+00	0.00e+00	0.00e+00	0.00e+00	0.00e+00	0.00e+00	0.00e+00	0.00e+00	0.00e+00
21	0.00e+00	0.00e+00	7.82e+48	0.00e+00	0.00e+00	0.00e+00	0.00e+00	0.00e+00	0.00e+00	0.00e+00	0.00e+00	0.00e+00	0.00e+00	0.00e+00	0.00e+00	0.00e+00	0.00e+00	0.00e+00	0.00e+00	0.00e+00
20	0.00e+00	5.21e+48	0.00e+00	0.00e+00	9.09e+48	0.00e+00	0.00e+00	1.83e+50	0.00e+00	0.00e+00	0.00e+00	2.28e+49	2.28e+49	0.00e+00	0.00e+00	0.00e+00	0.00e+00	0.00e+00	0.00e+00	0.00e+00
19	0.00e+00	0.00e+00	2.05e+48	0.00e+00	2.60e+49	0.00e+00	0.00e+00	0.00e+00	0.00e+00	0.00e+00	0.00e+00	0.00e+00	0.00e+00	0.00e+00	0.00e+00	1.83e+49	1.83e+49	0.00e+00	0.00e+00	0.00e+00
18	2.89e+49	2.89e+49	9.63e+48	3.88e+50	1.44e+50	2.87e+49	4.50e+52	7.80e+50	3.77e+50	0.00e+00	0.00e+00	2.15e+49	2.15e+49	0.00e+00	0.00e+00	1.83e+49	1.83e+49	0.00e+00	0.00e+00	0.00e+00
17	0.00e+00	9.09e+49	0.00e+00	8.33e+51	1.15e+52	0.00e+00	1.04e+52	9.83e+50	2.23e+52	8.10e+51	2.07e+50	0.00e+00	0.00e+00	0.00e+00	0.00e+00	0.00e+00	0.00e+00	0.00e+00	0.00e+00	0.00e+00
16	4.10e+47	0.00e+00	0.00e+00	7.37e+49	5.38e+52	1.64e+48	0.00e+00	0.00e+00	0.00e+00	1.90e+51	1.09e+52	0.00e+00	0.00e+00	0.00e+00	0.00e+00	0.00e+00	0.00e+00	0.00e+00	0.00e+00	0.00e+00
15	2.89e+49	0.00e+00	8.21e+50	2.12e+52	7.09e+51	3.31e+52	1.59e+51	0.00e+00	0.00e+00	0.00e+00	1.61e+51	5.56e+51	0.00e+00	0.00e+00	0.00e+00	0.00e+00	0.00e+00	0.00e+00	0.00e+00	0.00e+00
14	6.82e+49	0.00e+00	1.74e+52	0.00e+00	0.00e+00	1.71e+52	0.00e+00	0.00e+00	0.00e+00	0.00e+00	7.86e+51	6.61e+50	2.28e+51	7.75e+49	0.00e+00	0.00e+00	0.00e+00	0.00e+00	0.00e+00	0.00e+00
13	4.10e+47	1.43e+53	3.15e+51	0.00e+00	0.00e+00	2.26e+51	0.00e+00	0.00e+00	0.00e+00	0.00e+00	0.00e+00	3.69e+49	1.83e+50	6.82e+49	1.94e+48	0.00e+00	0.00e+00	0.00e+00	0.00e+00	0.00e+00
12	0.00e+00	5.62e+50	4.19e+52	9.85e+49	0.00e+00	0.00e+00	8.28e+50	0.00e+00	2.58e+51	7.03e+52	0.00e+00	0.00e+00	0.00e+00	0.00e+00	0.00e+00	0.00e+00	0.00e+00	0.00e+00	0.00e+00	0.00e+00
11	1.23e+48	8.90e+50	1.82e+52	8.21e+48	4.18e+50	0.00e+00	0.00e+00	0.00e+00	0.00e+00	0.00e+00	0.00e+00	0.00e+00	0.00e+00	0.00e+00	0.00e+00	6.15e+50	0.00e+00	0.00e+00	8.21e+47	8.21e+47
10	4.86e+52	6.21e+52	2.91e+52	2.29e+52	0.00e+00	0.00e+00	0.00e+00	0.00e+00	0.00e+00	0.00e+00	9.14e+50	8.54e+52	2.26e+51	1.95e+52	8.21e+48	6.89e+50	1.32e+51	0.00e+00	0.00e+00	0.00e+00
9	5.51e+52	6.88e+52	3.17e+52	3.28e+52	5.17e+49	0.00e+00	0.00e+00	0.00e+00	4.10e+48	0.00e+00	2.92e+50	0.00e+00	0.00e+00	0.00e+00	0.00e+00	0.00e+00	3.02e+51	2.61e+49	0.00e+00	0.00e+00
8	1.39e+50	0.00e+00	0.00e+00	0.00e+00	4.10e+48	5.62e+50	2.07e+50	1.03e+50	4.02e+50	0.00e+00	0.00e+00	0.00e+00	0.00e+00	0.00e+00	0.00e+00	7.38e+50	1.14e+51	0.00e+00	0.00e+00	0.00e+00
7	0.00e+00	8.21e+48	1.23e+48	8.21e+48	4.34e+51	4.57e+49	0.00e+00	1.23e+49	1.23e+49	0.00e+00	0.00e+00	0.00e+00	0.00e+00	0.00e+00	0.00e+00	7.55e+51	1.64e+49	0.00e+00	1.23e+48	0.00e+00
6	4.54e+48	1.23e+48	4.10e+47	0.00e+00	0.00e+00	0.00e+00	9.14e+49	2.59e+50	1.04e+49	0.00e+00	2.07e+50	2.67e+50	2.33e+51	4.14e+50	5.21e+50	1.23e+48	3.69e+49	8.21e+47	1.64e+49	0.00e+00
5	4.54e+48	1.23e+48	4.10e+47	0.00e+00	0.00e+00	0.00e+00	0.00e+00	1.55e+49	0.00e+00	0.00e+00	9.14e+48	1.83e+50	0.00e+00	0.00e+00	2.59e+50	0.00e+00	0.00e+00	0.00e+00	2.38e+49	9.15e+49
4	9.14e+49	9.14e+49	2.28e+49	1.83e+49	0.00e+00	0.00e+00	0.00e+00	0.00e+00	0.00e+00	0.00e+00	0.00e+00	4.57e+48	5.81e+49	0.00e+00	0.00e+00	1.83e+50	0.00e+00	6.48e+48	2.27e+48	0.00e+00
3	9.14e+49	9.14e+49	2.28e+49	1.83e+49	0.00e+00	0.00e+00	0.00e+00	0.00e+00	0.00e+00	0.00e+00	0.00e+00	0.00e+00	0.00e+00	4.57e+48	0.00e+00	0.00e+00	0.00e+00	0.00e+00	0.00e+00	7.77e+47
2	0.00e+00	0.00e+00	0.00e+00	0.00e+00	0.00e+00	0.00e+00	0.00e+00	0.00e+00	0.00e+00	0.00e+00	0.00e+00	0.00e+00	0.00e+00	0.00e+00	0.00e+00	0.00e+00	0.00e+00	0.00e+00	0.00e+00	9.71e+47
1	0.00e+00	0.00e+00	0.00e+00	0.00e+00	0.00e+00	0.00e+00	0.00e+00	0.00e+00	0.00e+00	0.00e+00	0.00e+00	0.00e+00	0.00e+00	0.00e+00	0.00e+00	0.00e+00	0.00e+00	0.00e+00	0.00e+00	9.71e+47

Table 20: Expected energy emission in erg by stars formed in the last 20 Myrs integrated starting 10 Myr ago. Rows: DEC-Bin, Columns: RA-Bin (as in images), binsize $12' \times 12'$, conversion to coordinates in table 1.

	20	19	18	17	16	15	14	13	12	11	10	9	8	7	6	5	4	3	2	1
23	0.00e+00	0.00e+00	8.38e+50	0.00e+00	0.00e+00	7.02e+48	6.25e+50	1.47e+49	8.46e+49	9.69e+49	9.69e+49	0.00e+00	0.00e+00	3.93e+49	3.93e+49	0.00e+00	0.00e+00	6.62e+47	6.62e+47	0.00e+00
22	0.00e+00	0.00e+00	3.12e+51	1.44e+50	0.00e+00	0.00e+00	0.00e+00	2.87e+48	0.00e+00	9.69e+49	9.69e+49	0.00e+00	0.00e+00	3.93e+49	3.93e+49	0.00e+00	0.00e+00	6.62e+47	6.62e+47	0.00e+00
21	0.00e+00	0.00e+00	5.03e+50	1.28e+49	0.00e+00	0.00e+00	0.00e+00	0.00e+00	2.38e+48	0.00e+00	0.00e+00	0.00e+00	0.00e+00	0.00e+00	0.00e+00	6.30e+50	6.30e+50	3.71e+48	3.71e+48	0.00e+00
20	0.00e+00	1.02e+51	0.00e+00	0.00e+00	2.51e+50	1.95e+48	1.20e+48	7.95e+51	5.46e+48	0.00e+00	0.00e+00	9.37e+50	9.37e+50	0.00e+00	0.00e+00	6.30e+50	6.30e+50	3.71e+48	3.71e+48	0.00e+00
19	1.61e+51	0.00e+00	3.25e+50	1.25e+51	2.13e+51	5.41e+50	0.00e+00	1.27e+52	2.72e+50	0.00e+00	0.00e+00	1.25e+50	1.25e+50	2.74e+49	2.74e+49	1.75e+51	1.75e+51	3.71e+48	3.71e+48	0.00e+00
18	1.28e+51	4.65e+51	4.54e+51	1.98e+52	9.86e+50	1.16e+51	6.21e+52	1.55e+51	1.02e+51	1.62e+50	3.00e+51	1.87e+51	1.87e+51	6.74e+49	6.74e+49	1.75e+51	1.75e+51	0.00e+00	0.00e+00	0.00e+00
17	7.18e+50	5.32e+51	1.73e+52	2.59e+52	3.06e+52	1.23e+52	3.28e+52	2.59e+52	4.15e+52	2.37e+52	1.42e+52	5.55e+50	1.53e+51	4.45e+49	4.45e+49	0.00e+00	0.00e+00	0.00e+00	0.00e+00	0.00e+00
16	3.91e+50	3.55e+48	2.49e+52	1.99e+52	8.63e+52	5.33e+51	2.80e+49	0.00e+00	0.00e+00	3.12e+51	2.36e+52	5.65e+49	0.00e+00	3.19e+49	0.00e+00	1.94e+48	1.94e+48	0.00e+00	0.00e+00	0.00e+00
15	2.82e+51	1.77e+50	1.68e+51	4.25e+52	5.18e+52	1.21e+53	6.46e+52	1.96e+50	0.00e+00	2.53e+52	2.17e+52	1.74e+52	2.96e+49	0.00e+00	6.08e+49	0.00e+00	0.00e+00	0.00e+00	0.00e+00	0.00e+00
14	4.39e+51	3.44e+51	6.03e+52	1.87e+50	3.78e+49	4.91e+52	0.00e+00	0.00e+00	0.00e+00	0.00e+00	3.32e+52	1.43e+51	1.64e+52	4.15e+51	5.16e+51	3.97e+51	3.97e+51	0.00e+00	0.00e+00	0.00e+00
13	4.07e+50	1.73e+53	2.50e+52	1.52e+49	2.89e+49	3.32e+52	3.56e+50	0.00e+00	7.37e+50	0.00e+00	0.00e+00	1.30e+51	1.30e+52	4.39e+51	1.62e+51	2.00e+50	2.00e+50	7.09e+49	7.09e+49	7.09e+49
12	6.92e+50	1.41e+51	6.31e+52	2.40e+52	0.00e+00	0.00e+00	4.07e+52	0.00e+00	4.53e+51	1.10e+53	0.00e+00	0.00e+00	0.00e+00	0.00e+00	3.62e+51	0.00e+00	7.89e+49	0.00e+00	0.00e+00	0.00e+00
11	4.18e+50	1.75e+51	3.68e+52	7.31e+51	1.47e+52	9.13e+48	0.00e+00	0.00e+00	0.00e+00	4.68e+50	0.00e+00	0.00e+00	0.00e+00	0.00e+00	0.00e+00	1.22e+51	1.12e+51	0.00e+00	1.26e+50	1.26e+50
10	6.68e+52	7.76e+52	4.36e+52	4.26e+52	1.18e+52	0.00e+00	0.00e+00	0.00e+00	0.00e+00	4.50e+50	7.92e+52	1.77e+53	5.29e+51	5.22e+52	1.31e+51	1.38e+51	1.02e+52	0.00e+00	1.16e+49	2.22e+51
9	7.36e+52	9.42e+52	4.72e+52	5.14e+52	1.87e+52	1.65e+52	0.00e+00	0.00e+00	4.66e+50	1.04e+51	3.23e+52	1.53e+52	1.45e+49	0.00e+00	1.69e+52	4.70e+51	1.41e+52	3.41e+51	2.81e+50	2.22e+51
8	9.40e+50	0.00e+00	9.11e+50	2.47e+50	1.22e+51	1.54e+51	1.93e+52	1.72e+52	2.09e+51	0.00e+00	5.18e+51	2.09e+52	0.00e+00	1.99e+49	0.00e+00	1.59e+51	1.93e+51	1.70e+50	7.53e+49	3.36e+51
7	0.00e+00	5.59e+50	3.29e+50	6.38e+50	1.78e+52	1.79e+52	1.18e+52	6.84e+50	8.52e+50	4.87e+50	0.00e+00	1.40e+49	0.00e+00	0.00e+00	0.00e+00	2.51e+52	6.04e+50	6.25e+50	2.00e+50	0.00e+00
6	6.48e+50	1.61e+50	2.70e+50	2.27e+48	2.78e+48	0.00e+00	5.12e+51	6.98e+51	2.41e+51	2.85e+49	9.52e+51	9.44e+50	1.93e+52	1.10e+51	1.37e+51	1.78e+50	1.09e+51	1.39e+50	8.14e+50	1.13e+50
5	6.48e+50	1.61e+50	2.70e+50	2.27e+48	0.00e+00	6.15e+47	0.00e+00	3.69e+51	9.87e+50	0.00e+00	1.24e+51	4.75e+51	6.52e+51	0.00e+00	8.02e+51	7.24e+50	0.00e+00	6.63e+48	2.03e+51	2.53e+51
4	6.03e+51	6.03e+51	3.22e+51	6.58e+50	0.00e+00	7.31e+49	0.00e+00	1.91e+50	0.00e+00	0.00e+00	2.32e+51	1.88e+51	3.16e+51	2.24e+51	1.28e+49	7.49e+51	3.86e+51	1.41e+51	1.62e+51	2.80e+51
3	6.03e+51	6.03e+51	3.22e+51	6.58e+50	0.00e+00	0.00e+00	0.00e+00	0.00e+00	0.00e+00	0.00e+00	0.00e+00	4.91e+49	0.00e+00	1.51e+51	0.00e+00	1.18e+51	1.04e+50	0.00e+00	1.50e+51	4.01e+49
2	3.66e+50	3.66e+50	0.00e+00	0.00e+00	1.80e+51	0.00e+00	0.00e+00	0.00e+00	1.05e+51	0.00e+00	0.00e+00	2.10e+50	5.99e+50	0.00e+00	1.88e+51	0.00e+00	0.00e+00	0.00e+00	2.08e+51	2.85e+49
1	3.66e+50	3.66e+50	0.00e+00	0.00e+00	1.80e+51	0.00e+00	0.00e+00	0.00e+00	1.05e+51	0.00e+00	0.00e+00	2.10e+50	5.99e+50	0.00e+00	1.88e+51	0.00e+00	0.00e+00	0.00e+00	2.08e+51	2.85e+49

Table 21: Expected energy emission in erg by stars formed in the last 29 Myrs integrated starting 10 Myr ago. Rows: DEC-Bin, Columns: RA-Bin (as in images), binsize $12' \times 12'$, conversion to coordinates in table 1.

	20	19	18	17	16	15	14	13	12	11	10	9	8	7	6	5	4	3	2	1
23	0.00e+00	0.00e+00	0.00e+00	0.00e+00	0.00e+00	0.00e+00	6.82e+48	0.00e+00	1.94e+47	4.10e+47	4.10e+47	0.00e+00	0.00e+00	0.00e+00	0.00e+00	0.00e+00	0.00e+00	0.00e+00	0.00e+00	0.00e+00
22	0.00e+00	0.00e+00	0.00e+00	1.64e+48	0.00e+00	0.00e+00	0.00e+00	0.00e+00	0.00e+00	4.10e+47	4.10e+47	0.00e+00	0.00e+00	0.00e+00	0.00e+00	0.00e+00	0.00e+00	0.00e+00	0.00e+00	0.00e+00
21	0.00e+00	0.00e+00	7.82e+48	0.00e+00	0.00e+00	0.00e+00	0.00e+00	0.00e+00	0.00e+00	0.00e+00	0.00e+00	0.00e+00	0.00e+00	0.00e+00	0.00e+00	0.00e+00	0.00e+00	0.00e+00	0.00e+00	0.00e+00
20	0.00e+00	5.21e+48	0.00e+00	0.00e+00	9.09e+48	0.00e+00	0.00e+00	1.83e+50	0.00e+00	0.00e+00	0.00e+00	2.28e+49	2.28e+49	0.00e+00	0.00e+00	0.00e+00	0.00e+00	0.00e+00	0.00e+00	0.00e+00
19	0.00e+00	0.00e+00	2.05e+48	0.00e+00	2.60e+49	0.00e+00	0.00e+00	0.00e+00	0.00e+00	0.00e+00	0.00e+00	0.00e+00	0.00e+00	0.00e+00	0.00e+00	1.83e+49	1.83e+49	0.00e+00	0.00e+00	0.00e+00
18	2.89e+49	2.89e+49	9.63e+48	3.88e+50	1.44e+50	2.87e+49	4.50e+52	7.80e+50	3.77e+50	0.00e+00	0.00e+00	2.15e+49	2.15e+49	0.00e+00	0.00e+00	1.83e+49	1.83e+49	0.00e+00	0.00e+00	0.00e+00
17	0.00e+00	9.09e+49	0.00e+00	8.33e+51	1.15e+52	0.00e+00	1.04e+52	9.83e+50	2.23e+52	8.10e+51	2.07e+50	0.00e+00	0.00e+00	0.00e+00	0.00e+00	0.00e+00	0.00e+00	0.00e+00	0.00e+00	0.00e+00
16	4.10e+47	0.00e+00	0.00e+00	7.37e+49	5.38e+52	1.64e+48	0.00e+00	0.00e+00	0.00e+00	1.90e+51	1.09e+52	0.00e+00	0.00e+00	0.00e+00	0.00e+00	0.00e+00	0.00e+00	0.00e+00	0.00e+00	0.00e+00
15	2.89e+49	0.00e+00	8.21e+50	2.12e+52	7.09e+51	3.31e+52	1.59e+51	0.00e+00	0.00e+00	0.00e+00	1.61e+51	5.56e+51	0.00e+00	0.00e+00	0.00e+00	0.00e+00	0.00e+00	0.00e+00	0.00e+00	0.00e+00
14	6.82e+49	0.00e+00	1.74e+52	0.00e+00	0.00e+00	1.71e+52	0.00e+00	0.00e+00	0.00e+00	0.00e+00	7.86e+51	6.61e+50	2.28e+51	7.75e+49	0.00e+00	0.00e+00	0.00e+00	0.00e+00	0.00e+00	0.00e+00
13	4.10e+47	1.43e+53	3.15e+51	0.00e+00	0.00e+00	2.26e+51	0.00e+00	0.00e+00	0.00e+00	0.00e+00	0.00e+00	3.69e+49	1.83e+50	6.82e+49	1.94e+48	0.00e+00	0.00e+00	0.00e+00	0.00e+00	0.00e+00
12	0.00e+00	5.62e+50	4.19e+52	9.85e+49	0.00e+00	0.00e+00	8.28e+50	0.00e+00	2.58e+51	7.03e+52	0.00e+00	0.00e+00	0.00e+00	0.00e+00	0.00e+00	0.00e+00	0.00e+00	0.00e+00	0.00e+00	0.00e+00
11	1.23e+48	8.90e+50	1.82e+52	8.21e+48	4.18e+50	0.00e+00	0.00e+00	0.00e+00	0.00e+00	0.00e+00	0.00e+00	0.00e+00	0.00e+00	0.00e+00	0.00e+00	6.15e+50	0.00e+00	0.00e+00	8.21e+47	8.21e+47
10	4.86e+52	6.21e+52	2.91e+52	2.29e+52	0.00e+00	0.00e+00	0.00e+00	0.00e+00	0.00e+00	0.00e+00	9.14e+50	8.54e+52	2.26e+51	1.95e+52	8.21e+48	6.89e+50	1.32e+51	0.00e+00	0.00e+00	0.00e+00
9	5.51e+52	6.88e+52	3.17e+52	3.28e+52	5.17e+49	0.00e+00	0.00e+00	0.00e+00	4.10e+48	0.00e+00	2.92e+50	0.00e+00	0.00e+00	0.00e+00	0.00e+00	0.00e+00	3.02e+51	2.61e+49	0.00e+00	0.00e+00
8	1.39e+50	0.00e+00	0.00e+00	0.00e+00	4.10e+48	5.62e+50	2.07e+50	1.03e+50	4.02e+50	0.00e+00	0.00e+00	0.00e+00	0.00e+00	0.00e+00	0.00e+00	7.38e+50	1.14e+51	0.00e+00	0.00e+00	0.00e+00
7	0.00e+00	8.21e+48	1.23e+48	8.21e+48	4.34e+51	4.57e+49	0.00e+00	1.23e+49	1.23e+49	0.00e+00	0.00e+00	0.00e+00	0.00e+00	0.00e+00	0.00e+00	7.55e+51	1.64e+49	0.00e+00	1.23e+48	0.00e+00
6	4.54e+48	1.23e+48	4.10e+47	0.00e+00	0.00e+00	0.00e+00	9.14e+49	2.59e+50	1.04e+49	0.00e+00	2.07e+50	2.67e+50	2.33e+51	4.14e+50	5.21e+50	1.23e+48	3.69e+49	8.21e+47	1.64e+49	0.00e+00
5	4.54e+48	1.23e+48	4.10e+47	0.00e+00	0.00e+00	0.00e+00	0.00e+00	1.55e+49	0.00e+00	0.00e+00	9.14e+48	1.83e+50	0.00e+00	0.00e+00	2.59e+50	0.00e+00	0.00e+00	0.00e+00	2.38e+49	9.15e+49
4	9.14e+49	9.14e+49	2.28e+49	1.83e+49	0.00e+00	0.00e+00	0.00e+00	0.00e+00	0.00e+00	0.00e+00	0.00e+00	4.57e+48	5.81e+49	0.00e+00	0.00e+00	1.83e+50	0.00e+00	6.48e+48	2.27e+48	0.00e+00
3	9.14e+49	9.14e+49	2.28e+49	1.83e+49	0.00e+00	0.00e+00	0.00e+00	0.00e+00	0.00e+00	0.00e+00	0.00e+00	0.00e+00	0.00e+00	4.57e+48	0.00e+00	0.00e+00	0.00e+00	0.00e+00	0.00e+00	7.77e+47
2	0.00e+00	0.00e+00	0.00e+00	0.00e+00	0.00e+00	0.00e+00	0.00e+00	0.00e+00	0.00e+00	0.00e+00	0.00e+00	0.00e+00	0.00e+00	0.00e+00	0.00e+00	0.00e+00	0.00e+00	0.00e+00	0.00e+00	9.71e+47
1	0.00e+00	0.00e+00	0.00e+00	0.00e+00	0.00e+00	0.00e+00	0.00e+00	0.00e+00	0.00e+00	0.00e+00	0.00e+00	0.00e+00	0.00e+00	0.00e+00	0.00e+00	0.00e+00	0.00e+00	0.00e+00	0.00e+00	9.71e+47

Table 22: Lower limit energy emission in erg by stars formed in the last 20 Myrs integrated starting 10 Myr ago. Rows: DEC-Bin, Columns: RA-Bin (as in images), binsize $12' \times 12'$, conversion to coordinates in table 1.

	20	19	18	17	16	15	14	13	12	11	10	9	8	7	6	5	4	3	2	1
23	0.00e+00	0.00e+00	0.00e+00	0.00e+00	0.00e+00	0.00e+00	6.83e+48	0.00e+00	1.96e+47	4.20e+47	4.20e+47	0.00e+00	0.00e+00	0.00e+00	0.00e+00	0.00e+00	0.00e+00	0.00e+00	0.00e+00	0.00e+00
22	0.00e+00	0.00e+00	0.00e+00	1.68e+48	0.00e+00	0.00e+00	0.00e+00	1.45e+46	0.00e+00	4.20e+47	4.20e+47	0.00e+00	0.00e+00	0.00e+00	0.00e+00	0.00e+00	0.00e+00	0.00e+00	0.00e+00	0.00e+00
21	0.00e+00	0.00e+00	7.82e+48	0.00e+00	0.00e+00	0.00e+00	0.00e+00	0.00e+00	9.68e+45	0.00e+00	0.00e+00	0.00e+00	0.00e+00	0.00e+00	0.00e+00	0.00e+00	0.00e+00	0.00e+00	0.00e+00	0.00e+00
20	0.00e+00	5.21e+48	0.00e+00	0.00e+00	9.09e+48	1.45e+46	0.00e+00	1.83e+50	0.00e+00	0.00e+00	0.00e+00	2.28e+49	2.28e+49	0.00e+00	0.00e+00	0.00e+00	0.00e+00	0.00e+00	0.00e+00	0.00e+00
19	0.00e+00	0.00e+00	2.10e+48	0.00e+00	2.63e+49	0.00e+00	0.00e+00	0.00e+00	0.00e+00	0.00e+00	0.00e+00	0.00e+00	0.00e+00	0.00e+00	0.00e+00	1.83e+49	1.83e+49	0.00e+00	0.00e+00	0.00e+00
18	2.89e+49	2.89e+49	9.63e+48	3.88e+50	1.47e+50	2.94e+49	4.50e+52	7.97e+50	3.86e+50	0.00e+00	0.00e+00	2.15e+49	2.15e+49	0.00e+00	0.00e+00	1.83e+49	1.83e+49	0.00e+00	0.00e+00	0.00e+00
17	0.00e+00	9.09e+49	0.00e+00	8.33e+51	1.15e+52	0.00e+00	1.05e+52	9.87e+50	2.23e+52	8.11e+51	2.07e+50	0.00e+00	0.00e+00	0.00e+00	0.00e+00	0.00e+00	0.00e+00	0.00e+00	0.00e+00	0.00e+00
16	4.20e+47	1.45e+46	0.00e+00	7.37e+49	5.38e+52	1.68e+48	1.77e+47	0.00e+00	0.00e+00	1.94e+51	1.09e+52	2.29e+49	0.00e+00	0.00e+00	0.00e+00	0.00e+00	0.00e+00	0.00e+00	0.00e+00	0.00e+00
15	2.89e+49	1.94e+46	8.39e+50	2.12e+52	7.09e+51	3.31e+52	1.59e+51	9.88e+49	0.00e+00	1.42e+50	1.65e+51	5.56e+51	4.41e+46	0.00e+00	0.00e+00	0.00e+00	0.00e+00	0.00e+00	0.00e+00	0.00e+00
14	6.82e+49	0.00e+00	1.74e+52	0.00e+00	0.00e+00	1.72e+52	0.00e+00	0.00e+00	0.00e+00	0.00e+00	7.86e+51	6.76e+50	2.28e+51	7.75e+49	0.00e+00	0.00e+00	0.00e+00	0.00e+00	0.00e+00	0.00e+00
13	4.20e+47	1.43e+53	3.15e+51	1.77e+47	1.77e+47	2.35e+51	0.00e+00	0.00e+00	5.96e+50	0.00e+00	0.00e+00	3.78e+49	1.83e+50	6.82e+49	1.94e+48	0.00e+00	0.00e+00	0.00e+00	0.00e+00	0.00e+00
12	0.00e+00	5.75e+50	4.19e+52	1.01e+50	0.00e+00	0.00e+00	8.28e+50	0.00e+00	2.64e+51	7.08e+52	0.00e+00	0.00e+00	0.00e+00	0.00e+00	0.00e+00	0.00e+00	0.00e+00	0.00e+00	0.00e+00	0.00e+00
11	1.28e+48	9.11e+50	1.82e+52	8.39e+48	4.28e+50	0.00e+00	0.00e+00	0.00e+00	0.00e+00	2.25e+50	0.00e+00	0.00e+00	0.00e+00	0.00e+00	0.00e+00	6.29e+50	0.00e+00	0.00e+00	8.39e+47	8.39e+47
10	4.86e+52	6.21e+52	2.91e+52	2.29e+52	0.00e+00	0.00e+00	0.00e+00	0.00e+00	0.00e+00	2.52e+50	1.26e+51	8.54e+52	2.31e+51	1.95e+52	8.39e+48	7.05e+50	1.32e+51	0.00e+00	8.83e+46	0.00e+00
9	5.51e+52	6.88e+52	3.17e+52	3.28e+52	5.17e+49	0.00e+00	0.00e+00	0.00e+00	4.20e+48	0.00e+00	2.93e+50	0.00e+00	0.00e+00	0.00e+00	0.00e+00	4.41e+47	3.02e+51	2.61e+49	0.00e+00	0.00e+00
8	1.43e+50	0.00e+00	0.00e+00	0.00e+00	4.20e+48	5.75e+50	2.07e+50	1.03e+50	4.11e+50	0.00e+00	0.00e+00	0.00e+00	0.00e+00	0.00e+00	0.00e+00	7.55e+50	1.17e+51	0.00e+00	0.00e+00	0.00e+00
7	0.00e+00	8.57e+48	1.26e+48	8.39e+48	4.34e+51	4.57e+49	0.00e+00	1.26e+49	1.26e+49	0.00e+00	0.00e+00	0.00e+00	0.00e+00	0.00e+00	0.00e+00	7.55e+51	1.68e+49	0.00e+00	1.26e+48	0.00e+00
6	4.55e+48	1.26e+48	4.20e+47	0.00e+00	1.94e+46	0.00e+00	9.14e+49	2.59e+50	1.04e+49	0.00e+00	2.07e+50	2.73e+50	2.33e+51	4.24e+50	5.33e+50	1.26e+48	3.78e+49	8.39e+47	1.68e+49	1.94e+46
5	4.55e+48	1.26e+48	4.20e+47	0.00e+00	0.00e+00	0.00e+00	0.00e+00	1.55e+49	0.00e+00	0.00e+00	9.14e+48	1.83e+50	0.00e+00	0.00e+00	2.59e+50	0.00e+00	0.00e+00	2.47e+48	2.38e+49	9.15e+49
4	9.14e+49	9.14e+49	2.28e+49	1.83e+49	0.00e+00	0.00e+00	0.00e+00	0.00e+00	0.00e+00	0.00e+00	0.00e+00	4.57e+48	5.81e+49	0.00e+00	4.41e+46	1.83e+50	0.00e+00	6.48e+48	2.27e+48	0.00e+00
3	9.14e+49	9.14e+49	2.28e+49	1.83e+49	0.00e+00	0.00e+00	0.00e+00	0.00e+00	0.00e+00	0.00e+00	0.00e+00	0.00e+00	0.00e+00	4.57e+48	0.00e+00	0.00e+00	0.00e+00	0.00e+00	1.94e+46	7.86e+47
2	0.00e+00	0.00e+00	0.00e+00	0.00e+00	0.00e+00	0.00e+00	0.00e+00	0.00e+00	0.00e+00	0.00e+00	0.00e+00	0.00e+00	0.00e+00	0.00e+00	0.00e+00	0.00e+00	0.00e+00	0.00e+00	0.00e+00	9.82e+47
1	0.00e+00	0.00e+00	0.00e+00	0.00e+00	0.00e+00	0.00e+00	0.00e+00	0.00e+00	0.00e+00	0.00e+00	0.00e+00	0.00e+00	0.00e+00	0.00e+00	0.00e+00	0.00e+00	0.00e+00	0.00e+00	0.00e+00	9.82e+47

Table 23: Lower limit energy emission in erg by stars formed in the last 29 Myrs integrated starting 10 Myr ago. Rows: DEC-Bin, Columns: RA-Bin (as in images), binsize $12' \times 12'$, conversion to coordinates in table 1.

	20	19	18	17	16	15	14	13	12	11	10	9	8	7	6	5	4	3	2	1
23	1.57e+52	1.54e+52	1.87e+52	1.97e+52	1.71e+52	2.30e+52	2.55e+52	2.19e+52	1.95e+52	2.62e+52	2.62e+52	2.05e+52	2.05e+52	1.92e+52	1.92e+52	1.79e+52	1.79e+52	1.50e+52	1.50e+52	0.00e+00
22	1.42e+52	1.92e+52	2.71e+52	2.51e+52	0.00e+00	0.00e+00	0.00e+00	3.87e+52	2.48e+52	2.62e+52	2.62e+52	2.05e+52	2.05e+52	1.92e+52	1.92e+52	1.79e+52	1.79e+52	1.50e+52	1.50e+52	0.00e+00
21	1.47e+52	3.52e+52	2.78e+52	4.51e+52	0.00e+00	0.00e+00	0.00e+00	3.31e+52	3.00e+52	0.00e+00	0.00e+00	1.83e+52	1.83e+52	2.14e+52	2.14e+52	2.07e+52	2.07e+52	2.02e+52	2.02e+52	0.00e+00
20	2.47e+52	3.67e+52	5.02e+52	7.44e+52	8.17e+52	4.86e+52	3.94e+52	5.16e+52	3.12e+52	0.00e+00	0.00e+00	1.99e+52	1.99e+52	2.14e+52	2.14e+52	2.07e+52	2.07e+52	2.02e+52	2.02e+52	0.00e+00
19	4.03e+52	5.95e+52	9.12e+52	8.17e+52	7.01e+52	6.23e+52	6.00e+52	7.04e+52	4.21e+52	0.00e+00	0.00e+00	2.49e+52	2.49e+52	1.90e+52	1.90e+52	2.40e+52	2.40e+52	2.02e+52	2.02e+52	0.00e+00
18	4.95e+52	9.33e+52	8.94e+52	9.87e+52	8.52e+52	7.38e+52	1.40e+53	7.87e+52	6.44e+52	5.25e+52	3.31e+52	3.11e+52	3.11e+52	2.08e+52	2.08e+52	2.40e+52	2.40e+52	0.00e+00	0.00e+00	0.00e+00
17	6.78e+52	8.70e+52	8.07e+52	1.11e+53	1.33e+53	1.14e+53	1.40e+53	1.35e+53	1.34e+53	9.65e+52	6.07e+52	3.81e+52	2.41e+52	2.33e+52	2.33e+52	2.02e+52	2.02e+52	0.00e+00	0.00e+00	0.00e+00
16	4.88e+52	5.93e+52	9.67e+52	1.31e+53	2.31e+53	9.82e+52	6.77e+52	5.19e+52	5.37e+52	9.89e+52	8.68e+52	5.10e+52	2.92e+52	2.23e+52	1.91e+52	2.06e+52	2.06e+52	0.00e+00	0.00e+00	0.00e+00
15	5.08e+52	6.98e+52	8.31e+52	1.44e+53	2.22e+53	3.20e+53	2.88e+53	9.51e+52	1.28e+53	1.60e+53	1.12e+53	7.30e+52	4.80e+52	3.19e+52	2.22e+52	2.05e+52	2.05e+52	0.00e+00	0.00e+00	0.00e+00
14	6.18e+52	7.68e+52	1.57e+53	6.88e+52	6.61e+52	2.55e+53	1.36e+53	1.14e+53	1.18e+53	9.90e+52	1.35e+53	7.39e+52	6.78e+52	3.80e+52	3.69e+52	3.13e+52	3.13e+52	0.00e+00	0.00e+00	0.00e+00
13	6.46e+52	3.03e+53	1.09e+53	5.89e+52	6.18e+52	2.60e+53	6.73e+52	1.05e+53	1.64e+53	1.49e+53	1.17e+53	8.97e+52	6.50e+52	5.66e+52	3.46e+52	3.01e+52	3.01e+52	2.65e+52	2.65e+52	2.65e+52
12	6.76e+52	8.96e+52	1.60e+53	1.49e+53	4.62e+52	7.25e+52	1.95e+53	1.01e+53	1.72e+53	4.09e+53	1.36e+53	1.19e+53	1.11e+53	7.28e+52	5.97e+52	3.27e+52	2.69e+52	2.26e+52	2.24e+52	2.24e+52
11	6.32e+52	8.71e+52	1.25e+53	1.15e+53	1.37e+53	5.32e+52	4.37e+52	4.84e+52	1.47e+53	2.73e+53	1.95e+53	1.57e+53	1.29e+53	9.42e+52	8.29e+52	6.42e+52	3.22e+52	2.58e+52	2.93e+52	2.93e+52
10	1.50e+53	1.48e+53	1.09e+53	1.34e+53	1.32e+53	5.04e+52	4.97e+52	5.56e+52	1.64e+53	2.27e+53	3.83e+53	4.43e+53	1.94e+53	2.31e+53	9.02e+52	6.72e+52	5.32e+52	3.75e+52	3.26e+52	4.20e+52
9	1.61e+53	1.90e+53	1.20e+53	1.36e+53	1.13e+53	1.27e+53	5.26e+52	5.08e+52	7.53e+52	1.40e+53	2.51e+53	1.68e+53	1.36e+53	4.36e+52	1.24e+53	7.28e+52	6.77e+52	5.84e+52	4.90e+52	4.20e+52
8	6.21e+52	6.05e+52	6.59e+52	9.22e+52	8.35e+52	9.30e+52	1.18e+53	1.32e+53	1.34e+53	5.22e+52	1.52e+53	2.40e+53	1.12e+53	6.37e+52	1.11e+53	7.95e+52	7.27e+52	6.00e+52	5.38e+52	4.77e+52
7	5.78e+52	5.86e+52	6.83e+52	7.13e+52	8.35e+52	8.82e+52	7.91e+52	6.72e+52	8.01e+52	9.67e+52	4.88e+52	5.09e+52	4.05e+52	4.94e+52	4.11e+52	1.09e+53	7.92e+52	6.49e+52	5.99e+52	5.71e+52
6	5.62e+52	5.63e+52	6.91e+52	7.05e+52	5.92e+52	5.20e+52	5.09e+52	5.20e+52	6.78e+52	6.01e+52	6.54e+52	6.75e+52	8.12e+52	6.57e+52	7.85e+52	7.54e+52	7.46e+52	7.12e+52	6.85e+52	5.97e+52
5	5.62e+52	5.63e+52	6.91e+52	7.05e+52	4.75e+52	4.06e+52	3.61e+52	4.32e+52	3.72e+52	3.24e+52	3.79e+52	4.65e+52	5.08e+52	5.90e+52	6.06e+52	6.48e+52	5.76e+52	4.84e+52	5.55e+52	6.98e+52
4	4.86e+52	4.86e+52	4.24e+52	3.76e+52	5.05e+52	3.48e+52	3.03e+52	3.61e+52	3.24e+52	2.39e+52	3.30e+52	3.31e+52	3.46e+52	4.23e+52	3.89e+52	4.22e+52	4.05e+52	3.73e+52	4.64e+52	4.85e+52
3	4.86e+52	4.86e+52	4.24e+52	3.76e+52	5.05e+52	2.95e+52	3.16e+52	2.76e+52	2.61e+52	2.95e+52	2.68e+52	3.02e+52	2.80e+52	2.82e+52	2.45e+52	2.90e+52	3.34e+52	2.75e+52	4.00e+52	4.14e+52
2	2.99e+52	2.99e+52	3.35e+52	3.35e+52	3.29e+52	3.03e+52	3.05e+52	3.47e+52	2.90e+52	2.76e+52	2.73e+52	2.61e+52	2.33e+52	2.40e+52	3.12e+52	2.11e+52	2.62e+52	2.11e+52	2.46e+52	2.50e+52
1	2.99e+52	2.99e+52	3.35e+52	3.35e+52	3.29e+52	3.03e+52	3.05e+52	3.47e+52	2.90e+52	2.76e+52	2.73e+52	2.61e+52	2.33e+52	2.40e+52	3.12e+52	2.11e+52	2.62e+52	2.11e+52	2.46e+52	2.50e+52

Table 24: Upper limit energy emission in erg by stars formed in the last 20 Myrs integrated starting 10 Myr ago. Rows: DEC-Bin, Columns: RA-Bin (as in images), binsize $12' \times 12'$, conversion to coordinates in table 1.

	20	19	18	17	16	15	14	13	12	11	10	9	8	7	6	5	4	3	2	1
23	1.57e+52	1.55e+52	1.87e+52	1.98e+52	1.71e+52	2.30e+52	2.55e+52	2.19e+52	1.95e+52	2.63e+52	2.63e+52	2.05e+52	2.05e+52	1.92e+52	1.92e+52	1.79e+52	1.79e+52	1.50e+52	1.50e+52	0.00e+00
22	1.43e+52	1.92e+52	2.72e+52	2.51e+52	0.00e+00	0.00e+00	0.00e+00	3.88e+52	2.48e+52	2.63e+52	2.63e+52	2.05e+52	2.05e+52	1.92e+52	1.92e+52	1.79e+52	1.79e+52	1.50e+52	1.50e+52	0.00e+00
21	1.47e+52	3.52e+52	2.79e+52	4.52e+52	0.00e+00	0.00e+00	0.00e+00	3.32e+52	3.00e+52	0.00e+00	0.00e+00	1.83e+52	1.83e+52	2.14e+52	2.14e+52	2.07e+52	2.07e+52	2.02e+52	2.02e+52	0.00e+00
20	2.47e+52	3.67e+52	5.03e+52	7.44e+52	8.18e+52	4.87e+52	3.94e+52	5.16e+52	3.12e+52	0.00e+00	0.00e+00	1.99e+52	1.99e+52	2.14e+52	2.14e+52	2.07e+52	2.07e+52	2.02e+52	2.02e+52	0.00e+00
19	4.04e+52	5.96e+52	9.13e+52	8.17e+52	7.01e+52	6.23e+52	6.01e+52	7.05e+52	4.22e+52	0.00e+00	0.00e+00	2.49e+52	2.49e+52	1.90e+52	1.90e+52	2.40e+52	2.40e+52	2.02e+52	2.02e+52	0.00e+00
18	4.95e+52	9.34e+52	8.95e+52	9.88e+52	8.53e+52	7.39e+52	1.40e+53	7.88e+52	6.45e+52	5.25e+52	3.31e+52	3.11e+52	3.11e+52	2.08e+52	2.08e+52	2.40e+52	2.40e+52	0.00e+00	0.00e+00	0.00e+00
17	6.79e+52	8.71e+52	8.08e+52	1.11e+53	1.33e+53	1.14e+53	1.40e+53	1.35e+53	1.34e+53	9.66e+52	6.07e+52	3.81e+52	2.41e+52	2.33e+52	2.33e+52	2.02e+52	2.02e+52	0.00e+00	0.00e+00	0.00e+00
16	4.88e+52	5.93e+52	9.68e+52	1.31e+53	2.31e+53	9.83e+52	6.79e+52	5.20e+52	5.38e+52	9.91e+52	8.68e+52	5.11e+52	2.92e+52	2.24e+52	1.91e+52	2.06e+52	2.06e+52	0.00e+00	0.00e+00	0.00e+00
15	5.09e+52	6.99e+52	8.33e+52	1.44e+53	2.22e+53	3.21e+53	2.88e+53	9.54e+52	1.29e+53	1.60e+53	1.12e+53	7.31e+52	4.80e+52	3.20e+52	2.22e+52	2.06e+52	2.06e+52	0.00e+00	0.00e+00	0.00e+00
14	6.18e+52	7.68e+52	1.57e+53	6.89e+52	6.63e+52	2.55e+53	1.36e+53	1.14e+53	1.18e+53	9.91e+52	1.36e+53	7.40e+52	6.78e+52	3.80e+52	3.70e+52	3.13e+52	3.13e+52	0.00e+00	0.00e+00	0.00e+00
13	6.46e+52	3.03e+53	1.09e+53	5.90e+52	6.19e+52	2.60e+53	6.75e+52	1.05e+53	1.65e+53	1.49e+53	1.17e+53	8.98e+52	6.51e+52	5.67e+52	3.46e+52	3.01e+52	3.01e+52	2.65e+52	2.65e+52	2.65e+52
12	6.77e+52	8.97e+52	1.60e+53	1.49e+53	4.63e+52	7.26e+52	1.95e+53	1.01e+53	1.72e+53	4.10e+53	1.36e+53	1.19e+53	1.11e+53	7.29e+52	5.98e+52	3.27e+52	2.69e+52	2.26e+52	2.24e+52	2.24e+52
11	6.33e+52	8.73e+52	1.25e+53	1.15e+53	1.37e+53	5.33e+52	4.38e+52	4.84e+52	1.47e+53	2.73e+53	1.95e+53	1.58e+53	1.29e+53	9.43e+52	8.29e+52	6.43e+52	3.23e+52	2.58e+52	2.94e+52	2.94e+52
10	1.50e+53	1.48e+53	1.09e+53	1.34e+53	1.33e+53	5.05e+52	4.98e+52	5.57e+52	1.65e+53	2.28e+53	3.83e+53	4.44e+53	1.95e+53	2.31e+53	9.03e+52	6.73e+52	5.33e+52	3.75e+52	3.26e+52	4.21e+52
9	1.61e+53	1.90e+53	1.20e+53	1.36e+53	1.14e+53	1.28e+53	5.27e+52	5.09e+52	7.54e+52	1.40e+53	2.51e+53	1.68e+53	1.37e+53	4.36e+52	1.24e+53	7.29e+52	6.78e+52	5.85e+52	4.91e+52	4.21e+52
8	6.22e+52	6.05e+52	6.60e+52	9.24e+52	8.36e+52	9.32e+52	1.18e+53	1.32e+53	1.34e+53	5.23e+52	1.52e+53	2.40e+53	1.12e+53	6.38e+52	1.12e+53	7.96e+52	7.28e+52	6.01e+52	5.38e+52	4.77e+52
7	5.79e+52	5.87e+52	6.84e+52	7.14e+52	8.36e+52	8.83e+52	7.91e+52	6.73e+52	8.02e+52	9.68e+52	4.89e+52	5.10e+52	4.05e+52	4.95e+52	4.11e+52	1.10e+53	7.93e+52	6.50e+52	6.00e+52	5.72e+52
6	5.63e+52	5.63e+52	6.91e+52	7.06e+52	5.93e+52	5.20e+52	5.09e+52	5.20e+52	6.78e+52	6.02e+52	6.55e+52	6.76e+52	8.13e+52	6.58e+52	7.86e+52	7.55e+52	7.47e+52	7.12e+52	6.86e+52	5.98e+52
5	5.63e+52	5.63e+52	6.91e+52	7.06e+52	4.76e+52	4.06e+52	3.61e+52	4.32e+52	3.72e+52	3.25e+52	3.80e+52	4.65e+52	5.08e+52	5.90e+52	6.06e+52	6.49e+52	5.77e+52	4.85e+52	5.55e+52	6.98e+52
4	4.87e+52	4.87e+52	4.24e+52	3.76e+52	5.06e+52	3.49e+52	3.03e+52	3.61e+52	3.25e+52	2.39e+52	3.30e+52	3.32e+52	3.46e+52	4.23e+52	3.90e+52	4.23e+52	4.05e+52	3.73e+52	4.64e+52	4.85e+52
3	4.87e+52	4.87e+52	4.24e+52	3.76e+52	5.06e+52	2.95e+52	3.16e+52	2.76e+52	2.61e+52	2.96e+52	2.69e+52	3.02e+52	2.80e+52	2.82e+52	2.45e+52	2.91e+52	3.34e+52	2.75e+52	4.00e+52	4.14e+52
2	2.99e+52	2.99e+52	3.36e+52	3.36e+52	3.29e+52	3.03e+52	3.05e+52	3.47e+52	2.90e+52	2.77e+52	2.73e+52	2.62e+52	2.33e+52	2.40e+52	3.12e+52	2.11e+52	2.63e+52	2.11e+52	2.46e+52	2.50e+52
1	2.99e+52	2.99e+52	3.36e+52	3.36e+52	3.29e+52	3.03e+52	3.05e+52	3.47e+52	2.90e+52	2.77e+52	2.73e+52	2.62e+52	2.33e+52	2.40e+52	3.12e+52	2.11e+52	2.63e+52	2.11e+52	2.46e+52	2.50e+52

Table 25: Upper limit energy emission in erg by stars formed in the last 29 Myrs integrated starting 10 Myr ago. Rows: DEC-Bin, Columns: RA-Bin (as in images), binsize $12' \times 12'$, conversion to coordinates in table 1.

Selbstständigkeitserklärung

Hiermit bestätige ich, dass ich diese Arbeit selbstständig und nur unter Verwendung der angegebenen Hilfsmittel angefertigt habe.

Ort, Datum

Unterschrift